Pre-synaptic Terminal Dynamics in the Hippocampus

Inauguraldissertation

zur

Erlangung der Würde eines Doktors der Philosophie

vorgelegt der Philosophisch-Naturwissenschaftlichen Fakultät

der Universität Basel

von

Vincenzo De Paola

aus Italien

Basel, 2003

Friedrich Miescher Institut
Maulbeerstrasse 66
4058 Basel
Schweiz

Genehmigt von der Philosophisch-Naturwissenschaftlichen Fakultät

auf Antrag von

Prof. Markus Rüegg, PD Dr. Caroni, Prof. Andrew Matus

Basel, den**_____08-07-2003____**

_____

Dekan

Contents

Summary 1

1. Introduction 2

Overview 2

1.1. Plasticity in the adult brain 2

1.1.1. Experience-dependent synaptic plasticity 3

1.1.1.1. Experience-dependent structural synaptic plasticity 4

1.1.2. Mechanisms of activity-dependent synaptic plasticity 5

1.1.2.1. Glutamate receptor-dependent synaptic plasticity 6

1.1.2.2. Other pathways underlying synaptic plasticity 9

1.2. Synapse formation and remodelling 11

1.2.1. Overview of synaptogenesis 11

1.2.1.1. Pre- and post-synaptic differentiation at glutamatergic synapses 13

1.2.2. Spine dynamics as an example of synapse remodelling 13

1.2.3. Synaptic stability 15

1.3. A model system for studying mechanisms of plasticity: the hippocampus 17

1.3.1. Memory processing and the hippocampus 17

1.3.2. Main areas and connectivity of the hippocampus 19

1.3.3. The mossy fiber pathway 21

1.3.4. A model for studying the hippocampus in vitro: the hippocampal slice culture technique 23

1.4. Starting point and goal of the thesis 24

2. Results 25

2.1. Targeted-GFP expression in adult neurons of transgenic mice 26

2.1.1. Summary 27

2.1.2. Introduction 28

2.1.3. Results 31

2.1.4. Discussion 39

2.1.5. Material and methods 42

2.1.6. Figures 45
2.1.7. Figure legends 54

2.2. Presynaptic terminal dynamics in mature hippocampal networks 59
2.2.1. Introduction 61
2.2.2. Results 63
2.2.3. Future perspectives and Discussion 72
2.2.4. Material and methods 75
2.2.5. Figures 83
2.2.6. Figure legends 97

3. Discussion and future prospects 105

3.1. Overview 105

3.2. Genetic tools to study live synaptic dynamics and fine details of neuronal morphology 105
3.2.1. Main achievements and relevance of results 105
3.2.2. Future applications of the genetic tools 107
3.2.3. Conclusions 110

3.3. Presynaptic terminal dynamics in the hippocampus 110
3.3.1. Main findings, open questions and follow-ups 110
3.3.2. Biological relevance of pre-synaptic plasticity 115
3.3.3. Conclusions 118

3.4. Discussion figures 120

3.5. Outlook 123

4. Appendix 125

4.1. Defining molecular basis of motor neuron subpopulations 125

4.1.1. Overview and rationale of approach 125
4.1.2. Results 126
- Protocadherins cloning and expression pattern in the mouse spinal cord and DRGs
- Backlabeling from different skeletal muscles and isolation of correspondent motor neurons
4.1.3. Discussion 127
4.1.4. Material and methods 128
4.1.5. Figures 131
4.1.6. Figure legends 133

5. References 134

Curriculum Vitae 155

Acknowledgements

I would like to thank the many people who gave me help and support in the time that I spent at this fantastic place that is the Friedrich Miescher-Institute.
First of all I would like to thank Pico Caroni. He gave me the unique possibility of making my graduate studies in an exceptional scientific environment. His enthusiasm for science and his critical and experimental approach together with his acute insights have been an invaluable guide for my development as a graduate student.
I am very grateful for the support and never ending discussions I had from my colleagues, especially for wise advice and patience of Stefano Fumagalli, Maddalena Lino, Thorsten Laux, Dunja Frey, Martin Hund. San Pun, Corinna Schneider, Lan Xu, Stefan Wacha, Tami Golub, Alex Santos for support. I thank “my” student Igor Dodevsky for his enthusiastic support in deciding to spend a summer with me quantifying data. Members of the Muller lab, Martin, Marco, Sandra, Diana, Amanda, for sharing their experiences and beers with me.
A special thank goes to all the members of the Matus lab, especially Martjn, Pingwei, Virginie, Heike, Manuel, Andreas, who were always ready to help and share with me their technical experience in many circumstances. Also, I thank Maria Fischer and Uta Wagner for their help with my first attempts in culturing “green” neurons. Marlin Moosmayer (Dominique Muller lab) for her kindness in introducing me to the slice culture technique and for teaching me all the “tricks”. Mathias Abegg and Massimo Scanziani for their help with electrophysiology.
I would like to thank Markus Ruegg for his kindness to present my thesis to the faculty, Andrew Matus for acting as "Coreferent" and Denis Monard for being my chair, Uli Muller for discussions and advice.
I would also like to acknowledge the financial support of The Swiss Foundation for Muscle Research.
And last but not least I want to thank my family who constantly supported my studies, and Janis Bennion for her constant encouragement, critical discussions during my last years as a PhD student, and for being the marvellous person she is.

Abbreviations

Acetycholine (**ACh**), α-amino-3-hydroxy-5-methy-4-isoxazoleproprionate (**AMPA**), botulinum toxin A (**BotA**), brain-derived neurotrophic factor (**BDNF**), central nervous system (**CNS**), dorsal root ganglion (**DRG**), extracellular matrix (**ECM**), γ-aminobutyric acid (**GABA**), Growth Associated Protein 43 (**GAP43**), granule cell (**GC**), calcium concentration (**[Ca^{2+}]**), long term depression (**LTD**), long term potentiation (**LTP**), neuromuscular junction (**NMJ**), N-methyl-D-aspartate (**NMDA**), peripheral nervous system (**PNS**), postsynaptic density (**PSD**), Large Mossy Terminals (**LMT**), Large Mossy Terminal Filopodia (**LMTfil**), en passant varicosities (**epV**), mossy fibers (**MF**), dentate gyrus (**DG**), plasmamembrane-targeted GFP (**mGFP**), synaptophysin-targeted GFP (**spGFP**), cytosolic-GFP (**cGFP**), synaptic vesicle (**SV**), tetrodotoxin (**TTX**)

TABLE OF CONTENTS

Summary 1

1. INTRODUCTION 2

Overview 2

1.1. Plasticity in the adult brain 2

1.2. Synapse formation and remodelling 11

1.3. A model system for studying mechanisms of plasticity: the hippocampus 17

1.4. Starting point and goal of the thesis 24

2. RESULTS 25

2.1. Targeted-GFP expression in adult neurons of transgenic mice 26

2.2. Presynaptic terminal dynamics in mature hippocampal networks 59

3. DISCUSSION AND FUTURE PROSPECTS 105

3.1. Overview 105

3.2. Genetic tools to study live synaptic dynamics and fine details of neuronal morphology 105

3.3. Presynaptic terminal dynamics in the hippocampus 110

3.4. Discussion figures

3.5. Outlook 123

4. APPENDIX 125

4.1. Defining molecular basis of motor neuron subpopulations 125

5. REFERENCES 134

Summary

This thesis work dealt with the study of synaptic plasticity in the adult brain. This is an area of intensive investigation because instability of synapses is believed to underlie cognitive processes like learning and memory in the CNS, and adaptation to injury or paralysis in the PNS.

Structural changes involving large-scale growth and retraction of neuronal processes or fine-tuning of connections are well documented in the developing nervous system and are thought to naturally decrease in mature systems. Evidence for post-synaptic structural changes in the adult brain is numerous. In contrast, rearrangements of pre-synaptic terminals are much less studied and we simply do not know their capacity for plastic changes.
To investigate these issues we generated mice expressing membrane- and/or synaptic vesicle-targeted spectral variants of GFP in neuronal subsets to image identified presynaptic terminals.
This unique tool allowed us, for the first time, to follow individual presynaptic terminals over long periods of time by confocal and conventional time-lapse microscopy. Because of its prominent role in learning and memory we have chosen the hippocampus as a model system. The use of *in vitro* and *ex vivo* preparations (hippocampal slice culture and whole mount preparations) enabled us to investigate the molecular mechanisms of pre-synaptic terminal plasticity in the hippocampus. Our main findings are:
1) Pre-synaptic terminal numbers in mature hippocampal networks are in a state of dynamic equilibrium. 2) Mature mossy fibers display short-term dynamic behaviors resembling those typical during development. 3) Distinct types of terminals of the same neuron exhibit unique dynamic properties. 4) Stable terminals can be reversibly converted into dynamic ones by patterned electrical activity. 5) This process is mediated through AMPA-receptor activation, PKA and protein synthesis. We conclude that stable presynaptic terminals in mature hippocampal networks can be converted into dynamic ones by synaptic activity, demonstrating regulated pre-synaptic rearrangements in these networks.

The usefulness of the targeted-GFP transgenic mice for many fields of neuroscience research was also demonstrated in several additional experimental designs and applications.

1. INTRODUCTION

Overview

The ability of the brain to change in response to everyday experience or upon learning and memory is called plasticity and has been the subject of thorough studies for centuries especially with respect to synaptic changes. Since this is the context where my thesis work can be best placed, I will start the introduction by giving a summary of how experience can alter synapses (1.1.1.). In the following subsections (1.1.1.1 to 1.1.2.2.) I will attempt to describe at which levels synaptic plastic phenomena could occur: namely at the biochemical (e.g. changes in ion channel currents), molecular (e.g. modifications in key synaptic proteins) and morphological level (e.g. changes in shape, size or numbers of synapses). The mechanisms of synaptic plasticity will be treated in a separate subsection (1.1.2.), which will include both classic studies from Aplysia and LTP literature, and also recent views about other possible pathways underlying activity-dependent modifications of synapses. How synapses form, disassemble and remodel will be the subject of the second section (1.2), with a particular emphasis on synapse number changes.

The third section (1.3) deals with the hippocampus as a model system to study synaptic plasticity in the brain, primarily focusing on its role in memory processing. This is followed by a part on the anatomy of hippocampal circuits, together with the functional roles of the mossy fiber pathway, which will be important for the later interpretation of the second part of the results (2.2). A critical evaluation of the slice culture technique will end the introduction.

1.1. Plasticity in the adult brain

Anybody who has ever observed a child trying to grasp a toy must have realized that the adult perceptual and motor skills are not innate but need to develop with time through practice.

Before the developing brain acquires the full capacity to elaborate and analyse sensory experience, experience itself will leave a ‘fingerprint’ on brain tissues. Even if, after birth, the brain does not undergo modifications of its fundamental organization, structural and functional details maintain a certain capacity to change for some time. This capacity of the brain is called plasticity and persists into adulthood. Importantly, this plasticity is thought to allow us to adapt our behaviour to experience, to acquire new tasks, to remember past things and recognise objects. But, how can experience modify the organization of the brain?

1.1.1. Experience-dependent synaptic plasticity

Experience can shape the brain at specialized interneuronal connection sites, the synapses. Formation of synapses during development is thought to depend upon both genetic and environmental factors. Initial establishment of synaptic connections occurs independently of experience, followed by a period of experience-dependent refinement. A common view was that, after this critical period of fine-tuning, the configuration of synaptic connections remained unaltered throughout the lifetime of the animal. However, research over the last decade has shown evidence for widespread experience-dependent plasticity in the adult brain (Gilbert, 1998). Some of the most detailed accounts of experience-dependent plasticity, including mechanistic studies, have been performed in the rodent barrel cortex. This is the location where tactile information from the facial vibrissae is processed. There are several advantages in using this cortical region in the mouse for studies of experience-dependent plasticity. For example, contrary to the rodent visual system (the visual system is mainly studied in cats and monkeys), this region comprises a clear columnar structure, which is both easy to define functionally and easy to view with histochemical stainings (Woolsey and Van der Loos, 1970). In layer IV of this somatosensory cortex, neurons are arranged in discrete clusters called “barrels”. Each whisker activates neurons primarily in a single identifiable barrel, and the spatial arrangement is topographic, such that neighbouring whiskers map to neighbouring barrels. Manipulations of the sensory periphery during development and in the adult mouse (usually, a period around 6 months is considered as adult, corresponding to 20 years in humans, and 3-4 years in a cat), such as through clipping whiskers, can change the receptive fields of cortical neurons. Thus, experience-dependent plasticity can be measured as soon as 1 day after whisker clipping (e.g., (Diamond et al., 1993)). The cortex is still plastic up to 15 months in a mouse (Fox, 2002). According to most models, the cellular basis of this experience-dependent plasticity is in modifications of existing synapses, such as reorganization of active zones (Lnenicka et al., 1986), postsynaptic spines (Fifkova and Anderson, 1981; Chang and Greenough, 1984) or long-term potentiation and depression (Buonomano and Merzenich, 1998; Martin et al., 2000). But studies on the biology of memory have clearly demonstrated that experience can also alter synapse numbers in adult brain (Bailey and Kandel, 1993).

1.1.1.1. Experience-dependent structural synaptic plasticity

There are several types of structural changes associated to various forms of activity-dependent alterations in both vertebrates and invertebrates. Early examples come from studies of sensory deprivation during critical periods of postnatal development.

In kittens, using monocular deprivation Hubel and Wiesel found that lack of visual experience during early development, but not after this critical period, leads to permanent alteration in perceptual capabilities later in life. These behavioural changes are accompanied by morphological and physiological changes consistent with alteration in the number and pattern of synaptic connections (Hubel and Wiesel, 1970). The so-called ocular dominance columns do not form in kittens when all activity in retinal ganglion cells and optic nerves is blocked by injections of tetrodotoxin into each eye, meaning that during the critical period segregation of afferent fibres and the establishment of ocular dominance columns can be altered by changing the balance of input activity from the two eyes (Stryker and Harris, 1986).

In primates, depending on the level of injury, large-scale functional reorganization of cortical maps representing body sensation and movement has been described to be caused by limb deafferentation or amputation or peripheral injury (Florence et al., 1998; Merzenich, 1998). Similarly, studies of recovery from brain damage have also demonstrated dendritic as well as synaptic structural changes, like enhanced dendritic arborization and/or increased spine density (Jones and Schallert, 1994; Kolb et al., 1996; Schallert et al., 1997).

Interestingly, in songbirds, morphological studies on vocal centres within their brain have shown a correlation between neuronal numbers and synaptic connectivity changes, and various aspects of the song features, such as seasonal variations or time spent singing (Nottebohm, 1981). Furthermore, structural plasticity correlated to learning and memory has been studied at identified synapses of higher invertebrates like the marine mollusc *Aplysia californica*. In fact the simplicity of this model system has allowed the analysis of short- and long-term forms of memory at the molecular and cellular level (see later). Thus, upon long-term sensitisation following behavioural training of the gill and siphon-withdrawal reflex, there is an increase in sensory neuron varicosities, and an enlargement of the axonal arbor at the sensory to motor synapse (Bailey and Chen, 1988). This elementary form of non-associative learning has been instrumental for the study of the time course of structural changes: these studies revealed that some aspects of synaptic structure are transient (like modulation of active zone size that lasts only few days) while others (like active zone and synapse number) endure for weeks and parallel the behavioural time course of memory (Bailey and Chen, 1989).

A broad body of work has associated the addition of synapses with learning and memory formation also in higher vertebrates verifying the theory introduced by Cajal that memory is stored as an anatomical change in the strength of synapses (Cajal, 1894). Adult animals housed in complex, toy filled cages have thicker cerebral cortical tissue, more highly branched neuronal dendritic fields and more synapses per neuron than animals housed in standard laboratory cages. Subsequent work demonstrated that standard learning tasks evoked similar changes (Turner and Greenough, 1985; Moser et al., 1997). Another type of learning, motor learning, has also been associated to changes in number and patterns of synaptic connections. The number of synapses per Purkinje cell was elevated by a 30-day period of acrobatic motor learning in adult rat cerebellar cortex. In contrast, simple motor exercise was ineffective, suggesting that only those aspects of activity that are related to the acquisition of a particular learning task lead to changes in synaptic organization (Black et al., 1990). Finally, with the aid of sophisticated methodology experience-dependent changes in spine turnover on a time-scale of days have been recently observed in mouse barrel cortex (Knott et al., 2002; Trachtenberg et al., 2002), but see (Grutzendler et al., 2002). How does this compare to humans? In a recent study, the anatomy of the brains of London taxi drivers has been compared with that of age-matched non-taxi drivers (Maguire et al., 2000) using voxel-based morphometry analysis of structural MRI scans. Significant differences in grey matter volume between the two groups were found only in the hippocampus, with the posterior hippocampus being larger on both sides in taxi drivers and anterior hippocampus being smaller. Moreover the increase in right posterior hippocampus correlated with the time spent in the job. This study provides an intriguing example of experience-dependent structural plasticity in the human brain and suggests a close link between navigation and the hippocampus in humans (see later).

1.1.2. Mechanisms of activity-dependent synaptic plasticity

Mechanisms underlying synaptic plasticity have been studied mainly in the context of learning and memory. These studies developed rapidly in the late 40's and early 50's with the introduction of cellular techniques to study synaptic connections, including intracellular microelectrode recording or electron microscopy. The plastic changes that underlie memory are thought to follow a so-called homosynaptic rule, that is, the events responsible for triggering synaptic strengthening occur at the same synapse that is being strengthened. This rule was postulated in 1949 by Donald Hebb, who proposed that the strength of the connection between two neurons is increased for a long period of time when the firing of the presynaptic

and postsynaptic neuron are closely correlated in time. Importantly, synaptic strengthening is input-specific, meaning that other synapses on either neuron remain unchanged. Synaptic strengthening can also occur as a result of the firing of a third neuron, a modulatory interneuron, whose terminals end on and regulate the strength of a specific synapse (the so called heterosynaptic rule). These changes can result in an increase (facilitation) or decrease (depression) in synaptic strength (Bailey et al., 2000). As mentioned above the simplicity of the neural circuit represented by the sensory neurons that innervate the siphon in the mollusc *Aplysia* allowed more detailed molecular studies. Thus, upon sensitization, serotonin (5-HT) released by a class of modulatory interneurons, activates G-protein-coupled receptors on the sensory neuron presynaptic terminals. As a consequence, either adenylyl cyclase or the cyclic AMP-dependent protein kinase (PKA) or protein kinase C (PKC) are activated leading to enhanced transmitter release (Brunelli et al., 1976). This facilitation can be transient, lasting only few minutes, when only one intense stimulus is given to the tail of *Aplysia* (or when only one pulse of 5-HT is given in a culture system that reconstitutes the elements of the neural circuit) and requires only covalent modifications of pre-existing proteins. Repetitive stimuli (or spaced applications of 5-HT in the culture), instead lead to long-term sensitization that lasts several days. This long-term phenomenon requires both new protein and mRNA synthesis. Repetitive 5-HT applications recruit PKA and mitogen-activated protein kinase (MAPK) that translocate to the nucleus and activate the transcription factor CREB (for cAMP response element binding protein). CREB in turn activates a cascade of genes that lead to the growth of new synaptic contacts between the sensory and the motor neurons and to facilitation of synaptic strength that persists for days. It seems, thus, that the distinction of memory phases in short- and long-term phases at the behavioural level has a counterpart at the cellular level.

1.1.2.1. Glutamate receptor-dependent synaptic plasticity

Long-lasting synaptic enhancement has also been discovered in the mammalian hippocampus as a consequence of repetitive stimulation of excitatory synapses (Bliss and Lomo, 1973). Since this landmark study, a lot of progress has been made to characterise this so-called long-term potentiation (LTP) of synaptic transmission. Although there are many unanswered questions regarding the role of LTP as a cellular mechanism of memory storage (Martin et al., 2000), it is clear that the study of LTP has provided a way to identify and characterize molecular mechanisms that potentially underlie memory storage. LTP is not a unitary phenomenon, but a family of processes that vary in their cellular and molecular mechanisms.

The existence of these various forms of LTP was first found in the three main areas of hippocampus, but other variants were discovered in the cerebellum, in the lateral nucleus of the amygdala and in prefrontal cortex (Blair et al., 2001), (Vickery et al., 1997). Some of the properties of LTP are shared among the different systems. Thus, there is an early phase (e-LTP) and a late phase (l-LTP) of LTP. This latter one requires new protein and mRNA synthesis. Moreover, the induction of l-LTP requires in part cAMP, PKA and MAPK. The triggering of LTP requires activation of postsynaptic *N*-methyl-D-aspartate (NMDA) glutamate receptors. To activate the NMDA receptor, and to initiate LTP, two events need to occur simultaneously: glutamate has to bind to the receptor and the postsynaptic membrane needs to be depolarised sufficiently by the activation of α-amino-3-hydroxy-5-methy-4-isoxazoleproprionate (AMPA) receptors to dissociate magnesium from the binding site within the receptor. This allows Ca^{2+} and Na^{+} to enter the postsynaptic dendritic spine. This local source of Ca^{2+} is the trigger of LTP and accounts for its input-specificity (but see (Schuman, 1997)). Thus, the NMDA receptor may act as a molecular coincidence detector in Hebbian plasticity because of its dual requirement for depolarisation and glutamate.

Synaptic plasticity is greatly influenced by the properties of the activation signal. A 100 Hz stimulus (tetanus) protocol activates the kinases required for e-LTP, but this phase only lasts a few hours. Use-dependent modulations of the efficacy of synaptic transmission can last for seconds to minutes (paired-pulse facilitation and post-tetanic potentiation) (reviewed by (Zucker and Regehr, 2002). In contrast, multiple tetani are required to induce long lasting l-LTP. This intense stimulation recruits calcium-calmodulin-dependent protein kinase II (CaMKII), a key component of the molecular machinery of LTP. An important property of CaMKII is that when autophosphorylated on Thr^{286}, its activity is no longer dependent on Ca^{2+}-calmodulin. This allows its activity to continue long after the Ca^{2+} signal has returned to baseline (Lisman et al., 1997). Other biochemical pathways induced by Ca^{2+} and required for the increase in synaptic strength characteristic of LTP, include cAMP intracellular elevation and consequent activation of PKA and MAPK, which activate CREB-mediated transcription (Abel et al., 1997). It is clear that the dynamics and magnitude of Ca^{2+} increase in the dendritic spine, as well as the modes of Ca^{2+} entry, are critical for the form of the resulting synaptic plasticity induced. In fact, short-term potentiation that decays to baseline over 5 to 20 minutes or long-term depression (LTD), a persistent decrease of synaptic strength that can be due to a reversal of the mechanisms underlying LTP, can also be generated by an increase in Ca^{2+}.

The third class of ionotropic glutamate receptor is called kainate receptor (after the name of the agonist) type. Kainate receptors are ubiquitous in the nervous system and, as for the other two types, NMDA and AMPA receptors, are tetramers in which each monomer carries its own ligand-binding site. There is now compelling evidence that they act both pre- and post-synaptically in modulating transmitter release and short- and long-term synaptic plasticity. Synaptic responses mediated by kainate receptors were primarily found at hippocampal mossy fiber synapses (Castillo et al., 1997). Interestingly, at mossy fibers these receptors function as autoreceptors that sense the synaptically released glutamate, enhancing glutamate release in a frequency dependent manner. So, these presynaptic kainate receptors significantly contribute to the short-term plasticity (frequency-dependent facilitation) of mossy fiber synapses (Contractor et al., 2000). These receptors seem also to be involved in long-term plastic phenomena. Indeed, mossy fiber LTP is completely prevented, in a reversible manner, by a specific antagonist of GluR5-(one of the five cloned kainate receptor subunits)-containing receptors (Bortolotto et al., 1999). Although the precise mechanism of action needs further investigation, it has been found that GluR5 and GluR6 interact with PDZ domain containing proteins like GRIP (glutamate-receptor-binding-protein), PICK1 (protein that interacts with C kinase 1) and PSD-95 (postsynaptic density 95). PKC-mediated phosphorylation of kainate receptors results in the stabilization of anchored receptor at the synapse. This is in contrast with the PKC-dependent phosphorylation of AMPA receptors that allows them to enter into a recycling process, making them available for insertion into the membrane (Daw et al., 2000). So, differential effects of PDZ-interacting proteins on AMPA and kainate receptor types constitute a potential molecular mechanism to account for the activity-dependent changes observed at synapses that contain AMPA and kainate receptors.

Compared with our understanding of the roles of ionotropic glutamate receptors (AMPA, NMDA and Kainate receptors), much less is known about the roles of the metabotropic glutamate (mGluR) receptor family in synaptic plasticity. These are G-protein coupled receptors (both pre- and post-synaptic) that have modulatory functions on neuronal excitability, transmitter release, and synaptic plasticity in the CNS. Phosphorylation (by PKC or PKA) and dephosphorylation (PP2B/calcineurin) are events that play a major role in their regulation. There are 8 cloned mGluRs divided in 3 groups based on sequence homology, mechanisms of transduction and pharmacology. Postsynaptic Group I (mGluR1/mGluR5) are selectively activated by 3,5-dihydroxy-phenylglycine (DHPG) and coupled to inositol phospholipid

hydrolysis. They are coupled to various calcium, potassium, and non-selective cationic channels, thus modulating excitability of hippocampal neurons directly. Presynaptic group II (mGluR2/mGluR3) and group III (mGluR4/mGluR6/mGluR7/mGluR8), which are linked to inhibition of the cAMP cascade in receptor-transfected cell lines, are selectively activated by 2-(2,3-dicarboxycyclopropyl)-glycine (DCG-IV) and 2-amino-4-phosphonobutyrate (L-AP4), respectively. They suppress transmitter release in various regions by inhibiting voltage-dependent calcium channels and/or interfering directly with the release machinery. The critical role of mGlu in LTP and LTD of synaptic transmission in the hippocampus is also well established due to the aid of a series of agonists and antagonists and to mGluR knockouts (Lu et al., 1997; Fitzjohn et al., 1998).

Interestingly, pharmacological evidence exists that the late phase of LTP, which requires PKA and protein synthesis, has a further requirement for heterosynaptic modulatory (dopamine, noradrenaline) input that recruits the cAMP cascade at various pathways. Whether dopamine and noradrenaline axons are directly activated by the high frequency stimulation, or whether there is glutamate spillover-induced transmitter release at these modulatory axon terminals is not clear at present (Whitton, 1997). Blockade of ß-adrenergic receptors interferes with the formation of emotional memory in humans, whereas infusion of ß-adrenergic agonists into the amygdala in animals enhances memory consolidation. These results suggest that these modulatory pathways are important for regulating memory storage.

1.1.2.2. Other pathways underlying synaptic plasticity

In the search for molecules that could mediate the structural synaptic changes that underlie long-term memory in *Aplysia*, a number of proteins were found. One group of such proteins is constituted by the *Aplysia* homologs of NCAM-related cell adhesion molecules (apCAM). Upon serotonin or cAMP, there is a decrease in the expression of these different *Aplysia* isoforms and, notably, also a loss of pre-existing proteins from the membrane of the sensory neurons within 1h after addition of the stimulus. Further experiments revealed that upon 5-HT there is a rapid internalisation of apCAM, and thus a regulation of the internal membrane system of sensory neurons which closely resemble the changes induced by growth factors in non neuronal cells (e.g. NGF effect on PC12 cells). Thus, learning related synapse formation is accompanied by activation of an endocytic pathway. This could serve the double function of destabilizing synaptic contacts to facilitate their disassembly and of redistributing membrane components that would favour synapse formation (Bailey et al., 1992).

Another class of proteins whose role in synaptic plasticity is well recognized are the neurotrophins.

They have classically been known for their role in neuronal growth and survival, but there is an increasing amount of reports that point to an action in establishing connections between neurons during development, in the mature CNS and after injuries. Synaptic activity can regulate expression, secretion, and function of neurotrophins which in turn can influence both acute and long-term electrophysiological and structural synaptic plasticity (Poo, 2001). Neurotrophins can act like neurotransmitters altering the functional state of neurons within milliseconds (Kafitz et al., 1999), with their actions restricted to the local environment. In fact there is evidence that BDNF could induce a spatially-restricted potentiation of synaptic transmission which requires local protein synthesis in the axon (Zhang and Poo, 2002). The threshold to induce LTP is lower when exogenous BDNF is added, and BDNF knockout mice have impaired hippocampal LTP. TrkB signalling appears to be required for both the early and late phase of LTP, although this varies with the stimulation protocol used (Kang et al., 1997). Interestingly, NGF and NT-3 (that act on different receptors) do not have these effects. Moreover, the establishment of ocular dominance columns in the visual cortex, a model of activity-dependent developmental plasticity, also involves neurotrophin action (McAllister et al., 1999).

The silent synapse hypothesis states that synapses can be either presynaptically silent (releasing little or no glutamate), postsynaptically silent (containing non-functional AMPA receptors or not having them at all), or both (Liao et al., 1999). There is electrophysiological evidence that LTP expression is associated with the insertion of AMPA receptors in the postsynaptic membrane (Shi et al., 1999). BDNF can trigger the increase of AMPA receptor proteins in cultured hippocampal neurons (Narisawa-Saito et al., 1999) suggesting that it may play a role in activity dependent conversion of silent synapse into functional ones. Consistent with a role of exocytosis in this process, introduction into CA1 pyramidal neurons of compounds like botulinum toxin prevents LTP. Finally, there is also evidence that LTD involves increased endocytosis of AMPA receptors (Wang and Linden, 2000). Thus the activity-regulated trafficking of receptors at synapses provides a further molecular mechanism for changing synaptic weight.

A last example of a possible method of synaptic modulation by neural activity is local protein synthesis. Both anatomical and biochemical evidence exist for protein translation near synapses, and several mechanisms for the regulation of this translation and for potential roles

in synaptic plasticity have been described recently (Steward and Levy, 1982; Scheetz et al., 1997; Jiang and Schuman, 2002). Indeed polyribosomes are translocated to spines during synaptic plasticity (Ostroff et al., 2002). One of the proteins synthesized under neurotransmitter regulation (e.g. following mGluRI activation) is the fragile-X mental retardation protein (FMRP). This RNA binding protein can regulate translation in both cell body and dendrites (Brown et al., 2001). The idea is that by keeping the protein synthesis machinery nearby, each synapse can operate as an autonomous entity and change its transmission efficacy independent of others. These new plasticity-related proteins would be transferred to activated synapses and act to induce long-lasting synaptic enhancement or depression (Kang and Schuman, 1996; Huber et al., 2000).

Are the molecular mechanisms underlying synaptic plasticity conserved throughout evolution? With the recent isolation and initial characterisation of the NMDA receptor complex (more than 80 proteins, including PKA regulatory and catalytic subunits), it is becoming clear that the similarity between mechanisms of plasticity in various model systems is greater than their apparent differences. In support of this unified view of the molecular basis of synaptic plasticity, cAMP/PKA signalling pathways have been shown to be involved in hippocampal LTP, barrel formation, in learning and memory paradigms in *Drosophila* and *Aplysia* and in the plasticity of receptive field properties of visual cortical neurons (Beaver et al., 2001).

1.2. Synapse formation and remodelling

The final step in wiring up the brain is synapse formation. It involves three highly regulated steps: 1) the formation of selective contact sites between the developing axon and its targets, followed by 2) presynaptic and 3) postsynaptic differentiation.

1.2.1. Overview of synaptogenesis

Axo-dendritic contact can be initiated by the axonal and dendritic growth cone, as well as by dendritic and axonal filopodia (Ziv and Garner, 2001). This critical process seems to be mediated by various classes of cell-cell adhesion molecules including the cadherins and the neuroligin-neurexin complex. Particularly relevant in the context of the considerable heterogeneity of synaptic connectivity in the CNS (Craig and Boudin, 2001), is the discovery of the structural features of synaptic cadherin-related neural receptors (CNRs) or protocadherins. The striking variability of their extracellular domains, could provide a mechanism by which initial contact would be established by cells expressing complementary

sets of these molecules (Kohmura et al., 1998). This, in turn, would ensure that precision in the connections between developing neurons is achieved.

The most complete picture of synaptogenesis presently available is at the synapse between motor neurons and skeletal muscles. Although many differences between neuromuscular junction (NMJ) and CNS synaptogenesis are obvious, one emerging similarity is that in both systems, a synapse editing process takes place to get rid of an initial surplus of synapses. For example, each Purkinje cell in the cerebellum is initially innervated by multiple climbing fibers (coming from the inferior olive) during early postnatal life. Over the course of several weeks, however, every Purkinje cell is eventually innervated by only one climbing fiber, due to an activity-dependent process that eliminates the other inputs. In the periphery, during embryonic and early postnatal life most vertebrate muscle fibers are innervated by several motor neurons, but adult muscle fibers typically are innervated by only one of them. This process is thought to be mediated by activity and by local competitive interactions that take part at different times within each neuromuscular junction (Keller-Peck et al., 2001). Consistent with a role of neurotransmitter release in synapse elimination, when pre- and postsynaptic activity is not temporally correlated, silent synaptic sites are destabilized (Personius and Balice-Gordon, 2002). A key pathway involves the synthesis and axonal secretion of the extracellular matrix protein agrin by motor neurons. Agrin activates a receptor tyrosine kinase known as muscle-specific kinase (MuSK), which, in turn, initiates clustering of ACh receptors and other proteins at the developing synapse. Both the extracellular domain of MuSK, which plays a role in signal transduction and is not only required for activation by the ligand, and its intracellular domain, seem to be necessary for this function (Zhou et al., 1999). The postsynaptic specialization also leads to presynaptic differentiation, in a process that probably involves a retrograde signal (DeChiara et al., 1996; Glass et al., 1996). However, even if neural agrin is missing, ACh receptors are still found concentrated during embryonic development (Yang et al., 2001). Thus it seems that agrin is not required for the formation of small ACh receptor aggregates at early stages, but is necessary for their maturation (Lin et al., 2001). Further players in synaptic differentiation at NMJs are neuregulin, which promotes transcription of synaptic proteins, including Ach receptors, and Neural-CAM, a cell-adhesion molecule (not neuron-specific even though termed “neural”) that seems to be required for presynaptic maturation (Polo-Parada et al., 2001).

1.2.1.1. Pre- and post-synaptic differentiation at glutamatergic synapses

In contrast to the formation of NMJs in the periphery, synapse formation in the CNS is less well understood, and most data about potential mechanisms involved come mainly from *in vitro* studies. Whether and how these mechanisms contribute to synaptogenesis *in vivo* is not yet clear.

Presynaptic sites are assembled from active zone precursor vesicles that upon fusion with the presynaptic plasma membrane lead to the rapid formation of new active zones (Ziv and Garner, 2001). The exact location of docking and fusion seem to be defined by large scaffold proteins like the presynaptic protein Piccolo and Bassoon (Garner et al., 2000). At present, it is not known how the different vesicle types are involved in presynaptic assembly, but these vesicles seem to carry numerous components of the presynaptic active zone (Ahmari et al., 2000; Zhai et al., 2001). Potential inducers of presynaptic differentiation are Narp (neuronal activity-regulated pentraxin), EphB receptors and syndecan.

In contrast to presynaptic sites, postsynaptic sites seem to be assembled in situ, in an ordered and sequential manner, from individual elements or distinct classes of vesicular intermediates that carry only limited types of postsynaptic proteins. This point is well illustrated considering that even different subunits of the same receptor type differ in their dynamics of insertion in the postsynaptic membrane and in their dependence on synaptic activity for insertion. An important role in postsynaptic assembly is played by scaffold or adaptor molecules like PSD95, PICK, Stargazin, proSAP1. These proteins have multiple binding sites for both glutamate receptors and additional scaffold and cytoskeletal proteins and thus they might be important for clustering and stabilizing receptors at postsynaptic locations.

Once formed, synapses are characterised by a certain capacity for remodelling as well documented for postsynaptic spines.

1.2.2. Spine dynamics as an example of synapse remodelling

Dendritic spines are the primary targets of excitatory transmission in the mature brain. They are sub-cellular compartments protruding from the dendritic shaft, and contain high concentrations of actin filaments (Matus et al., 1982), which are oriented longitudinally in the neck and form a dense network in the head (reviewed by (Harris, 1999a)). Spines have remarkably diverse structures even on the same dendritic segment. Differences in spine structure can be important for spatially restricting calcium signals and biochemical cascades, or for modulating synaptic response properties (Majewska et al., 2000). Thus, due to the specific

morphology of spines (narrow necks), even a relatively low rise in [Ca^{2+}] is locally restricted and can reach substantially high levels. This may decrease the threshold for triggering calcium-mediated signalling specifically in the spine and lead to short- or long-term synaptic plasticity (Malenka and Nicoll, 1999). Furthermore, limiting the spread of calcium may provide input specificity (Yuste and Denk, 1995), and protect dendritic shaft and soma, which are especially sensitive to calcium-induced excitotoxicity.

The entry of Ca^{2+} through activated NMDA receptor channels, and Ca^{2+} release from intracellular stores in dendritic spines are critical factors in determining whether maintenance, growth or spine retraction occur (Harris, 1999b; Luscher et al., 2000). Dendritic spines are highly variable in both number and shape on time scales ranging from seconds to days. Regulation of the actin cytoskeleton is fundamental to spine motility. It does not only induce changes in receptor distribution (mainly AMPA-R, (Zhou et al., 2001)), but also alters the morphology of the spine itself. Thus spontaneous spine motility over seconds is actin-dynamic dependent (Fischer et al., 1998) and is blocked by volatile anesthetics and by low concentrations of AMPA (Kaech et al., 1999; Fischer et al., 2000). It is also developmentally regulated as it decreases dramatically during the first postnatal weeks in vitro (Dunaevsky et al., 1999). The fragile-X mental retardation protein, FMRP, is thought to regulate Rac 1 (a member of the Rho family of GTPases, which are central actin organization regulators) function, and in fact the knockout of FMRP results in defects in the maturation and pruning of synapses during development and adulthood (Comery et al., 1997). LIMK-1 (Meng et al., 2002), Ca2+ via Ras, Rap or MAPK (Zhu et al., 2002), PSD proteins like SPAR, spinophilin, kalirin and shank (Naisbitt et al., 1999; Pak et al., 2001; Penzes et al., 2001) are further important players in regulating actin cytoskeleton and thus spine dynamics.

Pathological conditions can also change spines. Loss of spines can be due to epileptic seizures both in humans (Isokawa and Levesque, 1991), and in animal models (Drakew et al., 1996). Spine loss in the hippocampus may involve NMDA-R-mediated excitotoxic effects caused by strong synaptic activation. It can also be due to partial deafferentiation of pyramidal cells due to death of their afferents and loss of spines has been reported after sensory deprivation or lesions of synaptic afferents in rats (Valverde, 1971). These phenomena can be mimicked in vitro in hippocampal slice cultures (McKinney et al., 1999). Blockade of AMPA receptors or treatment with Bot-A (but not with TTX) induced loss of spines on pyramidal neurons, suggesting that deafferentiation causes loss of spines because the postsynaptic side cannot sense presynaptically released quanta of glutamate. The signalling pathways that translate

changes in AMPA or NMDA receptor activation into a change in dendritic spine configuration are unknown. Finally, numerous studies have attempted to correlate LTP with changes in spine morphology (Fifkova and Anderson, 1981; Desmond and Levy, 1988) (Geinisman et al., 1991), and dendritic spine growth (Engert and Bonhoeffer, 1999; Maletic-Savatic et al., 1999), associated with synapses (Toni et al., 1999) has been reported in response to hebbian changes in synaptic efficacy in vitro.

1.2.3. Synaptic stability

Once synapses are formed, very little is known about their maintenance and modifications. The recent evidence that neurons continue to be generated in adulthood suggests that synaptogenesis must continue in the adult brain. Although in the PNS the accessibility of junctions has allowed studies over long periods of time in living animals (Lichtman et al., 1987; Herrera et al., 1990), it is not clear whether CNS synapses are stable over a lifetime. In the late 80s, pioneering experiments were made to follow terminals on central parasympathetic ganglion cell soma in living mice. These experiments revealed extensive remodelling of terminal organization on the surface of these cells over periods of weeks (Purves et al., 1987).

Synapse turnover is known to occur in the adult rat hippocampus across the estrous cycle (Woolley, 1999) when spine density fluctuates by 22-45 % over the course of a few days. Similar transient increases in spine density can be induced by estradiol and progesterone in ovariectomized animals. Interestingly, the new spines are selectively arranged in multiple synapse boutons, indicating formation of new postsynaptic elements on pre-existing presynaptic sites (Woolley et al., 1996). Moreover the effects are dependent on the action of NMDA receptors (Woolley and McEwen, 1994).

Spine density also decreases naturally during normal aging (Bondareff and Geinisman, 1976). Two recent studies (see also subsection 1.1.1.1) analysed the issue of synaptic stability in adult brains, through a direct approach. Both groups followed GFP-labelled spines in the barrel and visual cortex of living mice (> two month-old), for periods of up to several months with the aid of two-photon microscopy. Although they reached somewhat different conclusions they both detected structural spine plasticity in adult animals. Grutzendler et al. found, that 20 % of spines were either added or eliminated over a four-month period in the visual cortex, whereas Trachtenberg et al. found a value of 40 % dynamic spines over a 8-day period in the barrel cortex. In both cases such numbers are not negligible indicating that adult neural circuits continuously remodel. The results seem to suggest that the size of the spines is a measure of

their stability. Thus, large spines appeared to be more stable (up to months or years) than small (thin or filopodia-like) spines (characterised by rapid disappearance or appearance events) in adult cortical circuits. The molecular mechanisms for these differences are not known. A potential candidate to regulate spine formation in mature networks is BDNF. Consistent with this possibility, TrkB signalling seems to be important for regulating spine number and their morphology in cerebellar cortex (Shimada et al., 1998), and BDNF can act as a dendritic morphogen (Horch et al., 1999).

1.3. A model system for studying mechanisms of plasticity: the hippocampus

1.3.1. Memory processing and the hippocampus

The hippocampus is an ideal system to study the relation between circuitry and brain function because of its importance for memory processing, the amount of information known, and the tools available (especially animal models, electrophysiological and imaging techniques). Hippocampal damage in experimental animals or amnesic patients leads to two devastating consequences: loss of the ability to form new declarative memories (anterograde amnesia) and a loss of recently formed memories (retrograde amnesia). Thus, the hippocampus is necessary for the brain to convert short-term memory into long-lasting memory, a crucial process known as memory consolidation. Hippocampal function can also be characterised as a cognitive map theory (O'Keefe, 1979), according to which the hippocampus of rats and other animals represents their environment, locations within those environments, and their contents, thus providing the basis for spatial memory and navigation. In humans, the right hippocampus is viewed as encoding spatial relationships and the left part is rather associated with verbal or narrative memories (Frisk and Milner, 1990). Moreover, the temporal information derived from the frontal lobes that is needed for a spatio-temporal contextual or episodic memory system is also thought to reside in the hippocampus. In fact, it is clear that even within memory, the role of the hippocampal region is selective both to a particular time window (after you learn you need the hippocampus only temporarily) and a particular aspect of memory processing (Bontempi et al., 1999; Teng and Squire, 1999). For example, immediate memory, the ability to repeat or recognize items just brought into consciousness, is intact in patients with damage to the hippocampal region (Squire et al., 1993), as are other cognitive functions. It seems that there are several memory systems in the brain: the neostriatum and cerebellum mediate procedural memory, the acquisition of motor skills and habits. A system that includes the amygdala mediates emotional learning and modulates the strength and consolidation of memories in other memory systems. Cortical regions are critical in short-term working memory, in the recognition of recently experienced stimuli, as well as in long-term declarative memory (Eichenbaum, 2000). A key principle that defines the role of the hippocampus in memory is the linkage of episodic memories through their common events and places, to link related recollections and thus to solve new problems.

The discovery of LTP marked the beginning for the exploration of memory at the molecular and cellular level (Bliss and Collingridge, 1993). The role of NMDA receptor dependent

synaptic plasticity in learning and memory has been explored using both second (region specific) and third generation (region-specific and inducible) gene-knockout techniques. For example, these sophisticated experiments show that the CA1-hippocampal NMDA receptor is required for the formation of hippocampus-dependent spatial and non-spatial memories (Tsien et al., 1996), (Rampon et al., 2000; Shimizu et al., 2000). In contrast CA3-NMDA receptors are dispensable for memory formation and retrieval but seem to be necessary for the reconstruction of spatial maps using previously stored memories (that is CA3 NMDA receptors are necessary for the association of events and places) (Nakazawa et al., 2002). For a long time it has been thought that the mechanism that allows the hippocampus to consolidate and process memories ultimately uses structural changes in synapses. However, since synaptic structures and synaptic receptors are not stationary in the brain, but continuously turn over, and since the time window in which consolidation of memory is thought to occur is too large (weeks in rodents and years in humans), consolidation probably does not involve a single molecular cascade. The evidence that inducible knockout of the CA1-NMDA receptor during the fourth week after training (but not soon after training) had no effect on the retrieval or storage of memory (Shimizu et al., 2000) suggests the existence of alternative mechanisms. For example, memory consolidation could require multiple rounds of NMDA receptor-dependent synaptic modification to reinforce the synaptic changes initiated during memory acquisition (a process called synaptic re-entry reinforcement or SRR). Without such reinforcement single memories would be lost due to synaptic decay. Of course, not all memories would have the same likelihood of being reactivated and consolidated. Preference would be given to particular memories important for the animal.

Moreover, by providing a coherent input, the hippocampus would induce reinforcement of synaptic connections between cortical neurons, via cortical SRR. In other words, the hippocampus would act as a coincidence-regenerator for the coordinated reactivation of cortical neurons leading to a strengthening of their connections.

According to this model conscious recall or sleep could trigger SRR (for a role of sleep in memory consolidation see review by (Siegel, 2001). Finally, it is intriguing to note that in this context, adult dentate granule cell neurogenesis could serve as a means to extinguish outdated memories that would otherwise overload the system.

1.3.2. Main areas and connectivity of the hippocampus

The hippocampal formation comprises four relatively simple cortical regions. These include the dentate gyrus (DG), the hippocampus proper (which can be divided into three sub-fields, namely CA3, CA2 and CA1), the subicular complex and the entorhinal cortex (Amaral and Witter, 1989).

The hippocampus and DG appear as an elongated structure medially in the temporal horn of the lateral ventricle, produced by the invagination of the ventricular wall by the hippocampal sulcus (Figure 1). They belong to the allocortex and have a simplified laminar pattern compared with the neocortex.

Two aspects of hippocampal connectivity are crucial for its functional role: the presence of extensive two-way connections with various cortical association areas, and of the direct and indirect connections with other limbic structures such as the cingulate gyrus and septal nuclei. The predominant afferent inputs to the hippocampus arise in the entorhinal area. The fields in the hippocampal formation are linked by unique and largely unidirectional connections. Neurons in the entorhinal area send their axons forming the so-called perforant path, to the hippocampus, where many end in the DG (but also to pyramidal cells). The axons of the granule cells of the DG (the mossy fibers (MF)), end primarily on the apical dendrites of the pyramidal cells in CA3. CA3 pyramidal cells send Schaffer collaterals to the apical dendrites of CA1 pyramids, and also extensive collaterals that terminate within CA3. From area CA1 a significant part of the information goes to the subiculum, and from there to the entorhinal cortex, thus closing the circuit. The entorhinal area receives afferents from nearby areas in the temporal lobe, and more distant cortical areas. All are association areas (that is not primary sensory or motor regions), which integrate various kinds of sensory information. Further afferents come from the septal nuclei (acetylcholine), monoaminergic cell groups in the brain stem, raphe nuclei (serotonin), and the locus coeruleus (norepinephrine). These modulatory pathways appear to control the firing rate of hippocampal cells (together with various kinds of interneurons, notably GABA-ergic basket cells that inhibit the pyramidal cells) in response to specific information from the entorhinal area. These may be related to degrees of attention and motivation, which we know have a profound influence on both learning and memory.

Efferents of the hippocampal formation are directed via the subiculum towards association area of the temporal and frontal lobes and towards the cyngulate gyrus via the mammilary bodies and the anterior thalamic nucleus. These pathways are topographically arranged, so that regions of the subiculum project to different areas according to their relative position.

Finally a large number of commissural fibers connect the hippocampus of the two brain sides, mediating a close cooperation between them.

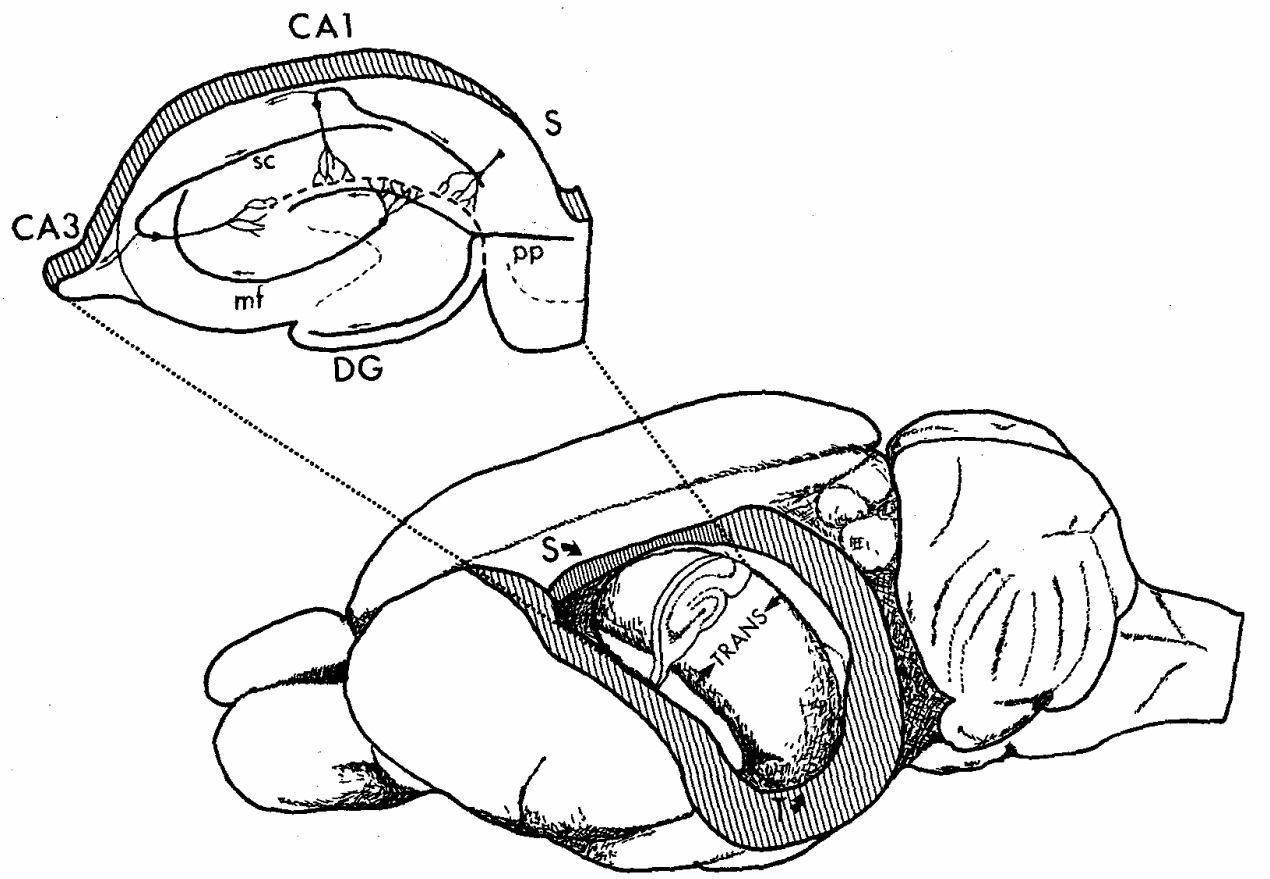

Figure 1: The position of the hippocampal formation in the rat brain is shown in this drawing of a preparation in which the cortical surface overlying the hippocampus has been removed. The hippocampus is an elongated, C-shaped structure with the long or septotemporal axis running from the septal nuclei rostrally (S) to the temporal cortex (T) ventrocaudally. The short or tansverse axis (TRANS) is oriented perpendicular to the septotemporal axis. The major fields of the hippocampal formation (except for the entorhinal cortex) are found in slices taken approximately midway along the septotemoral axis. The slice pictured at top left is a representation of the summary of the major neuronal elements and intrinsic connections of the hippocampal formation. Abbreviations: DG, dentate gyrus; mf, mossy fibers; pp, perforant path; sc, schaffer collaterals. From Amaral and Witter 1989.

1.3.3. The mossy fiber pathway

The term “mossy fiber” (MF) was first used by Cajal (Cajal, 1911) to describe fibers in Golgi preparations of the hippocampus that anatomically resembled the fibers found in the cerebellum. The large varicosities and filamentous extensions of the cerebellar and hippocampal MFs are reminiscent of moss and thus suggested the name of these structures. However it was Golgi (1886) who discovered that the mossy fibers are the axons of the dentate granule cells (GC) and that they form an extensive collateral plexus in the hilus before passing into the CA3 region. In rats, each of the approximately 1 million GCs (approximately 15 million in humans) gives rise to a single unmyelinated MF axon that leaves the hilus to travel through area CA3 in a narrow band called the stratum lucidum. For most of its course through area CA3, the MF pathway can be considered the only true lamellar fiber system of the hippocampal formation because it shows only a limited degree of septo-temporal divergence. However, the MF pathway does make a significant longitudinal projection in the temporal direction (1-2 mm) once it reaches the border of CA1 (Amaral and Witter, 1989). Pyramidal cells in rodent area CA3c also receive a limited MF projection to the proximal basilar dendrites that is referred to as the infrapyramidal projection. The extent of the infrapyramidal projection varies across species and even across strains within species, and seems to correlate with the animal performance in spatial tasks (Blackstad et al., 1970; Schwegler and Crusio, 1995).

The dentate granule cells have a unique mode of generation. All telencenphalic neurons, with the exception of the dentate granule cells, are formed in either the ventricular zone lining the lateral ventricles or in the overlying subventricular zone. Both zones are relatively far away from the sites where the mature neurons are found. The majority of the granule cells, however, are formed closer to the sites they occupy when they are mature. Only a few of them are derived directly from the ventricular zone. In the rat the dentate ventricular zone is active between embryonic days 14 ad 17. Before the cessation of mitotic activity in the ventricular zone neuroblast and glioblast migrate from the dentate ventricular zone into the area of the future hilus where the cells establish a secondary proliferative zone referred to as displaced subventricular zone (Gaarskjaer, 1986). Granule cell development varies according to species: for example in the monkey, at least 80% of granule cells in the dentate gyrus are generated before birth, whereas only 15% of dentate granule neurons in the rat are born prenatally. The vast majority of granule cells are generated during the first 3 weeks after birth in the rat and few continue to be added at a slower rate through the first year of life (Rihn and Claiborne, 1990). The temporal sequence of MF growth clearly reflects the pattern of granule cell

neurogenesis. From the level at which they originate, the fibers diverge along the septo-temporal axis in such a way that the oldest GCs have the most extensive projections. MFs form synapses with excitatory and inhibitory cells of the hilus and area CA3. In the hilus the majority of synapses are with inhibitory interneurons and only a minority with excitatory mossy cells (140 versus 10 synapses of a single GC axon). In CA3 each MF provides 11-18 synapses with CA3 pyramidal cells (at specialised multispine complexes called thorny excrescences). The MF projection to CA3 also provides a strong innervation of all types of interneurons that have dendrites in the stratum lucidum. These comprise both spiny and aspiny interneurons. Thus activation of the MF pathway may cause a net inhibition of the hippocampal CA3 network. But to determine the extent of this inhibition it would be critical to know whether or not interneurons activated by a given MF make synaptic contacts on pyramidal cells that also receive (excitatory) input from the same MF axon.

In electrophysiological terms, to understand the role of the MF pathway, one would need to know by how much the firing rate of a given postsynaptic cell (e.g. CA3 pyramidal neuron) would change, for a given change in the average firing rate of a population of presynaptic cells (such as dentate granule cells). Anatomical and physiological considerations suggest that the perforant path provides by far the most input. In fact there are about 41 thorny excrescences/CA3 pyramidal neuron. From the elegant three-dimensional reconstructions of Chicurel and Harris (1992) and Acsady et al., (1998) we know that most single excrescence are contacted by just one mossy fiber bouton; moreover a single mossy fiber bouton innervates only a single pyramidal neuron (Chicurel and Harris, 1992). Thus, roughly 50 granule neurons could synapse onto a single CA3 pyramidal neuron (in contrast to e.g. single CA1 pyramidal neurons that may be contacted by as much as 13,750 CA3 pyramidal neurons from each side). This is to be compared to 4,000 perforant path synapses and 12,000 synapses from collateral axons that represent a much greater input to CA3 pyramidal neurons (Amaral et al., 1990). Even though the mean amplitude of unitary MF excitatory postsynaptic currents (EPSCs) recorded in CA3 pyramidal cell bodies is about 10-fold larger than that of collateral synapses, it seems reasonable that the MF pathway as a whole is expected to play a small role in the overall activity of CA3 pyramidal cells. Given also the relatively low and variable GC firing rate under normal conditions in vivo, it was proposed that one possible role of the MF input is to shift the function of the CA3 network (Urban et al., 2001). The MF pathway is distinct from other pathways in the hippocampus also because LTP induction is independent of NMDA receptor activation. The involvement of mGluRs, which interestingly appear to be differentially

expressed at MF presynaptic terminals (Shigemoto et al., 1997), instead, seems to be similar to their involvement at other hippocampal synapses. In fact, as in Schaffer and perforant path synapses, LTP induction is blocked by an antagonist of a novel mGluR (Bashir et al., 1993). LTD of synaptic transmission at MF synapses is mGluR2-dependent and involves a presynaptic decrease of both cAMP and PKA activity (Tzounopoulos et al., 1998).

1.3.4. A model for studying the hippocampus in vitro: the hippocampal slice culture technique

Questions related to the neurobiological basis of learning and memory made the hippocampus one of the most extensively studied areas of the mammalian brain. In particular, the investigation of the cellular mechanisms involved, requires a preparation in which detailed observation and manipulation of the basic anatomical, electrophysiological and pharmacological features are possible.

The acute slice preparation of the adult rat (Skrede and Westgaard, 1971), and cultures of dissociated cells of the embryonic hippocampus (Banker and Cowan, 1977) are commonly used in vitro preparations for physiological, developmental, and pharmacological studies. The prominent advantage of acute slices is that they retain the original cellular and connective organization of the hippocampus. Unfortunately, their short survival time in vitro, and the difficulty in identifying healthy cells and processes represent a limitation of this preparation. In contrast, in dissociated cell cultures, individual cells can be readily identified; however the separation of the cells leads to an artificial neuronal network that lacks the typical structural features of intact hippocampus. Organotypic slice cultures combine a number of advantages of the previously described systems. The intrinsic circuitry and cell types of the hippocampal formation are conserved, and the network matures to a large extent thus enabling developmental studies. The wiring of connections is of course changed in the layers normally dominated by extrinsic afferents like the perforant pathways, but synapses formed in response to their absence are most likely abnormal only with regard to location and number, just like the synapses formed after denervation of the layers in the brain (Zimmer and Gahwiler, 1984). Moreover these preparations persist for weeks in vitro, thus allowing long-term manipulations.

1.4. Starting point and goal of the thesis

Structural changes at the synaptic level in adult brains are at present the most widely accepted mechanism to explain behavioural processes such as long-term learning and memory. Mainly due to intrinsic difficulties in studying pre-synaptic contributions, most attempts have focused so far on demonstrating activity-dependent changes at post-synaptic sites. Thus axonal dynamics of mature Central Nervous System neurons have not been studied extensively, and nothing was known about the stability of presynaptic terminals before this study. This issue, however, is important because it will tell us more about the extent and modes of structural plasticity in the brain and thus more about cellular and molecular principles underlying learning and memory.

The goal of the thesis has been to investigate the relationship between anatomical rearrangements of axons, and in particular of pre-synaptic terminals, and synaptic activity. The expectation was that to study the activity-dependency of structural changes, if any existed, would provide potential indications about their physiological relevance. We tried to answer the following fundamental questions: 1) Do pre-synaptic terminals rearrange in mature networks? 2) If so over which time scale? 3) By which mechanisms?. These studies are reported in section (2.2).

To label and thus visualize axons and pre-synaptic terminals, we generated transgenic mice over-expressing different types and combinations of GFP-fusion proteins, specifically in subsets of neurons in the adult mouse. The careful characterization of this tool in various experimental settings was one of the first important aims in this PhD work. This was necessary not only to validate the use of the mice for our study, but also to demonstrate their significant advantages compared to previous technology, and their possible general usefulness in many other fields of neurobiology. The section (2.1) provides an account of these efforts.

2. RESULTS

2.1. High Resolution Visualization of Synaptic Morphology and Dynamics in Transgenic Mice Expressing GFP-Fusion Proteins In Single Neurons

[1]Vincenzo De Paola, [1]Anirban Sadhu, [1]Katri Pajusola, [1]San Pun, [1]Lan Xu, [2]Silvia Arber [3]R.A. McKinney and [1]Pico Caroni

To be submitted as *Neurotechnique*

[1]Friedrich Miescher Institut
Maulbeerstrasse 66, CH-4058 Basel, Switzerland
[2]Friedrich Miescher Institut and Biozentrum University of Basel
Klingelbergstrasse 70, CH-4056 Basel, Switzerland
[3]Brain Research Institute, University of Zurich
Winterthurerstrasse 190, CH-8057 Zurich

2.1.1. SUMMARY

The level at which neurons and their synapses can be visualised in situ has consistently been a critical limiting factor to progress in neuroscience. With the advent of live imaging techniques it has become possible, in principle, to monitor the dynamics of neurons at the subcellular and molecular level. The present challenge is to apply those tools to single, identified neurons in a circuit. Here we generated and characterized targeted-Green Fluorescent Protein (GFP) transgenic mice that allow high resolution imaging of the neuronal membrane, the presynaptic compartment, or both simultaneously in single neurons in the mouse, and used this approach in three experimental paradigms to prove their general usefulness. First, high resolution confocal imaging of dendrites and spines in cytosolic versus membrane-targeted-GFP transgenic tissues shows that cytosolic markers are less suitable than membrane-targeted ones for visualizing the fine details of neuronal structure. Second, using membrane-targeted-GFP mice and live imaging we show that immature hippocampal granule cells in mature networks might use similar mechanisms to developing granule cells, in order to integrate into adult networks. Third, by time-lapse imaging in synaptophysin-targeted-GFP mice, we show that the dynamics of synaptic vesicles at developing NMJs can be followed in real time in living animals

Our results indicate that these genetic tools could be advantageous to gain unique and deeper insights into the fine structure and dynamics of both central nervous system (CNS) and peripheral nervous system (PNS) synapses.

2.1.2. INTRODUCTION

Techniques to visualize neuronal morphology and synapses

To understand fully at the molecular, cellular and circuit level the renowned complexity of the nervous system, both anatomical and functional studies are needed. These approaches may be extremely diverse, depending on the questions and interests that are addressed with the research. Traditionally, researchers, e.g. of neocortical microcircuits, have studied their function and deduced information on their connectivity (Martin, 2002). Recently, *in vitro* slice experiments on microstructure and physiology have provided a greater level of detail in the attempt to relate the structure of circuits to their function. This information is critical for understanding the processes that lead to brain dysfunction. Despite this effort, it is clear that we simply do not know enough about the fine anatomical structure of the mammalian brain. This information would also provide a cellular basis for cognitive processes and behavior. To this end, neuroscientists have developed a variety of techniques to visualize projections and connections of interest. Some of these methods, from the traditional use of staining techniques and dyes to more recent reporter based tracers, are briefly outlined here. A particular emphasis has been given to synaptic labeling techniques that are illuminating our view on the nervous system.

Since the fundamental functional unit of the brain is the synapse, it is not surprising that an important aim was to try to visualize synaptic morphology and plasticity. Synaptic junctions are specialized dynamic structures, sites of extensive changes in response to a variety of stimuli. There are two classes of changes (Bailey and Kandel, 1993): changes in the strength of pre-existing synapses without alterations of interneuronal connectivity ((Tanzi, 1893), for a review see (Martin et al., 2000)) and changes in circuit connectivity due to formation and elimination of synapses (Cajal, 1893, Dailey and Smith, 1996; Darian-Smith and Gilbert, 1994; Engert and Bonhoeffer, 1999; Harris and Woolsey, 1981; Lendvai et al., 2000; Maletic-Savatic et al., 1999; O'Rourke and Fraser, 1990; Purves and Hadley, 1985; Rajan and Cline, 1998; Toni et al., 1999; Wong et al., 2000). This dynamic view of the nervous system is starting to be widely accepted especially now that imaging techniques capable of visualizing synapses in real time are being further developed.

Staining techniques, dyes (FM-dyes), reporter-based methods

Traditionally, ultra structural and immunocytochemical studies gave us a static picture of synapses. Nevertheless, in particular the *Golgi technique* (Golgi, 1873) has had a tremendous impact since its introduction at the beginning of the 20th century and it is still the technique of

choice for investigation of samples that are not amenable for molecular genetic approaches (e.g. human samples). Other methods introduced in the 1970s and 1980s include staining for specific transmitters, or cell-type specific molecules, as well as microinjection of a wide range of anterograde and retrograde tracers (e.g. horseradish peroxidase, biocytin, the cytoplasmic lucifer yellow, etc.) (Callahan et al., 1998). With the advent of fluorescent dyes such as the carbocyanine DiI and DiO, it also became possible to look at neuronal morphology in living tissue, thus allowing the possibility of studying the dynamics of neurons and neuronal processes (Honig and Hume, 1989). One application of this approach is the study of synapse morphology, formation and remodelling at the Neuromuscular Junction (NMJ) using dyes that label organelles concentrated at NMJ (Magrassi et al., 1987) (Balice-Gordon and Lichtman, 1990) and the use of lipophilic dyes (e.g. FM-dyes) to investigate synaptic vesicle (SV) trafficking at NMJ *in vitro* (Betz et al., 1992a) and SV dynamics in cultured neurons (Ahmari et al., 2000; Friedman et al., 2000). FM-dyes are based on the internalization of the compound during membrane recycling and represented the approach of choice to investigate activity-dependent SV dynamics in cultured cells and whole mount preparations for more than a decade. However, although they proved very useful, these techniques have intrinsic limitations. Dye labeling depends on the possibility of identifying and accessing the neurons of interest. For many classes of neurons this is not a feasible task. Some of the dyes present unspecific labeling and background problems and can even interfere with synaptic function (Balice-Gordon, 1997), and, as in the case of FM-dyes, an activity-dependent protocol of staining is necessary.

Since discrete populations of neurons can be defined by patterns of gene expression, reporter-based tracers have greatly increased the ability to label subsets of neurons and their processes. Markers like the *lac*-z product ß-gal have then been used to label specific populations of cells, and in the attempt to label processes a number of ß-gal fusion proteins have been introduced as first attempts in *Drosophila,* and also in mice (Mombaerts et al., 1996).

GFP-based methods

The discovery of Green Fluorescent Protein (GFP) and its variants ten years ago (Chalfie et al., 1994) is leading to a revolution in cell biology allowing the ability to visualize and quantify molecules and events in living cells with high spatial and temporal resolution. One of the major advantages of genetically encoded fluorophores is that they can be fused to virtually any protein of interest and thus allow to study their subcellular localization. To exploit the GFP technology for the study of synaptic morphology and dynamics, ways to deliver the proteins in subsets of neurons have been devised. For example, by particle mediated gene transfer (gene gun) or viral-

based approaches, GFP fusion proteins can be targeted in specific brain areas (Gan et al., 2000; Haas et al., 2001; Lo et al., 1994; Moriyoshi et al., 1996). Unfortunately these methods are labor intensive, difficult to control, often compromise cell viability extensively, and, e.g. in the case of gene gun, do not specifically label neurons (see Supplementary figure 1).

To overcome this, genetic methods to express GFP or GFP fusion proteins in particular sets of neurons are available in model systems like *Drosophila* (Edwards et al., 1997), *zebrafish* (Higashijima et al., 2000), *C. elegans* (Nonet, 1999) and in mouse (van den Pol and Ghosh, 1998). In particular, the use of a neuron specific promoter, the Thy.1 expression cassette (Caroni, 1997) to drive the expression of different spectral variants of cytosolic fluorescent proteins**,** proved to be a valuable tool to study neuronal morphology and dynamics in vivo (Feng et al., 2000; Walsh and Lichtman, 2003); (Grutzendler et al., 2002; Trachtenberg et al., 2002). However, the cytosolic nature of the fluorescent proteins could represent a serious problem when detailed morphological analysis is needed. In fact, small compartments like filopodia and tiny protrusions may be poorly represented, as the fluorescent signal is proportional to the amount of fluorophore that diffuses in a particular neuronal structure. Moreover, a way to monitor in vivo subcellular compartment (e.g. pre-synaptic compartments) dynamics in a non-invasive manner in the mouse is currently lacking. Such a tool would allow imaging of specifically labeled sub-cellular compartments in living mammalian neurons without invasive manipulations.

To address this problem, we generate transgenic mice expressing membrane- and/or synaptic vesicle-targeted spectral variants of GFP in a wide range of subsets of neurons and used this approach in a recent study that focused on presynaptic terminal dynamics in the hippocampus (De Paola et al., 2003). We now provide evidence from three experimental paradigms that this new approach can contribute a great deal to the study of synaptic structure and dynamics, both in the CNS and in the PNS. We thus document here the characterization of these mice in terms of expression patterns, morphology and physiology of expressing neurons. We then prove the potential of the tool in three different contexts.

1) We first compared a cytosolic-GFP (cGFP) tracer with our plasmamembrane-targeted GFP (mGFP) marker in transgenic tissues. We demonstrated that our mGFP marker overcomes the intrinsic limitations of a cytosolic tracer to label entirely small neuronal structures, especially dendritic spines.

2) We studied the dynamics of Synaptic Vesicles (SVs) at NMJs *in vivo*. This is the first report on the long-term behavior of SV clusters in living mice. SV clusters rapidly reorganize their

arrangement in developing NMJs. This molecular dynamism could be involved in presynaptic maturation and/or elimination.

3) Finally, to demonstrate the importance of mGFP mice in the study of axonal plasticity we compared the dynamics of young versus mature hippocampal granule cell processes in the same mature neuronal network. This is the first report on the fine morphological details and dynamics of immature granule cell axons and dendritic spines in a mature network. These data provide evidence that some of the dynamic properties of synaptic structures are intrinsic to the neuron and not a property of the state of maturation of the network.

Thus, targeted-GFP expression in a wide variety of transgenic mouse neurons allows visualizing the neuronal membrane and the presynaptic compartment in a non-invasive manner in both *in vitro* preparations and intact tissues. This may represent a decisive advantage for in vivo studies of both CNS and PNS synaptic junctions.

2.1.3. RESULTS

Generation of transgenic mice

Mice are designated as follows: *Thy1-mGFP* (mGFP) express a plasmamembrane-targeted form of EGFP; *Thy1-spGFP* (spGFP) express synaptophysin-GFP fusion proteins; and *Thy1-mGFP/spRFP* (mGFP/spRFP) co-express plasmamembrane-targeted EGFP and synaptophysin-RFP in the same neurons (**Fig. 1**).

Mice expressing GFP constructs specifically in adult neurons were generated using the mouse Thy1.2 expression cassette, as described (Caroni, 1997). We used two membrane-targeting domains fused to GFP: one consisted of the first 41 amino acids of the protein MARCKS, a plasmalemmal targeting sequence (Wiederkehr et al., 1997), fused to EGFP. The amino-terminal of MARCKS was modified to include palmitoylation sites at residues 3 and 4; the second used the first 41 amino acids of the growth-associated protein GAP43 (Aigner et al., 1995). No difference in cell morphology was found when the two different membrane-targeting domains were used in transfected cell experiments. spGFP or spRFP consisted of full-length synaptophysin fused to EGFP (Li and Murthy, 2001) or RFP (Red Fluorescent Protein). The appropriate localization was initially tested in both fibroblast cell lines (Cos-7 cells), and hippocampal neurons in culture (**Fig**. **1**). As already reported (Moriyoshi et al., 1996) plasmamembrane-targeted GFP does not alter cell morphology and visualizes the whole cell membrane effectively. In contrast EGFP expression alone, diffuses very poorly in cells and in processes of cells in culture (**Fig. 1**). We tested further mGFP, spGFP and spRFP targeting in intact brain and muscle tissues (see later).

We generated 25 transgenic lines expressing a membrane bound form of EGFP (mGFP), 17 expressing a synaptophysin-EGFP (SpGFP) fusion protein and 6 of synaptophysin-RFP/mGFP double transgenics. About 30 % transgenic lines expressed transgene in subsets of neurons (see also reference (Feng et al., 2000)). The relatively high number of lines was needed to be able to reliably select the ones with useful expression patterns (see discussion).

The over expression of the fusion proteins does not cause any detectable phenotype

The transgenic mice had no detectable phenotype, and the expression of these transgenes did not affect neuronal physiology and morphology at the neuromuscular junction (NMJs) synapse. At spGFP-expressing end plates, quantal content (a measure of synaptic function) was not affected (**Fig**. **2**). Moreover, to further characterize the behavior of spGFP clusters we tested their dispersal kinetics upon α-latrotoxin. This toxin stimulates vesicular exocytosis leading to massive neurotransmitter release. Upon α-latrotoxin application, spGFP containing Synaptic Vesicle (SV) clusters converted to a diffuse signal, suggesting that they fused to the membrane and followed the expected localization and dynamics of SVs upon neurotransmitter release (Fig. 2). Paralysis-induced nerve sprouting at NMJs, a phenomenon severely deregulated in mice overexpressing full length GAP43 (Aigner et al., 1995) was within wild type levels in both GAP-GFP, and MARCKS-GFP-expressing nerve terminals (**Fig. 2**). Finally, neurons expressing different levels of the mGFP transgene exhibited undistinguishable morphologies in brain slices (not shown). These data confirm previous reports from the literature that indicate that mGFP and spGFP are suitable markers for the visualization of the neuronal membrane and presynaptic compartments respectively (Callahan et al., 1998; De Paola et al., 2003; Li and Murthy, 2001; Moriyoshi et al., 1996) and validate the use of membrane- and SV-targeted GFP markers in transgenic mice.

Expression patterns in both CNS and PNS

To find useful transgenic lines we characterized the expression patterns of more than 40 different lines. As expected, the Thy.1 promoter drove expression mainly in neurons throughout the nervous system. Moreover, transgene expression at the protein level was occasionally found around blood vessels, and in glia, fibroblast and ependymal cells (not shown).

In situ hybridization and conventional fluorescence microscopy were used to detect transgene expression at the mRNA and protein level respectively (**Fig. 3**). Besides the previously described property of the Thy.1 promoter of driving expression in a characteristic, yet unique, pattern from one line to the other (Caroni, 1997), we report also striking region-specific patterns

that can be exploited with the aid of targeted-GFP markers. For example, in the molecular layer of the DG, no expression, or spGFP specific expression in the Inner or Outer Molecular Layer (IML or OML) were found in L5, L1 and L17 respectively (**Fig. 3a**). This may be exploited in hippocampal lesion paradigms to study Enthorinal Cortex (to OML) or Commissural/Associational (to IML) sprouting at the level of SVs.

Another compelling example of the utility of some expression patterns enabled by the Thy1 promoter is the possibility of using the double transgenic mice (i.e. *Thy1-mGFP/spRFP*) for contemporaneous imaging of pre- and post- synaptic sites. For example in L24 virtually all CA1 hippocampal neurons were positive whereas few pyramidal neurons were labeled in CA3 (**Fig. 3a**). Given the high number of expressing neurons in CA1, spRFP positive single Schaffer collateral axon terminals will have high chance of contacting mGFP-expressing CA1 apical dendrites. This could in turn allow the simultaneous visualization of pre-and post-synaptic sites in *Thy1-mGFP/spRFP* slices. Similarly, in the cerebellum, Purkinje cell broad labeling combined with few granule cells in the same mouse could also allow to study parallel fiber-to-Purkinje cell dendrite synapses in intact preparations of *mGFP/spRFP* mice (**Fig. 3a**).

Furthermore, in the retina of L23 mice, the few horizontal cells enable the visualization of their connections to the more numerous ganglion cells (**Fig. 3a**). Importantly, mGFP expressing single cortical axons are clearly visible in the intact mouse cortex (**Fig. 3b**). Similarly, spGFP positive discrete clusters are detected in intact cortical regions, opening the important possibility of studying their dynamics in living animals (**Fig. 3b,** see later).

Other regions of the Central Nervous System that presented transgene expression comprised main areas like cortex, hippocampus, cerebellum, brain stem, thalamus, all retina layers, and spinal cord but also less characterized nuclei (**Fig. 3**). In the Peripheral Nervous System (PNS) motor neurons and Dorsal Root Ganglia express transgenes with unique patterns in each line (**Fig. 3b**). To find out the percentage of expressing motor neurons in mGFP lines we compared the in situ patterns with cresyl violet staining (a staning protocol that reveals all cell bodies) in the lumbar spinal cord. For example in L5, L14 and L13 80 %, 26 % and 13 % of motor neurons express mGFP, respectively. This pattern was confirmed in a comparison of mGFP labeled axons and α-Bungarotoxin-red-labeled AcChR (Acetyl-choline receptors on muscle) that allowed to gain expression data for specific muscles. In the same mouse, different muscles contained different percentages of labeled motor axons. For example in L14 the diafragm muscle had almost 100 % of labeled terminals, whereas the pectoris muscle about 50 %. Thus independent analysis of the muscle of interest has to be undertaken to find the convenient expression in subpopulation of motor neurons. Finally, we provide two examples of the potential

represented by the *Thy1-mGFP/spRFP* double transgenic mice. First, in the cerebellum, MF glomerular terminals in the granular layer can be easily localized with the mGFP marker and both their morphology and the dynamics of the SVs inside (spRFP positive), eventually studied in whole mount cerebellar preparations from *mGFP/spRFP* mice (**Fig. 3b**). Second, at the NMJ, the expression of spRFP and mGFP in the same motor axon (**Fig. 3c**) should give the possibility of imaging (e.g. in the context of synaptic elimination) NMJ development and plasticity at the simultaneous level of identified terminals and SVs. Thus *Thy1-mGFP/spRFP* mice allow the contemporaneous imaging of the axonal membrane, important to identify the terminal type, and the correspondent SVs.

These data demonstrate the correct targeting of mGFP, spGFP and mGFP/spRFP at the membrane and presynaptic compartment of CNS and PNS neurons in intact neuronal tissues. This opens the possibility that imaging of the neuronal membrane, and more remarkably of presynaptic SVs, can be carried out *in vivo* without any further manipulation other than presenting the synapse to the microscope objective. They additionally provide an important and useful baseline for a wide variety of applications of such transgenic mice.

Examples of potential applications

To prove the usefulness of these transgenic mice for the study of both synapse dynamics and structure we provide here three examples.

1) *Thy1-mGFP*: high resolution imaging of dendritic spine morphology

We first tested the hypothesis that a plasmamembrane-targeted variant of GFP (mGFP) in transgenic tissues might reveal details of fine neuronal structures that appear absent in cytosolic GFP (cGFP, or YFP) variant-expressing cells from transgenic mice (Feng et al., 2000). Since cGFP is starting to be widely used also for the study of central synapses *in vivo* (Grutzendler et al., 2002; Trachtenberg et al., 2002), we studied this important issue in the context of dendritic spine research. First, by quantitative analysis, we report that spine densities and categories in mGFP mice are comparable to those from electron microscopy and other membrane staining techniques data from naïve animals (Richards, D.A., De Paola, V., Caroni, P., Gähwiler, B.H. and McKinney, R.A., (2003a) (**Fig. 4c)**. We then imaged dendritic branches from two of the most intensively studied brain regions: the hippocampus and the cortex. We compared cGFP-expressing neurons (from (Feng et al., 2000)) versus mGFP expressing ones with high resolution confocal microscopy and deconvolution softwares. Representative examples are shown in (**Fig 4 a, b**). At low magnification a major difference is evident: cGFP diffuses in apical pyramidal dendrites but, surprisingly, faintly labels the basal dendrites of CA1 and cortical pyramidal

neurons. mGFP, in contrast, labels both regions uniformly (compare **Fig. 4a A and B**). At higher magnification spines are visible in cGFP expressing neurons but outlines of spines are completely absent, limiting the use of this tool for spine size measurements and subtype classification. For example, all mushroom-shaped spines appeared to have a globular head in cGFP lines (**Fig. 4a a_1-a_4 and 4b a_1-a_3)**. In contrast mGFP expressing spines revealed the typical diverse shapes (including craggy appearances of mushroom-shaped spines) seen from electron microscopic reconstructions and other membrane labeling techniques (Fiala et al., 2002); Richards, D.A., De Paola, V., Caroni, P., Gähwiler, B.H. and McKinney, R.A., (2003a)) and are thus amenable for detailed size measurements and monitoring (**Fig. 4a b_1-b_4 and 4b b_1-b_3)**. Since spine size is closely related to synaptic strength (Nimchinsky et al., 2002) the advantage represented by the mGFP marker for high-resolution analysis of both spine structure and dynamics appears considerable. We noted the greatest difference between the two markers when the complexity of the spine arrangement along dendritic segments was maximal, as in primary dendritic branches. In fact, in these segments, the bright dendritic shaft fluorescence signal literally covers the numerous spines that emerge from the surface of it, thus limiting the use of this tool for high resolution imaging of complex dendritic regions. When the gain is reduced, several protrusions, with far less fluorescence signal than the one coming from the dendritic shaft, are no longer visible in cGFP dendrites. In contrast, under the same conditions, mGFP-labeled complex dendritic regions can still be detected at the level of single filopodia and spines (**Fig. 4b b_1**). To directly test the hypothesis that mGFP labels structures not labeled in cGFP neurons we are in the process of injecting membrane-labeling dyes (DiI) in cGFP expressing neurons. Thus, since mGFP expressing spines seem to reveal the known complex outlines of spine heads and necks, whereas cGFP spines do not, these data show that the cGFP marker is unsuitable for high-resolution confocal imaging of dendritic protrusions and indicate that mGFP could be an appropriate alternative.

2) *Thy1-spGFP*: SV dynamics *in vivo*

Information on the behavior of SVs in living animals is currently lacking primarily due to the fact that there are few possibilities to specifically label them. At present in fact, the closest approximation of in vivo behavior of SVs in mice has been achieved through staining live whole mount muscle preparations with fluorescent dyes (Betz et al., 1992a). Although elegant, this method has some limitations including the need of an activity-dependent protocol for staining that could itself influence SV dynamics, as outlined in the introduction. Information on the dynamics of SVs in unperturbed systems is important. For example, at the NMJ, such

information in living animals could give important insights into the precise defects that characterize motor neuron diseases. Are SVs dynamic in adult nerve terminals? Are SV dynamics perturbed in the diseased NMJ? To date there are no satisfying answers to these questions. We show here that with our approach these questions could begin to be answered. We report the successful *in vivo* repeated observations of SV clusters at developing NMJs using *Thy1-spGFP* transgenics. SV dynamics can be visualized at the level of individual clusters up to months without inducing photo toxicity or bleaching (**Fig. 5**). There are three lines of evidence that indicate that the SpGFP signal reflects the known arrangement of SVs at NMJs. First, in early postnatal stages of development (as early as P4), at low magnification, live spGFP signal was visible as a diffuse signal that outlined the motor axon and the terminal zone. In addition to this diffuse signal, discrete spGFP-containing vesicle pools (VP) with irregular shapes become visible at high resolution and magnification (**Fig. 5 b-d**). At later stages (P20) the spGFP signal was uniformly distributed at the terminal region and discrete puncta were evident at high magnification as more regular clusters both along the motor axon and at the terminal region (**Fig. 5 h**). This arrangement closely resembled the patterns found in different muscle types and in different species with presynaptic and SV markers including FM1-43, synaptophysin, synuclein and 4-di-2-ASP staining (Balice-Gordon and Lichtman, 1990; Betz et al., 1992a; Betz et al., 1992b) (Dekkers, 2001) (Brandon, 2003) (Quattrocchi et al., 2003). Second, although fixation protocols (see methods) lead to aggregation of spGFP signal (not shown), analysis of synaptophysin immunoreactivity in spGFP mice indicates that the vast majority of synaptophysin-containing vesicles are also spGFP positive (> 95%, n = 22 NMJs from 4 different muscles). Third, the data in Fig.2 together with these latter data support the notion that the spGFP signal has essentially a pre-synaptic localization consistent with the known VP arrangements. Repeated observations of SVs from tibial muscles *in vivo,* reveal that SV dynamics can be followed with high resolution using our approach. Discrete clusters reorganized their spatial arrangement over 1 day at living NMJs (n=12) (**Fig. 5 h-i**). We detected putative splitting events, fusion of smaller clusters into bigger ones as well as disappearance or appearance of clusters (**Fig. 5 f-i**).

Finally, it is remarkable to note that the spGFP signal appeared in a punctuate pattern also in the intact cortex and clusters were clearly visible with conventional fluorescence microscopy (**Fig. 3b**). We anticipate that with two-photon microscopy also central SV clusters in deeper cortical layers could be followed *in vivo*. In summary, *Thy1-spGFP* mice allow the study of peripheral as well as central SV dynamics in living animals. Such tool could be advantageous in defining

the properties of mammalian presynaptic compartments (e.g. sorting of synaptic vesicle proteins or trafficking of vesicles to terminals).

3) *Thy1-mGFP*: axonal and dendritic dynamics of immature granule cells

It is a well-established phenomenon that the adult mammalian hippocampus undergoes neurogenesis in the dentate gyrus. The rate of neurogenesis can be influenced by environmental factors. These newly generated GC extend the axon towards CA3, fire Action Potentials (AP) and receive inputs from the perforant path (van Praag et al., 2002). At present little is known about subcellular mechanisms that newly generated neurons employ to integrate in the adult network (Carleton et al., 2003). This knowledge might be important to better define the functional significance of these immature granule cells. At present few methods allow the visualization of new granule cells. These methods are either not suitable for structural analysis in living tissues (e.g. BrdU labeling), or use viral infection (van Praag et al., 2002), a notoriously invasive method. We found that the Thy1.2 expression cassette has the capability to turn on transgene expression in immature granule cells in a fraction of transgenic lines (**Fig. 6**). Anatomical observations suggest that the neurons corresponding to a fraction of imaged axons and dendrites are indeed immature granule cells. Characteristic features of young granule cells include: location in the Dentate Gyrus (DG), granular shape of cell body, simple dendritic arbor (mainly only one basal dendrite), virtually no spines on the dendrite, highly motile filopodia-like spines and highly motile growth cone filopodia at the end of axonal branches (**Fig. 6)**. These features were in sharp contrast with the ones we described for more mature axons and dendrites belonging to mature granule cells in the same hippocampal cell layer (De Paola et al., 2003), thus allowing for unequivocal discrimination of the two cell types (see methods). In summary, in *Thy1-mGFP* expressing slices it is possible to visualize with high resolution the neuronal membrane of young granule cells in a mature hippocampal network. Both the dendritic and axonal compartments with their post- and pre-synaptic structures are clearly visible (**Fig. 6**) thus allowing for the study of their arrangement and dynamics in living neurons and for a comparison with those of mature neurons. We used both hippocampal slice culture preparations and acute whole mount preparations to investigate these issues.

Immature granule cells extended their axons before their dendrites were fully developed, and started axonal branch formation independently of dendritic input (n = 4 granule cells). However, typical MF terminals were not yet present at this stage and probably need dendritic input to form. In contrast, numerous foci of filopodial dynamic protrusive activity (see later) as well as growth cones at their tips were detected along the axon of young granule cells (**Fig. 6**). This

appearance strongly resembled the morphology of developing MF (Dailey et al., 1994) raising the interesting possibility that these axons could use similar mechanisms to developing ones to navigate in a mature network.

To test this possibility further we repeatedly imaged young granule cell axons over days in mature slice cultures. In particular we asked the question of whether the young granule cell axons actually develop (branch, elongate or retract) in slices and if yes by which mechanism. Young granule cell axons elongated in mature hippocampal slices, resulting in a net increase in axonal complexity over 1d. Importantly, this increase was achieved by a subsequent process of extension-retraction likewise developing axons (**Fig. 6**).

One prediction of this scenario is that processes that accompany the development of axons in developing networks characterize also these developing axons in mature networks. For example, it is known that short-term axonal and dendritic dynamics, like rapid extension and retraction of filopodia, mediate axo-dendritic contact and synapse formation during development (Ziv and Garner, 2001) and to a less extent in mature systems (De Paola et al., 2003). To determine which plays a dominant role, the degree of the maturation of the neuronal network or the individual neuron, we compared short-term dendritic and axonal dynamics of young versus mature granule cells in the same *Thy1-mGFP* slices, by time-lapse fluorescent microscopy. Consistent with the notion that young granule cells in mature networks follow a cell autonomous program of maturation, we found that axonal varicosities and filopodia as well as dendritic spines from immature granule cells were more dynamic than mature MF in mature hippocampal slice cultures (Suppl. Videos 4-8). This was true for both the number of events per μm, and for the extent of each event (n = 13 granule cells). Moreover, we were able to demonstrate that young granule cells display similar morphology and behavior with respect to axonal filopodial motility, in intact whole mount preparations (**Fig. 6**). These data support the notion that axonal as well as dendritic STDs are an intrinsic property of the neuron and not a function of the maturity of the neuronal network. They also suggest that these newly born cells might use similar mechanisms to developing granule cells, in order to integrate into adult networks (Ziv and Smith, 1996).

2.1.4. DISCUSSION

The development of imaging techniques enabling the visualization of synapses in real time has recently led to a number of discoveries pointing to an unsuspected plasticity of synapses (for reviews see the “25 Oct 2002” issue of *Science*). We developed targeted-GFP transgenic mice with selective expression in many classes of neurons that could be useful in this context.

We first report the characterization of the expression patterns and targeting of the GFP-fusion proteins in *ex vivo* specimens. The GFP fusion proteins in intact specimens do not appreciably alter neuronal morphology and physiology, in accordance with previous studies predominantly made in dispersed culture systems.

We illustrated the unique applications of this tool with three examples.

We first compared our plasmamembrane-targeted variant of GFP (mGFP) with cGFP in transgenic tissues. The analysis was focused on dendritic spines because these tiny structures are sites of extensive studies given their direct involvement in synaptic communication and information processing. We found that cytosolic forms of GFP are less practical for high resolution imaging of these small protrusions, due to the fact that the fluorescence signal is proportional to the volume of the structure imaged. While cGFP transgenic lines enable relatively large compartments like cell bodies, primary dendritic shafts, or NMJ terminals to be clearly visible, they do not allow the proper visualization of the entire dendritic arbor and of outlines of spines and small protrusions. The information on the outlines of spines is precious. The outlines of spines disclose their enormous diversity and complexity of arrangements that underlie and hold important functional implications (Harris, 1999). Additionally, the ability to visualize the outlines of spines has the advantage of allowing spine shape monitoring over time. The ability to visualize spine shape changes in intact tissues in mGFP mice will encompass an important entry point to tackle the unknowns of spine motility research with particular regard to its functional role in vivo (Bonhoeffer and Yuste, 2002). Our method of visualization in living or fixed tissues enables the visualization of entire (both basal and apical) dendritic arbor including the outlines of complex spine regions (e.g. **Fig. 4b b_3**), thus overcoming the intrinsic limitations of cGFP tracers in neurons of transgenic mice. This method should thus allow *in vivo* imaging of dendritic as well as axonal dynamics with new and striking detail.

To establish the potential of synaptic vesicle targeted-GFP (synaptophysin-GFP, spGFP) and of mGFP/spRFP double transgenic mice, we studied the dynamics of Synaptic Vesicles (SVs) at NMJs *in vivo,* and show the first images of SVs in the mammalian cortex *ex vivo*. We show that the fusion protein is correctly targeted to synapses, and that we can visualize SV dynamics in living animals up to months without inducing photo toxicity or bleaching. What comprises the Vesicle Pool (VP) labeled by spGFP? Careful qualitative and quantitative analysis of hippocampal synapses expressing the marker shows that spGFP labels all SVs, including small active zone precursors known to carry SV membranes (Ahmari et al., 2000; De Paola et al., 2003; Li and Murthy, 2001). At NMJs the patterns of staining reflects the variability in VP arrangement and density known for different motor nerve terminals (Reid et al., 1999).

Moreover, postsynaptic receptors are apposed to spGFP clusters, suggesting that they are involved in terminal function. Finally, in mGFP/spRFP NMJs, RFP is clearly targeted to the terminal active zones by our SV targeting domain (**Fig. 3c**). Thus spXFP is a reliable SV marker at both central and peripheral terminals. When we used this approach to follow SV puncta at living motor neuron terminals we noticed a striking dynamism. At postnatal stages of development, after synapse elimination occurred (e.g. P18), clusters of SVs reorganized by changing their position, splitting or fusing over 1 day observation period. This was true also for sensory innervation known to contain synaptophysin microvesicles (De Camilli et al., 1988) (**Fig. 5 j-m**) suggesting that displacement of SV clusters may serve more general functions in living mammalian terminals. This molecular dynamism could be implicated in the maturation of presynaptic compartment at late postnatal NMJs. However, further experiments on earlier and later stages of development as well as employing mutant mice (e.g. NCAM KO) will clarify the implications of this dynamism for presynaptic function at PNS terminals.

Of note is that the spGFP signal is also detectable in a clear punctuate pattern in intact cortical regions (**Fig. 3b**). With the aid of two-photon microscopy (Denk and Svoboda, 1997) SV clusters could then be followed *in vivo* in deeper cortical areas. This approach could significantly contribute to the rapid elucidation of the plastic properties of presynaptic terminals in living mice (De Paola et al., 2003). Finally, in mGFP/spRFP mice, visualization of synapse (pre- and post- simultaneously) formation/elimination in living specimens could then be possible using lines that have a combination of broad and restricted expression patterns (e.g L24 Fig. 3a).

In summary, SV-targeted-XFP mice allow the study of central as well as peripheral SV dynamics in living animals in a non-invasive manner. We are currently crossing these mice with genetic models for motor neuron diseases (e.g. ALS) with the hope of characterizing the defects in nerve terminal function at this level.

Finally, to show further the applications of mGFP mice we compared the dynamics of young versus mature hippocampal granule cell processes in mature hippocampal tissues. We found that the Thy.1 expression cassette occasionally drives expression in newly born hippocampal granule cells. Thus, these young neurons appear as intermingled to mature granule cells in the same network. Given the expression of these lines in subsets of neurons and the great detail obtained with the mGFP marker, we were able to study the fine morphological details and dynamics of young granule cell processes and to compare them to mature granule cell ones in the same network. The biological function of adult neurogenesis is poorly understood. We began to appreciate the fine morphological details and dynamics of immature granule cell axons and dendritic spines in a mature network. We show that young neurons develop in culture and that

axons and dendrites are characterized by more prominent short-term dynamics than those of mature cells in the same mature network (Fig. 6 and supplementary videos). This is evidence that short-term neuronal process dynamics are a cell autonomous phenomenon. Since young axons elongate in the mature network with features typical of developing axons, these data suggest also that newly born cells might use similar mechanisms to developing granule cells, to integrate into adult networks. Consistent with this hypothesis is the recent report on the development of newly born olfactory neurons in the mouse olfactory bulb (Carleton et al., 2003). It will be important to study the regulation of young axon maturation processes with respect to both identity of guidance cues and roles of activity. We believe that our approach will have great impact in these investigations given the relative simplicity of the system and its ease of manipulation. These data outline the importance of this neuronal marker also for the study of axonal plasticity.

The main limitation of this genetic tool is that the identity of labeled neurons cannot be pre-selected. Several brain areas and subregions are "preferred" by the promoter (e.g. retina ganglion cell layer, all cortical layers, cerebellar GCL and PCL, hippocampal CA1). Yet, in our experience virtually all brain areas would occasionally have some detectable expressing neurons. A careful analysis of expression patterns is then needed to obtain labeled neurons of interest. Our approach promises to be a substantial aid to future research in a wide variety of fields of neurobiology, especially in the area of in vivo imaging of synaptic dynamics where the detail of investigation is crucial. Brain disease research is another context in which axonal and dendritic structure analysis are important. Moreover, the specific targeting of GFP in neuronal compartments of transgenic mice enables Fluorescence Recovery After Photobleaching (FRAP) analysis that could be helpful in investigating membrane as well as SV dynamics (Richards, D.A., De Paola, V., Caroni, P., Gähwiler, B.H. and McKinney, R.A., (2003b).

In conclusion, targeted-GFP expression in adult neurons of transgenic mice allows non-invasive, high resolution molecular imaging of both PNS and CNS synaptic junctions, *in vitro* and *in vivo*. This approach should be helpful in accelerating and deepening our understanding of synaptic development and plasticity at both CNS and PNS synapses.

2.1.5. MATERIALS AND METHODS

Constructs and mice. The first 41 aa of MARCKS and GAP-43 were generated by PCR using human MARCKS and GAP-43. pCDNA3 (clonetech) was the vector chosen to clone the EGFP-fusion proteins and the three different constructs were then cloned in the XhoI site of the linker sequence of a modified Thy1.2 promoter cassette (Evans et al., 1984; Kelley et al., 1994). pcDNA3-IRES-EGFP vector (Invitrogen, 5446 bp) was chosen to clone mGFP and spRFP on the same construct. IRES corresponds to an internal ribosomal entry signal sequence for bicistronic mRNA transcripts expressing mGFP and spRFP. The plasmid containing Thy1.2 expression cassette was cut with NotI and PvuI to remove vector sequences. The resulting constructs were checked by restriction digestion, purified and injected into pronuclei of B6 F1 zygotes according to established procedures (Hogan et al., 1994).

In all steps the EGFP fusion genes and all cloning junctions were checked by DNA sequencing. Transgenic founders were identified by either by fluorescence microscopy or by PCR analysis on mouse tail DNA, using primers EGFPSense (5'-xxxxx-3') and EGFPAntisense (5'-xxxxx-3') specific for EGFP sequences. PCR reactions were performed in 25 µl total volume containing 50 mM Tris-HCl (pH 9.2), 0.1% Tween-20, 0.2 mM dNTP, 2.5 U Taq polimaerase, and 1 µl mouse tail DNA. Mouse tail DNA was prepared by digesting 2–3 mm of mouse tails overnight at 55 ^{0}C with proteinase K (15µl of 10mg/ml stock solution) in TNES (Tris 50mM pH 8, EDTA 100mM, NaCl 36mM, 10% SDS, H2O). After 6' of centrifugation the supernatant was diluted 1:50 in ddH20 and 1µl of this dilution was then used for PCR screening.

The amplification of the DNA was performed in a Perkin Elmer Cetus Thermocycler using the following program: 1 initial cycle of 3 min denaturation at 94º, followed by 33 cycles of 30" at 94ºC, 30" at 58ºC and 40" at 72ºC and a final extension for 5' at 72º.

One transgenic founder was used to generate independent lines by crossing with wild-type animals (B6 males with C57B16 females).

Live imaging. For in vivo imaging of NMJs, animals of age between postnatal day 4 (P4) and 2 month were used. They were anesthetized with either brief (15' at 4 ^{0}C) exposure to cold temperature (for P4-P6 old animals), or a mixture of Rampoon and ketamine (for older animals). The hind limb muscle exposed by dorsal cut. Skin muscles and connective tissue removed to access directly the muscle. Confocal imaging and conventional microscopy were used to study nerve terminal dynamics in vivo. Mice were returned to their cages after suturing the wound with a surgical glue (Vet glue, CH).

Confocal imaging of dendritic spines. Mice (three months old) expressing the cytosolic form of YFP and the membrane tagged form of GFP under the Thy-1 promoter were perfused transcardially according to protocols described elsewhere. Briefly, mice were first perfused with Lactated Ringer's solution (Ringer's solution containing 50% sodium lactate) at 4 ^{o}C and subsequently with a fixative solution containing 4% paraformaldehyde at room temperature. Coronal sections of thickness 40-50 microns were taken in a vibratome.
Confocal images were taken in an Olympus Fluoview system, and deconvolved using the Huygens deconvolution software. Confocal stacks of thickness 0.15 microns were taken throughout the thickness of the dendrite and reconstructed to get the three dimensional view.

Histology, immunocytochemistry, cell culture. Neuromuscular synapses and their innervation patterns were visualized by the silver esterase reaction, as described (Caroni, 1997). Where indicated, purified Botulinum toxin A (Botox, clinical grade, Allergan AG, Lachen, Switzerland) was applied at 0.01 Units per g mouse (1-3 months old). For immunocytochemistry of muscle tissue mice were perfused with 4% paraformaldehyde-containing PBS, and cryostat sections were incubated with antibodies, as described (Caroni, 1997). Paralysis-induced nerve sprouting was analysed as described (Frey et al., 2000). Briefly, 0.01U per g of Botulinum toxin A were injected into one triceps surae, and cryostat sections were analysed with the combined silver esterase reaction 7-14 days after toxin treatment. Sprouting synapses in medial gastrocnemius and soleus were mapped systematically, and the results were displayed as percentages of synapses with sprouts along the synaptic band at a defined position of the muscle (Frey et al., 2000).
α-Bungarotoxin whole mount stainings of neuromuscular synapses were performed as following: freshly dissected medial gastrocnemius was placed into 4 °C L15 Medium (Gibco). After cooling down, the tissue was incubated with RITC α-Bungarotoxin 10-20 μg/ml for 2h on ice. After rinses with L15, the tissue was fixed in 2% parafomaldehyde (PBS) for 12h on ice.

Single fibres were pulled out and embedded for fluorescence microscopy.
Cell lines (monkey kidney epithelial cells COS-7) were obtained from American Type Cell Culture Collection, and cultured in DMEM supplemented with 10% FCS, or 10% horse serum and 5% FCS, respectively. Hippocampal neurons were isolated from newborn (P0-1) mice. Briefly, hippocampi were triturated and cells were washed in Hepes-buffered Hank's medium. Cells were then resuspended in culture medium (Neurobasal (GIBCO), with 0.5mM L-glutamine, 25mM glutamate, and 1% B27 supplement (GIBCO)), and plated at a density of 20'000 cells per 18mm poly-L-lysine coated coverslip.
Hippocampal slice cultures were transfected using the Helios Gene Gun System (Bio-Rad, CA). Plasmid (mGFP) was precipitated onto gold microcarrier particles (1 μm diameter). The DNA loading ratio was 8 μg/mg gold. Culture slices were transfected at 8–20 days in vitro (DIV) and returned to the incubator for 2–6 days post-transfection.

Electrophysiology. EDL or soleus muscles with their nerves were dissected from the mice under metofan anesthesia; subsequently animals were killed by cervical dislocation. Nerve-muscle preparations were pinned out in a Sylgard-coated recording chamber. The nerves were sucked tight into polyethylene stimulating electrodes pulled from polyethylene tubing.
Whole cell patch-clamp pipettes with a resistance of 5-10MΩ were pulled from borosilicate glass and filled with 3mM KCl. For Quantal Content measurement, standard electrophysiology techniques were used to record miniature endplate potentials (mepps) and evoked endplate potential (epps) in a high Mg^{2+} and low Ca^{2+} balanced salt solution (pH 7.4) containing (in mM): 150 NaCl, 5.4 KCl, 12 MgCl, 2 CaCl, 10 HEPES, 13 glucose. For Facilitation and Calcium Sensitivity measurements, evoked Epps (recorded at 1Hz for 1min) alone were recorded in normal balanced salt solution (pH7.4) containing (in mM): 150 NaCl, 5.4 KCl, 2 CaCl, 1 MgCl, 10 HEPES and 13 Glucose. 2.1μM d-Tubocurarine chloride was added to block muscle contraction. The stimulation frequencies for facilitation were 100 Hz for 1 sec.
Endplate potentials were recorded from two to three superficial layers of muscle fibers distributed over the whole muscle surface and single muscle fibers were impaled near the motor end plate. The initial resting potentials were between –65 to –80mV and remained stable throughout the duration of the experiments. EPPs were accepted when rising time was below 2ms. Potentials were recorded via an intracellular amplifier (AxonClamp 2B) and analyzed using digidata 1200 A and Axonscope software (20 kHz sampling rate; Axon instruments).

2.1.6. FIGURES

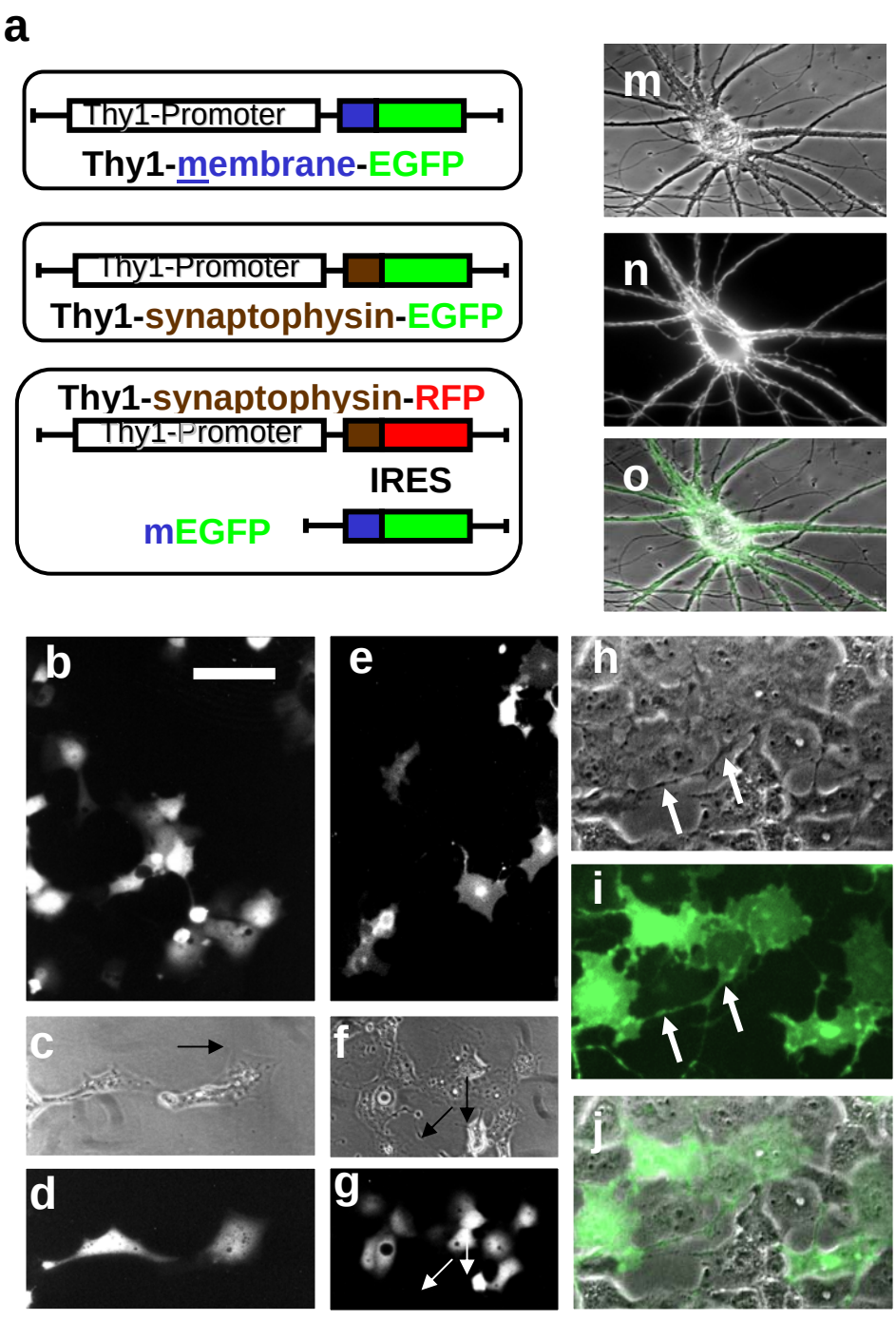

FIGURE 1

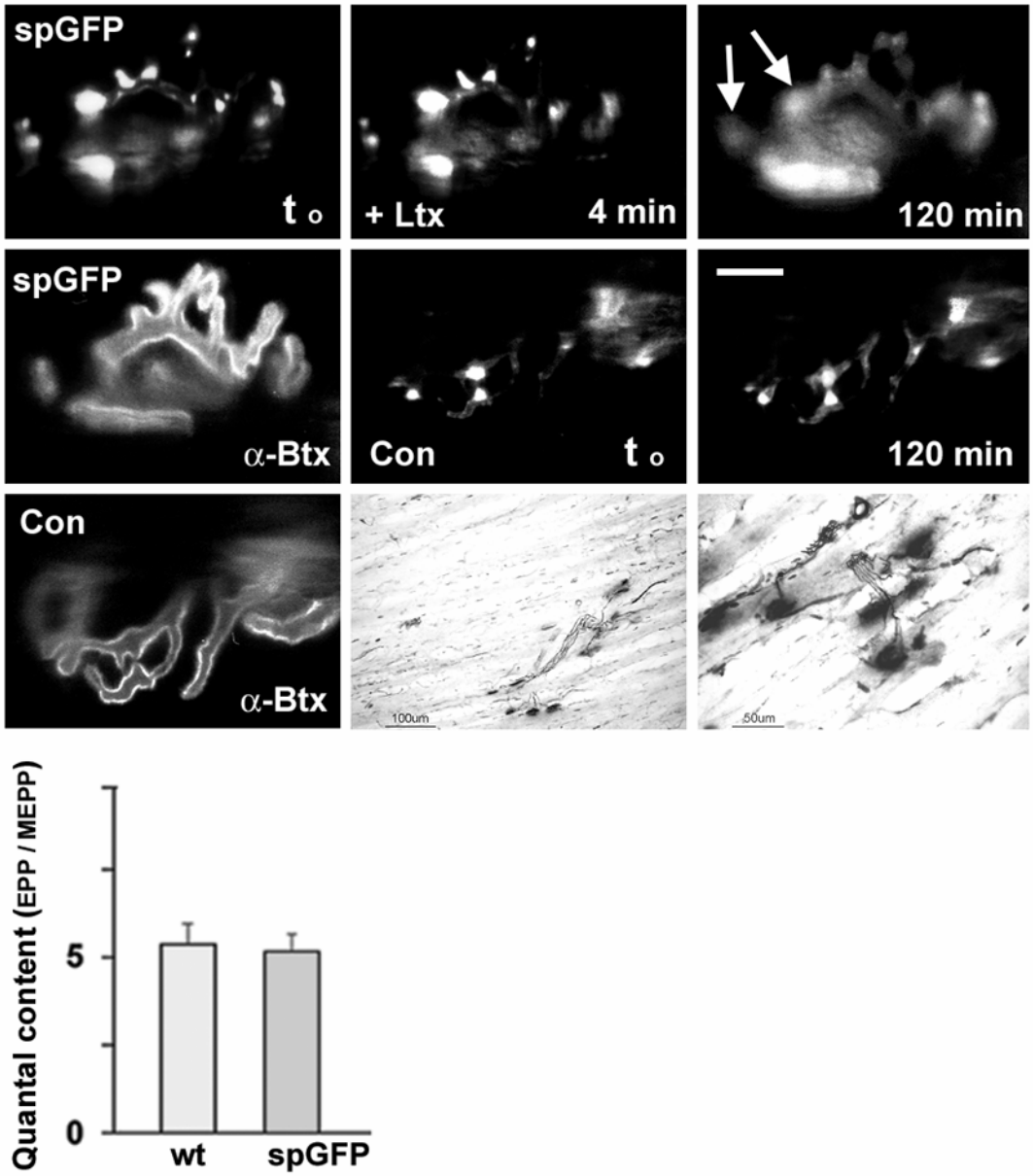
spGFP
t o
+ Ltx
4 min
120 min
spGFP
α-Btx
Con
t o
120 min
Con
α-Btx
100um
50um
Quantal content (EPP / MEPP)
5
0
wt
spGFP

FIGURE 2

a

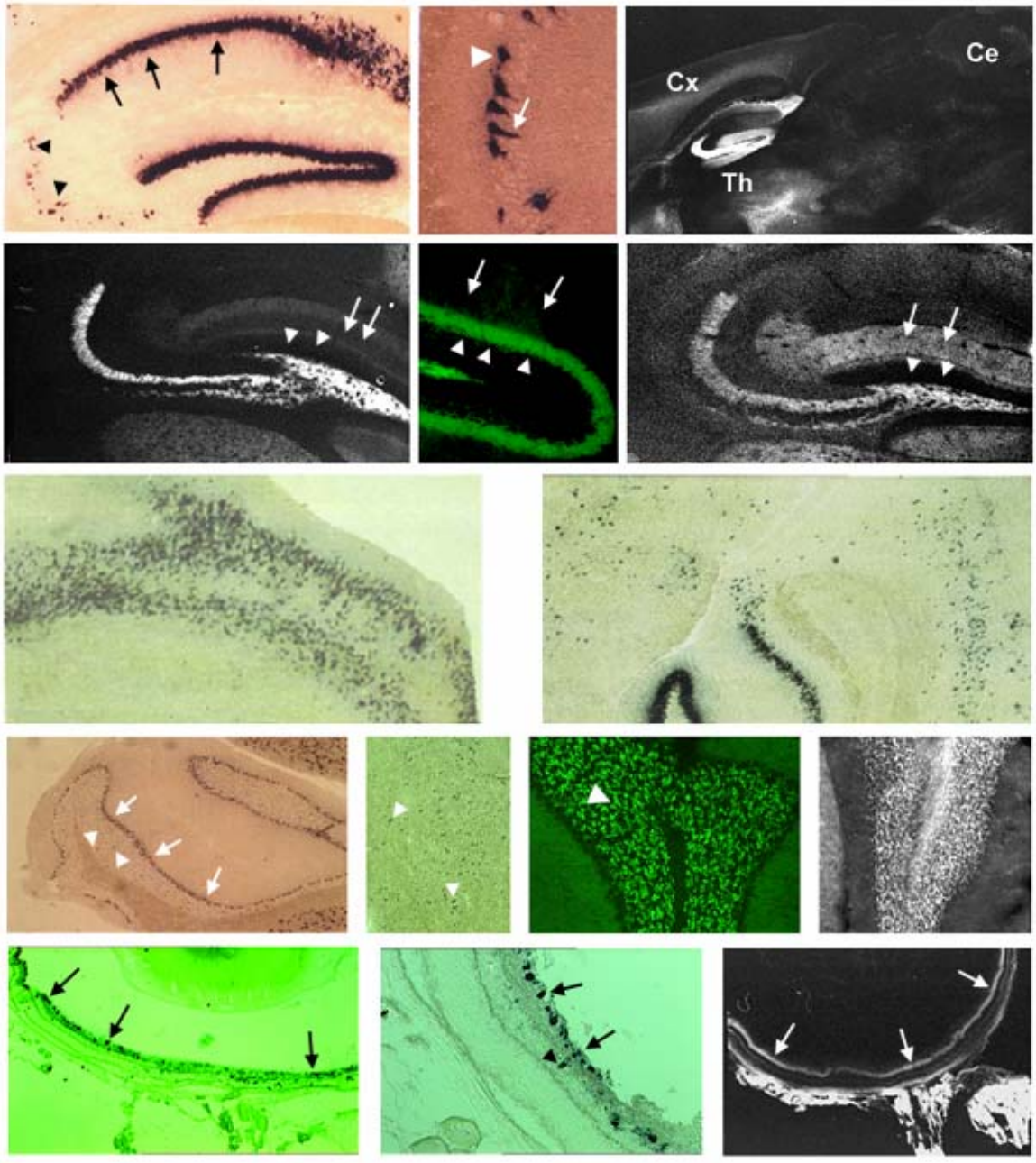

b

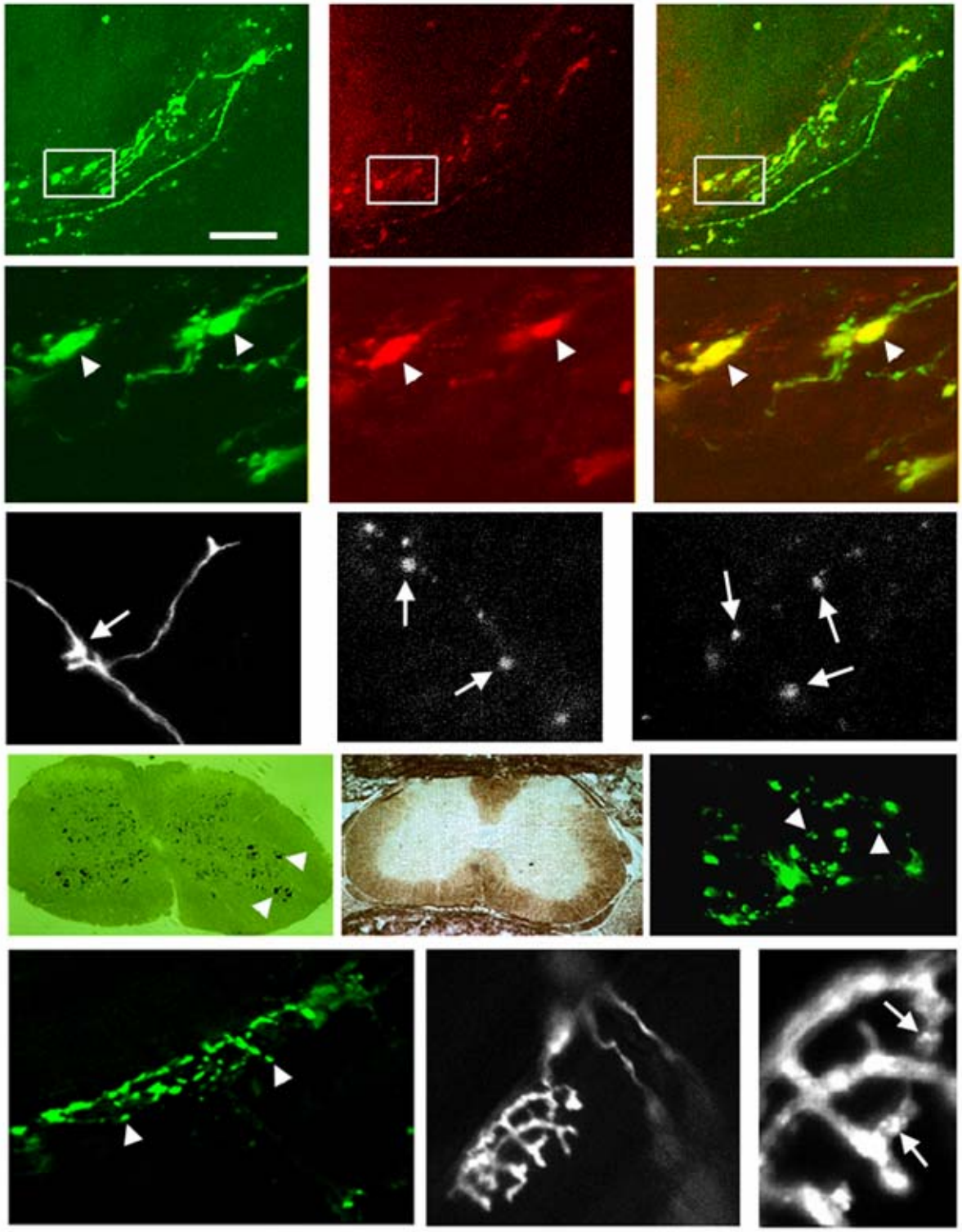

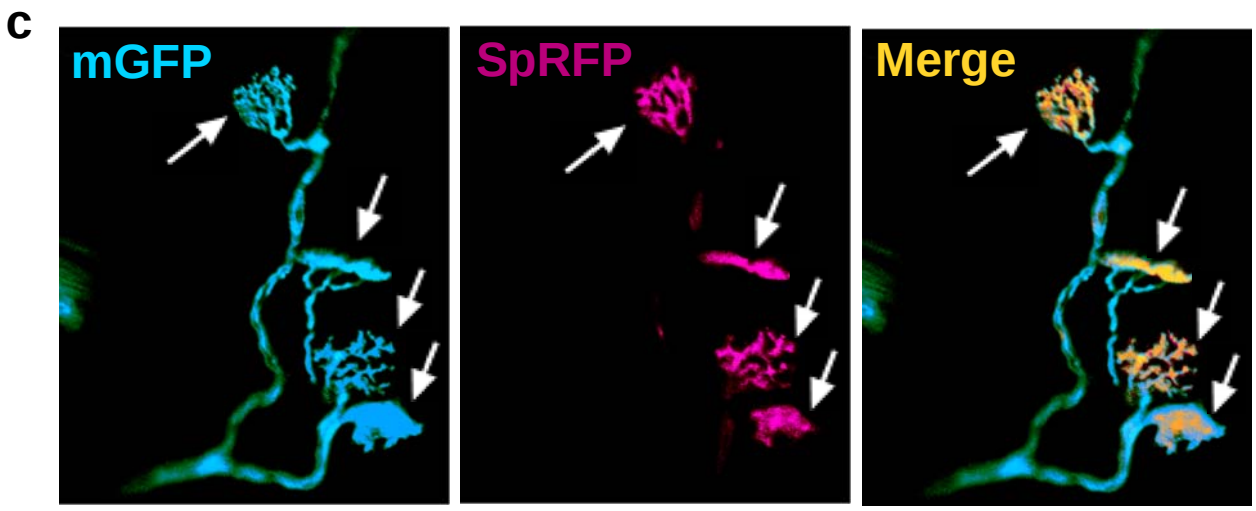

FIGURE 3

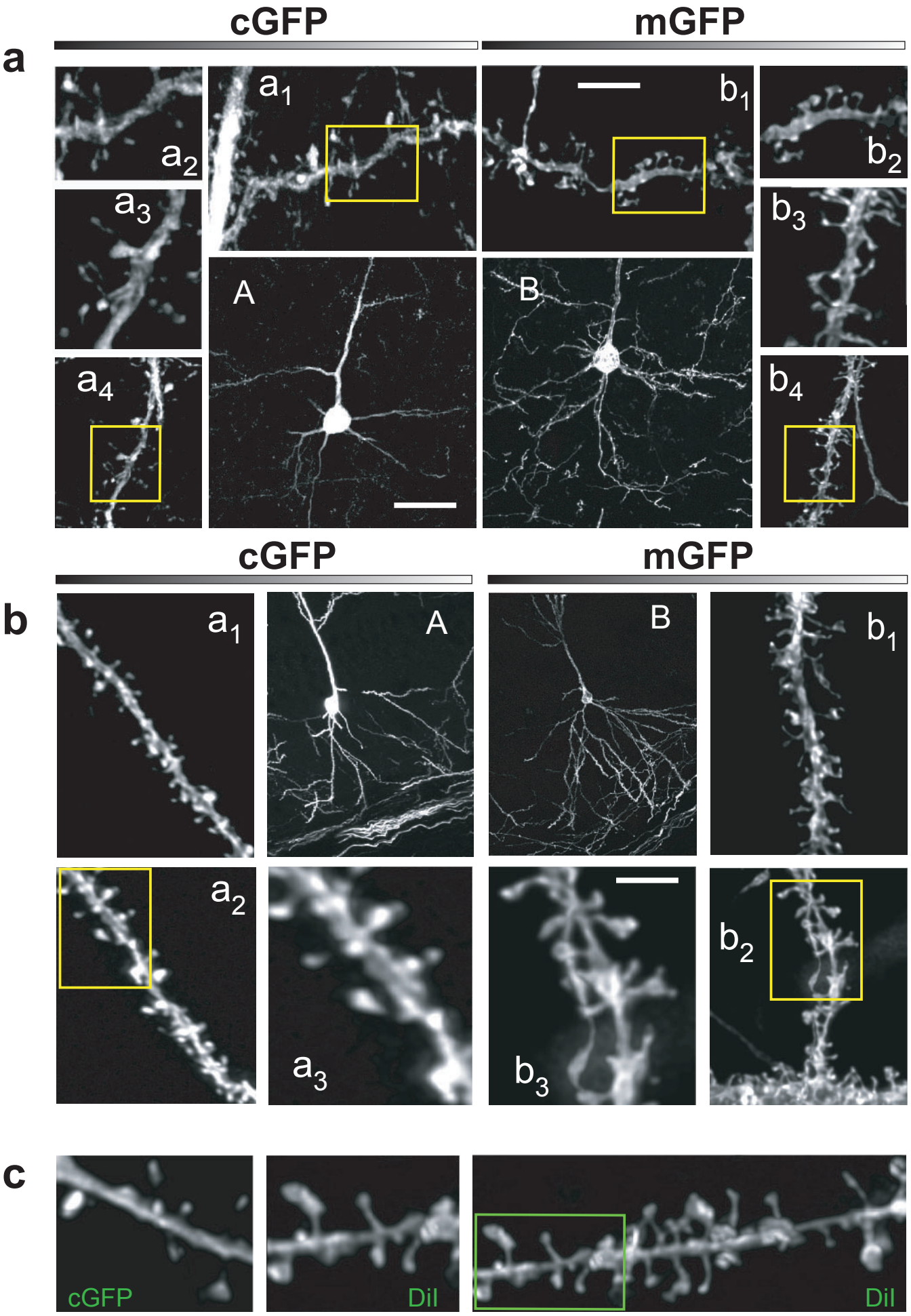
a
cGFP
mGFP
a1
a2
a3
a4
A
b1
b2
b3
b4
B
b
cGFP
mGFP
a1
A
B
b1
a2
a3
b3
b2
c
cGFP
DiI
DiI

FIGURE 4

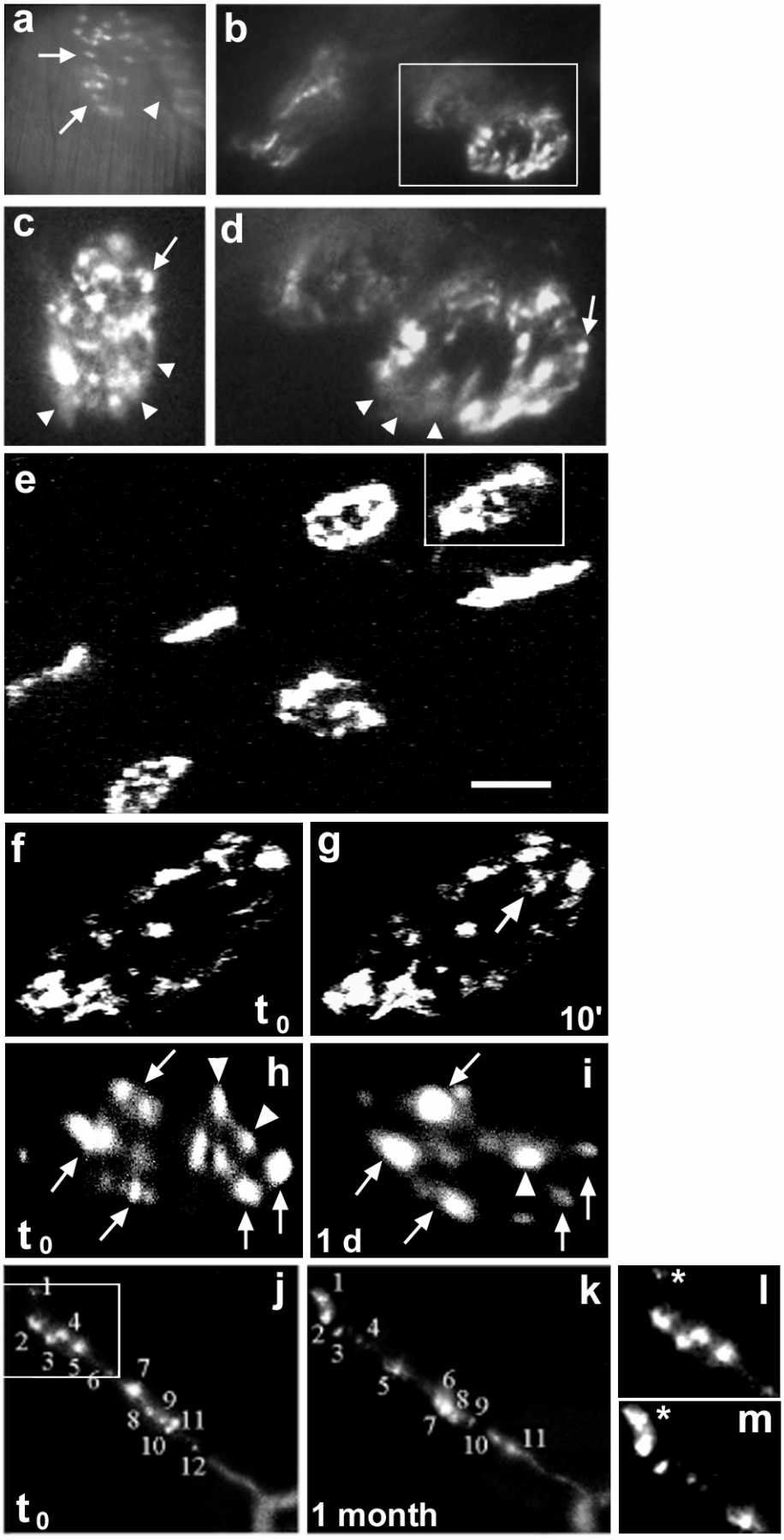

FIGURE 5

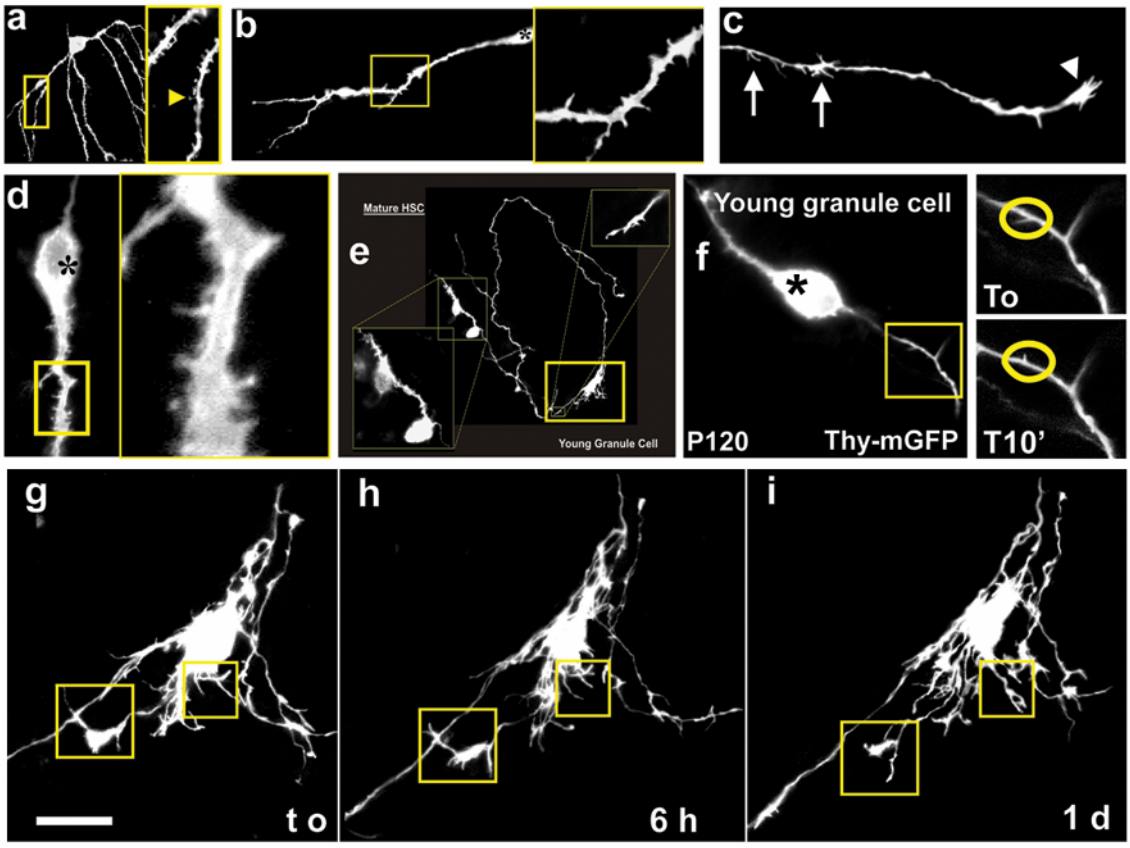
a
b
c
d
Mature HSC
e
Young Granule Cell
Young granule cell
f
P120
Thy-mGFP
To
T10'
g
t o
h
6 h
i
1 d

FIGURE 6

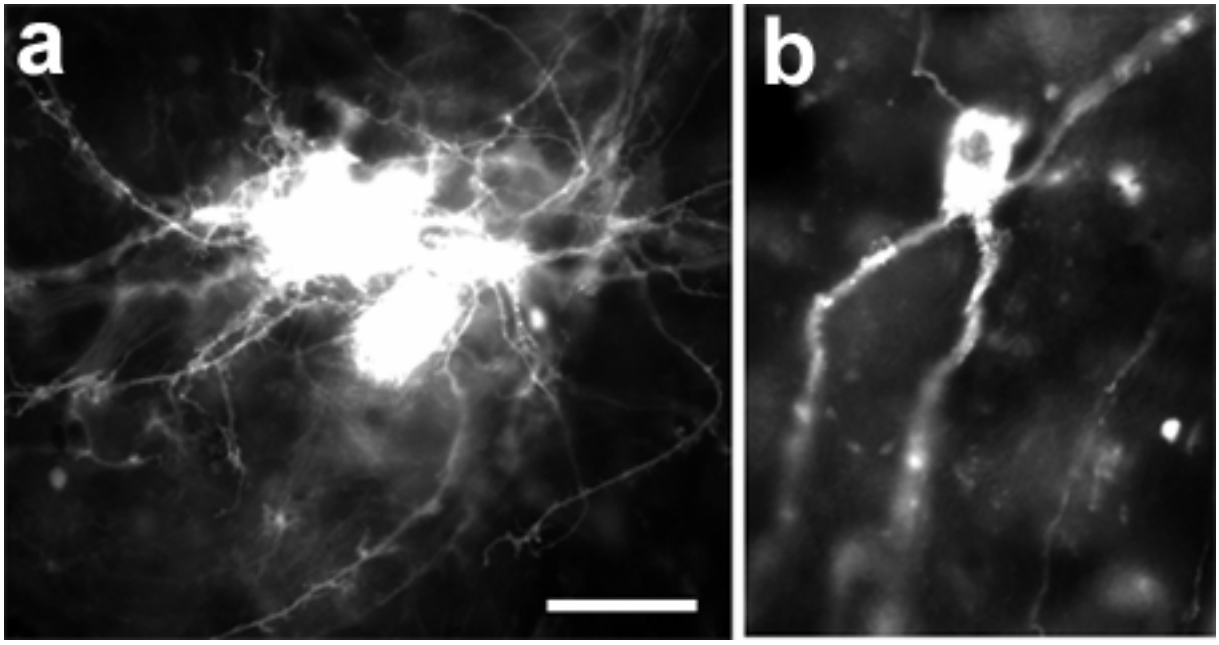

SUPPLEMENTARY FIG. 1

2.1.7. FIGURE LEGENDS

Figure 1: Constructs used for the generation of transgenic mice.
(**a**) Three different constructs were designed which resulted in the expression of three GFP fusion proteins in transgenic mice: a plasmalemmal-targeting domain fusion with GFP (mGFP), a synaptophysin-GFP fusion protein (spGFP), and a combination of the two (mGFP/spRFP).
(**b-o**) mGFP is a reliable marker of the neuronal membrane. (**b-d, f, g**) Cytosolic-EGFP-transfected Cos-7 cells. (**b**) Low magnification fluorescent picture showing a representative field. (**c, f**) Phase contrast pictures whose corresponding fluorescent pictures are in (**d)** and (**g)**. Note that the fluorescence signal, even at high levels diffuses poorly in the cytoplasm and fills neither the outline of these cells (arrows in d and g), nor their processes (arrows in g). (**e**) Low magnification of a representative field from mGFP-transfected fibroblasts. Note that cells appear completely stained, including their processes. (**h**) Phase contrast picture of mGFP positive cells. (**i**) Corresponding fluorescent view. (**j**) Merge. Note clear processes in (i) (arrows). (**m-o**) mGFP labels the axonal membrane in hippocampal neurons in culture. (**m**) Phase contrast picture of a neuron showing its cell body and processes at 25 DIV. (**n**) Corresponding fluorescent picture. Note clear signal around dendrites and cell body of mGFP positive axons surrounding a non-transfected neuron. (**o**) Merge of (m) and (n).

Figure 2: Transgenic mice over-expressing GFP fusion proteins have no detectable phenotype.
Top row: spGFP-expressing SV clusters fuse to the membrane upon α-latrotoxin (Ltx). The three top panels show repeated observations of the same spGFP expressing NMJ over a 120 min. observation period in whole mount soleus muscles. Note that spGFP clusters (arrows in first two panels) get diffuse 2h after Ltx applications (arrows in third panel), suggesting their correct fusion to the membrane. Second row: the first panel shows the Ach-R staining corresponding to the last image of first row (120 min). In the second and third panel a representative example of repeated observations in control conditions is displayed. Note cluster maintenance over the 2h period. The correspondent Ach-R staining is shown in the first panel of third row.
The second and third panels of third row show silver esterase staining of mGFP muscles. mGFP expressing NMJs do not exhibit sprouting.
Quantal content (EPP/MEPP) of spGFP muscle fibers is under control values (graph, fourth row). Scale bar: 15 μm.

Figure 3: Expression patterns of transgenic lines in both CNS and PNS.

(**a**) Expression of GFP transgenes in different brain areas. The first 2 panels show in situ hybridization on hippocampus of Line 24. Note broad expression in CA1 (black arrows in first panel) and restricted in few neurons in CA3 (arrowheads). A higher magnification view is shown in the second panel with arrows pointing to proximal apical dendrites that also express the transgenic mRNA. Overview of the brain of L14 (mGFP) at the protein level. Note DG specific expression in hippocampus and low expression in cortex (Cx) and cerebellum (Ce). Th, thalamus.

Second row: the hippocampus of L5, L1 and L17 (spGFP lines) are displayed in first, second and third panel respectively. Note no expression in the molecular layer (arrowheads, IML; arrows, OML) of the DG in L5; IML-specific expression (arrowheads) in L1 and OML-specific expression in L17. These lines might be useful to study sprouting in the hippocampus.

Third row: overview of frontal cortex at mRNA level in L20 (mGFP, first panel)). Enthorinal cortex and thalamus mRNA expression in L14 (mGFP, second panel).

Fourth row: Examples of different expression patterns in lines expressing in the cerebellum. First panel shows broad Purkinje cell labeling (arrows) and restricted expression in few neurons in the granular layer (arrowheads) of L6 (mGFP). Second panel shows mRNA expression in brain stem nuclei projecting to the cerebellum in L10. spGFP expression in the granular layer of the cerebellum (L5) is represented in the third panel. mGFP expression in the granular layer of the cerebellum (L13) is represented in the fourth panel.

Fifth row: expression patterns in the retina. First panel shows a low magnification of a transverse section through the L19 eye. Note mRNA positive-ganglion cells (arrows) and at higher magnification also few horizontal cells (arrowhead, second panel). Third panel presents an example of the protein (mGFP) expression in the ganglion cell layer (arrows) of L19.

(**b**) Glomerular synapses in a whole mount cerebellar preparation in a mGFP/spRFP mouse. mGFP, spRFP signal and the merge are shown in first, second and third panels of first row. Second row is a magnified view of the area delimited by a rectangle in first row. Note clear colocalization of mGFP and spRFP at glomeruli (arrowheads).

Single axon in the intact cortex of *ex vivo* preparations in a mGFP expressing transgenic line (first panel, third row). Note putative presynaptic structure (arrow).

Punctuate spGFP signals (arrows) are detectable in the intact cortex of *ex vivo* preparations (second and third panels, third row).

Fourth row: In situ hybridization on spinal cord sections. Note expression in motor neurons (arrowheads, first panel) and no signal with sense probe (second panel). Examples of spGFP

expressing NMJ (third panel) and spindle (first panel, fifth row) in whole mount muscle preparations. Note clear punctuate pattern indicating active zone labeling (arrowheads).
cGFP signal at NMJs appears non-uniform (arrows, third panel fifth row) at high magnification. A low magnification of the same NMJ is shown in the adjacent panel. Scale bar: 20 μm in first row, 7 μm in second, 8 μm in third, 80 μm in fourth first two panels, 15 μm third panel fourth row and first panel fifth row, 30 and 5 μm in second and third panels of fifth row.
(c) *Thy1-mGFP/spRFP* whole mount gluteus muscle. Note co localization of mGFP (blue) and spRFP (purple) at NMJs (arrows).

Figure 4: mGFP expressing spines reveal the known complex outline of spine heads and necks whereas cGFP spines do not.
(**a**) High resolution imaging of cortical dendritic spines in mGFP versus cGFP transgenic lines. (**A**, $\mathbf{a_1}$-$\mathbf{a_4}$) cGFP expressing cortical pyramidal neuron, (**B**, $\mathbf{b_1}$-$\mathbf{b_4}$) mGFP. Note the incomplete labeling of basal and apical distal dendrites (**A**) when compared to (**B**, mGFP cortical neuron). The entire dendritic tree and axons are sharper in m-GFP expressing pyramidal neurons (B). $\mathbf{a_1}$ (cGFP) versus $\mathbf{b_1}$ (mGFP) represent comparable regions from the apical dendrites. Note at high magnification (100X with 5X digital zoom), spines are not as clearly detected in the cGFP ($\mathbf{a_2}$, corresponding to the yellow rectangles in a_1) as is in case of the m-GFP ($\mathbf{b_2}$). In particular, the spine neck is not visible and the finer structures of the head as well as neck are not visible. $\mathbf{a_3}$ and $\mathbf{b_3}$ show the comparison for basal proximal dendrites. The distal region of the basal dendrites, where spine density is higher and the dendritic shaft is thinner, is shown in ($\mathbf{a_4}$, cGFP and $\mathbf{b_4}$, mGFP). Note the highly irregular structure of the spine neck and the head region in the mGFP example. Note also large number of spines in the m-GFP marker example, not visible with cGFP.
(b) High resolution imaging of hippocampal dendritic spines in mGFP versus cGFP transgenic lines.
(**A**) (cGFP) and (**B**) (mGFP) show the distribution of the cGFP and m-GFP markers in hippocampal pyramidal neurons at low magnification. Note strong cGFP signal only in cell bodies and proximal apical dendrites (top part of panel) and striking faint signal in distal parts of basal dendrites (bottom part of panel). mGFP, in contrast, labels effectively the whole neuronal membrane. At higher magnification (60X) in $\mathbf{A_1}$ (cGFP) and $\mathbf{B_1}$ (mGFP) note the more uniform signal around the neuronal membrane in mGFP. $\mathbf{a_1}$ (cGFP) versus $\mathbf{b_1}$ (mGFP) represent comparable regions of secondary apical dendritic segments. Note globular appearance of cGFP spine heads and diverse shapes in the mGFP example. This feature is also true for other cells in

the hippocampus (data not shown). **a_2**, cGFP, and **b_2**, mGFP, show pictures of primary basal dendrites close to the cell body. **a_3**, cGFP, and **b_3**, mGFP, show pictures of primary distal basal dendrites. Note here as well the varied shapes in the mGFP example but not in cGFP. **a_4** shows a high magnification view of the insert in **a_3**, whereas **b_4** corresponds to the green insert in **b_3**. Note that the mGFP marker visualizes complex spine regions in great details, highlighting its advantage for high-resolution imaging of fine dendritic structure.

(c) DiI labelling of naïve tissues reveals a similar population of spines in mGFP but not in cGFP expressing neurons.

Scale bar: 40 μm in low magnification pictures (**aA,B; bA,B**), 10 in magnified pictures.

Figure 5: SV dynamics at mammalian NMJs *in vivo.*

(**a**) Low magnification fluorescent picture of a mouse tibial muscle expressing spGFP transgene. Arrows mark the synaptic bend and the arrowhead a blood vessel that is useful to trace back the NMJ of interest. (**b**) Low magnification view of a 4 day-old spGFP mouse NMJ. Note at high magnification in (**d**) both diffuse (arrowheads) and clustered signal (arrow). In (**c**) another example of a NMJ belonging to a P4 mouse is shown. Confocal imaging stacks (12 μm in the Z-axis) of living tibialis NMJs are shown in (**e-g**). Note SV cluster reorganization over few minutes. The arrow in (g) shows an example of mobile SV clusters. Over 1day observation period, putative fusion (arrowhead in i) and disappearance of clusters (white arrowheads in h) are detectable in a NMJ from a 18-day-old spGFP mouse (**h-i**). Sensory innervation displays reorganization of microvesicle clusters over 1 month observation period *in vivo* (**j-m**). A spGFP positive sensory terminal is shown and its SV clusters numbered. Note changes in position of clusters but overall maintenance of total numbers. (**l**) and (**m**) are high magnification panels of the boxed region in j. GFP signal has been optimized in f-i to better reveal the SV clusters. Asterisk indicates the same cluster. Scale bar: 400 μm in (a), 40 μm in (b), 30 in (c), (d), (f-I), 50 μm in (e) and 60 in (j-k).

Figure 6: Young versus adult granule cells in the same mature hippocampal slice cultures.

(**a**) Typical example of a mature GC in the DG with its extensive basal dendritic arbor. The region delimited in yellow is magnified on the right to show details of spines. Note clear spine heads (arrowhead). (**b, d**) Typical examples of young granule cells with a simple basal dendrite. Note at high magnification the filopodia-like appearance of the dendritic protrusions (yellow inserts). Asterisk marks cell body. (**c**) Terminal axonal region of a young MF. Note widespread foci of filopodia extending from the shaft (arrows) and a growth cone at the tip (arrowhead). (**e**)

A young granule cell and its processes are reconstructed. Top right insert represents a growth cone at the main axon ending. Bottom left insert shows at high magnification the cell body and dendritic region. The large yellow insert shows a region that was repeatedly imaged over 1 day in (g-i). (**f**) Young granule cells are characterized by rapid extension-retraction of filopodia in hippocampal whole mount preparations. The region delimited by the yellow square was imaged over 10 min (shown in the two adjacent panels on the right). Note filopodia changes marked by the yellow circles. (**g-i**) Axons of young granule cells elongate and retract (bottom left insert) or extend progressively (top left insert) over a 1-day observation period.

Supplementary Figure 1: Gene gun mediated transfer of mGFP transgene in hippocampal slice culture is not specific for neurons. (a) Glia cell and processes are often labeled by the gene gun method because a layer of glia cells lies on the surface of the slice culture. (b) Granule cell in DG.

Supplementary videos 1-2: Young MF are characterized by more frequent and prominent dynamic activity than mature ones in the same neuronal circuit.
The videos show a young MF axon from a *Thy1-mGFP*^{s} slice imaged over a few minutes (Suppl. Video 2 is a high magnification view of video 1). The corresponding granule cell exhibited the characteristic features of young granule cells: including the location in the DG GCL, a granular shape of cell body, one basal dendrite, no mushroom spines on the dendrite but highly motile filopodia-like spines and highly motile growth cone filopodia at the end of axonal branches. Note multiple events of filopodial extension-retraction. Frames were captured at 10 sec intervals, and the video is shown at 15 frames/second.

Supplementary videos 3-5: Young GC dendrites are characterized by more frequent and prominent dynamic activity than mature ones in the same neuronal circuit. The videos show examples of young granule cell dendrites from a *Thy1-mGFP*^{s} slice imaged over a few minutes in mature hippocampal slice cultures. Note extensive dynamic filopodia-like protrusions. Frames were captured at 10 sec intervals, and the video is shown at 15 frames/second.

2.2. AMPA receptors regulate dynamic equilibrium of pre-synaptic terminals in mature hippocampal networks

[1]Vincenzo De Paola, [2]Silvia Arber, and [1]Pico Caroni

[1]Friedrich Miescher Institut
Maulbeerstrasse 66, CH-4058 Basel, Switzerland
[2]Friedrich Miescher Institut and Biozentrum University of Basel
Klingelbergstrasse 70, CH-4056 Basel, Switzerland

Correspondence should be addressed to P.C.:
tel: +41-61-6973727 fax:+41-61-6973976 email: caroni@fmi.ch

SUMMARY

The formation and disassembly of synapses in mature neuropil could provide a substrate to encode experience in the brain. While there is evidence for postsynaptic spine dynamics in mature systems, contributions to circuit rearrangements by presynaptic terminals have remained unclear. Here we use mice expressing membrane- and/or synaptic vesicle-targeted spectral variants of GFP in neuronal subsets to image identified presynaptic terminals. We find that in mature hippocampal slice cultures with no net changes in synapse numbers, subpopulations of presynaptic terminals appear and disappear within 1-3 days. Mature mossy fibers display short-term dynamic behaviors resembling those typical during development. The three terminal types established by mossy fibers exhibit distinct dynamic properties. High-frequency stimulation increases the fraction of dynamic terminals for 1-2 days, a process mediated through AMPA-receptor activation, PKA and protein synthesis. Thus, stable presynaptic terminals in mature hippocampal networks can be converted into dynamic ones by synaptic activity, providing a candidate mechanism to convert experience into changes of network connectivity.

2.2.1. INTRODUCTION

The cellular mechanisms for encoding experience in the brain are poorly understood, but most likely involve structural rearrangements of neuronal circuitry (Bailey and Kandel, 1993). This process may involve a turnover of presynaptic terminals and/or postsynaptic endings, resulting in the formation of new synaptic connections and/or the loss of existing connections. While the dynamic properties of postsynaptic sites have been characterized in some detail (Ziv and Smith, 1996; Kirov and Harris, 1999; Matus, 2000; Marrs et al., 2001; Yuste and Bonhoeffer, 2001), much less is known about rearrangements of axons and presynaptic terminals. Postsynaptic spines exhibit short-term actin-dependent motility, and can turn over within hours. This postsynaptic plasticity is mediated by Glutamate receptors and BDNF (Smart and Halpain, 2000), is affected by experience, and decreases as the nervous system matures (Lendvai et al., 2000). Consistent with the notion that a rearrangement of spines is involved in learning and in regulating behavior, new spines can be induced in response to long-term potentiation of synaptic transmission (LTP) (Engert and Bonhoeffer, 1999; Toni et al., 1999), or steroid hormone treatment (Woolley et al., 1996). In these experiments, new spines were associated with preexisting presynaptic boutons, leading to an increased number of synapses locally, and to an amplification of synaptic transmission through multi-spine boutons (Luscher et al., 2000; Yankova et al., 2001). These results would thus be consistent with the possibility that in mature systems synapse rearrangements predominantly involve postsynaptic remodeling, without concomitant reorganization of presynaptic structures.

Extensive turnover of presynaptic terminals has been detected during the innervation of the developing tectum in the frog, where it appeared to involve a dynamic balance between terminal appearance and disappearance events (Cline, 2001). In contrast, information about the possible existence of presynaptic terminal dynamics in mature, non-growing neuronal networks is currently lacking. Obtaining such information has been a challenging task due to the way in which presynaptic terminals are arranged along axons. Thus, in contrast to postsynaptic spines, where high numbers of individual structures are arranged in short intervals along any segment of a dendrite, presynaptic specializations of an individual axon are distributed at substantial distances along the axon. As a consequence, obtaining quantitative information about presynaptic terminal dynamics depends on being able to

repeatedly monitor long stretches of axons, and large populations of identified terminals over extended periods of time.

In this study we monitored individual, identified presynaptic terminals over periods of up to two weeks, analyzed quantitatively their dynamics, and identified molecular mechanisms that regulate them. To study long-term changes (days) in presynaptic structures under controlled experimental conditions we used organotypic hippocampal slice culture preparations (Stoppini et al., 1991). We initially focused our analysis on one defined type of axon, the mossy fiber (MF) of dentate gyrus granule cells, with its characteristic, anatomically recognizable terminals. As the MF pathway is essentially lamellar, its connectivity is well retained in the slice preparation (Zimmer and Gahwiler, 1984; Claiborne et al., 1986; Henze et al., 2000). MFs establish three distinct types of glutamatergic presynaptic terminals, the large mossy fiber terminals (LMT), the filopodial extensions of LMT (LMTfil), and the en-passant varicosities (epV) (Toth and McBain, 2000). LMT synapse on excitatory CA3 pyramidal dendrites, whereas LMTfil and epV synapse onto distinct inhibitory interneurons. The three types of terminals have been extensively characterized morphologically, ultrastructurally and functionally (Amaral, 1979; Acsady et al., 1998; Toth et al., 2000) and their presence on the same axon allowed us to compare the dynamic properties of distinct types of presynaptic terminals of the same neuron. To generalize our findings we also analyzed populations of synaptophysin-positive terminals in CA3a/b, an area also containing pyramidal neuron and interneuron terminals. We report that in hippocampal slices cultured for 1-3 months, with no net changes in synapse numbers, subpopulations of presynaptic terminals appear or disappear within a few days. Distinct types of terminals of the same neuron exhibited unique dynamic properties. High-frequency stimulation converted a fraction of stable terminals into dynamic ones for 1-2 days, a process involving AMPA-receptor activation, PKA, and de-novo protein synthesis. These findings reveal that in mature hippocampal networks, presynaptic terminal numbers are in a state of dynamic equilibrium subject to regulation by synaptic activity. Such dynamics may provide a substrate to convert experience into long-term changes of network connectivity.

2.2.2. RESULTS

Imaging identified presynaptic terminals

To investigate individual axonal processes and the dynamics of their presynaptic terminals in situ, we chose a genetic approach to visualize the plasmamembrane and synaptic vesicles of a small percentage of neurons in postnatal mice. The plasmamembrane marker was used to allow detailed monitoring of axonal outlines, including putative presynaptic structures, and the synaptic vesicle marker (Li and Murthy, 2001) to detect presynaptic terminals, where synaptic vesicles accumulated (**Fig. 1,** Suppl. Figs. 1-3). To achieve transgene expression in small subsets of neurons, we used a mouse Thy1.2 expression cassette, which in about a third of the transgenic lines leads to robust and constitutive expression of transgenes in a small fraction (< 0.1%) of postnatal neurons in several brain structures (see Methods). The transgenic lines used in this study were chosen for their expression in dentate gyrus granule cells in the hippocampus (**Fig. 1a**, Suppl. Fig. 1), and are designated *Thy1-mGFP*^{s} (expression of plasmamembrane-targeted EGFP in small subsets of neurons; **Fig. 1a, b**), *Thy1-spGFP*^{mu} (expression of synaptic vesicle synaptophysin-GFP in a majority of neurons; Suppl. Fig. 3), and *Thy1-mGFP/spRFP*^{s} (co-expression of plasmamembrane-targeted EGFP and synaptophysin-RFP in subsets of neurons; **Fig. 1a, b**). In addition to granule cells, transgene expression in the hippocampal formation was detected in small subsets of pyramidal cells and interneurons in CA3 and CA1.

The three distinct presynaptic structures of granule cell axons could be identified with the mGFP membrane marker (**Fig. 1a, b**). To determine whether anatomically identifiable *Thy1-mGFP*^{s} MF terminals correspond to synaptic sites, *Thy1-mGFP*^{s} and *Thy1-mGFP/spRFP*^{s} hippocampal slices were fixed and immunostained with antibodies against two synaptic markers: synaptophysin (pre-synaptic) and the NMDA receptor subunit NR1 (post-synaptic) (**Fig. 1b**). For signals to be considered as spatially related, they had to coincide on at least one confocal section. LMT could all (15/15) be counterstained with both synaptic markers. Quantitative analysis of confocal simultaneous two-channel images revealed that 91 ± 7% (mean ± SD; 54 epV, 6 slices) of epV could be counterstained for synaptophysin, and for at least 68 ± 12% of epV (42 epV, 5 slices) an NR1 cluster could be unambiguously visualized in apposition to the mGFP signal. All epV contacted by NR1 clusters contained

synaptophysin. 80 ± 11.0% of LMTfil (32 LMTfil, 6 slices) exhibited synaptophysin immunoreactivity, and at least 62 ± 6% (36 LMTfil, 6 slices) of them exhibited an NR1 cluster in close apposition. Nearly all epV (96 ±4%) and LMTfil (93 ± 6%) accumulated spRFP in living tissues (*Thy1-mGFP/spRFP^s* mice), and fractions of NR1 immunoreactivity apposed to small terminals were comparable to those detected for terminals identified anatomically in slices from *Thy1-mGFP^s* mice (epV, 63 ± 5% N = 24; LMTfil, 66 ± 9% N=28, 4 slices). Therefore, most anatomically identifiable MF terminals from *Thy1-mGFP^s* slices accumulate synaptic markers, suggesting that they correspond to functional synapses.

Stable numbers of terminals in mature slices

To analyze a system consisting of mature neuronal networks, we first determined whether and from when on total numbers of presynaptic terminals remained stable in the slice cultures. During the first three weeks in vitro, we observed a substantial degree of short-term (minutes and hours) dynamics by axons and dendrites, and a steady increase in the numbers of presynaptic terminals (*Thy1-spGFP^{mu}*, **Fig. 2b**). Growth and remodeling declined during the third week in vitro, and from 4 weeks on no growth cones, process elongation or branching were detected (*Thy1-mGFP^s*, 59 MFs, see supplementary fig.8). To determine whether net synapse numbers continued to change in hippocampal cultures with no overt process growth or rearrangements, we quantified the numbers of presynaptic structures that appeared or disappeared during repeated observations over periods of 1-4 days. To establish criteria distinguishing putative presynaptic structures from transport packages, i.e. pre-assembled synaptic precursor complexes that travel rapidly along the axon (Ahmari et al., 2000), we generated time lapse videos of spGFP puncta in CA3b (Suppl. Video 1). Quantification of these data for puncta > 1.5 μm and for putative transport packets (0.3-0.6 μm, long axis; 0.2-0.4 μm, short axis) (Ahmari et al., 2000) revealed two clearly distinct behaviors: 53/53 Sp-GFP clusters > 1.5 μm were never seen moving back or forth along the axon over periods of minutes, whereas smaller clusters (e.g. double arrowheads in **Fig. 2a**, arrows in Video 1) exhibited rapid translocation movements (see suppl. Methods). These data suggest that puncta substantially smaller than 1.5 μm represent synaptic vesicle transport packages, whereas those > 1.5 μm correspond to more stable synaptic contacts.

We then analyzed the turnover of putative CA3a/b presynaptic structures in slice cultures from *Thy1-spGFP^{mu}* mice (**Fig. 2**). Over days, only a minority of the larger spGFP structures appeared or disappeared between repeated observations, whereas the majority of them persisted for several days (**Fig. 2a, b**). As would be expected for a growing network, gains of spGFP puncta exceeded losses in young (1-3 weeks) slice cultures. In contrast, gains and losses of large spGFP puncta were comparable in slices older than 4 weeks, where numbers of new or lost terminals were remarkably closely matched (**Fig. 2b**). This was the case for both, the total population of large synaptophysin structures in CA3b (7.8 ± 1.2% gained, 7.9 ± 0.9% lost over a period of 24 hours; 40 days cultures), as well as a defined population of terminals (epV, see **Fig. 3b**). As synapse numbers are largely determined by the maturity and size of postsynaptic target regions (Davis and Bezprozvanny, 2001), these results suggest that from 4 weeks in vitro on, the hippocampal slice cultures consisted of neuronal networks with stable total numbers of presynaptic terminals. Surprisingly, this striking stability in total presynaptic structure numbers was maintained in the presence of a substantial turnover of individual terminal structures.

Dynamics of mossy fiber LMT

To investigate the dynamics of identified presynaptic terminals, we analyzed LMT, epV, and LMTfil separately. LMTs are multisynaptic complexes (> 3 μm diameter; up to 37 release sites), with varying numbers of LMTfil extending from any of them. Putative LMT structures of the appropriate size were restricted to MFs in the hilus and CA3 (*Thy1-mGFP^{s}* or *Thy1-spGFP^{mu}* slices, see Suppl. Figs. 1, 3), facilitating their unequivocal identification. We detected 5 to 16 LMT along any granule cell axon in our cultures (*Thy1-mGFP^{s}*), a range comparable to that reported for MFs in vivo (Acsady et al., 1998). Repeated observations of individual LMT over periods of up to 15 days failed to reveal any change in their numbers or positions (*Thy1-mGFP^{s}*: over 1 d (N > 100), 6 d (N = 9), 16 d (N = 6); *Thy1-spGFP^{mu}*: over 1 d (N = 37), 4 d (N = 12)), indicating that, as whole structures, LMT were stable. However, confocal time-lapse imaging revealed that within a few hours of observation LMTs altered both their outer shape (*Thy1-mGFP^{s}*) and the arrangement of synaptic vesicles inside the terminals (*Thy1-spGFP^{mu}*) (42/42 fully reconstructed LMTs from 16 separate cultures; see Suppl. Fig. 4). These dynamics may reflect alterations in LMT morphology without synapse turnover, and/or a rearrangement of individual active zones within the LMT.

Dynamics of mossy fiber epVs

EpV appeared as swellings of 1-2.5 μm of diameter along MFs (see Suppl. Methods). In agreement with previous reports, individual axons exhibited different densities of epV (range of 2-5, compared to 3-5/100 μm for hippocampal MFs in the adult brain (Claiborne et al., 1986)). There was no systematic relation between epV density in CA3b, and morphological features of granule cells, such as the extent of branching by the MF axon (the average branching value was 9 $\pm$ 2, predominantly in the hilus, N = 18 granule cells), the position of the granule cell body in the dentate gyrus (e.g., for 5 axons whose granule cell bodies were in the lateral blade, epV/100 μm were 0.9, 1.2,1.4, 4.5, 4.5; for 3 axons from the crest they were 1.8, 3.0, 4.2), or the morphology of its dendritic tree (typically characterized by 3 main basal branches, Supplementary fig.1). We followed 146 epV from 12 different slices over 3-5 time points for up to 6 days in > 40-day old organotypic slices. The same epV could be relocated reliably using positional landmarks such as LMT and axonal turns (for an example, see **Fig. 3a**, bottom image; *Thy1-mGFP*^{s}). The analysis showed that while the majority of epV was stable, a fraction of epV appeared or disappeared within this time frame (**Fig. 3a, b**). To determine whether epV may consist of subclasses with distinct dynamic properties, we related median fractions of dynamic epV to the time interval between repeated observations. While fractions of appearing/disappearing (i.e. dynamic) epV increased during the first 3 days of observation, they did not increase further when observation periods were extended to 4 and more days (**Fig. 3c**). These results are consistent with the existence of two main classes of epV along MF axons in these cultures: stable epV (about 91% of total; no detectable turnover within 1-week periods), and dynamic epV (about 9% of total; half-lives of approximately 1 day). The incidence of dynamic epV exhibited no apparent relation to epV density along the particular axon (median fractions of dynamic varicosities were 9.0% (MFs with 4-5 epV per 100 μm; N = 5) and 8.8% (MFs with 2-4 epV per 100 μm; N = 5)).

During development, axonal synaptogenesis involves rapid (seconds, minutes) protrusive activity from axonal varicosities (Dailey et al., 1994), and rapid filopodial extension-retraction events from the axonal shaft (Ziv and Garner, 2001). Together with corresponding dynamics at postsynaptic sites, these processes are thought to mediate the formation of synaptic sites. To determine whether similar short-term axonal dynamics, possibly involved in the

formation/disassembly of epV synapses, may exist in the mature slice cultures, we generated time-lapse videos, and quantified the short-term (seconds, minutes) dynamics of MF axons (see Methods, and Suppl. Videos 2 and 3). Consistent with the notion that new synaptic sites assemble over hours, but not a few minutes (Friedman et al., 2000), no gains or losses of epV (*Thy1-mGFP*^{s}) were detected within this time frame. A fraction of epV (12 ± 5% of total, 116 epV) exhibited protrusive lamellar activity comparable to that described for developing axons (Suppl. Video 2), and 39.5% of the filopodia along MF shafts (43 filopodia, from 1870 μm of MF) exhibited rapid extension-retraction events (> 1.5 μm). Like adult hippocampus, the slice cultures contain a small percentage of younger granule cells. These young granule cells occasionally appeared as new mGFP-positive neurons in the dentate gyrus during the time in culture, with characteristically growth cones at the end of their processes, only one dendrite, and low numbers of spines. As may be expected, the frequency and extent of dynamic events was much higher in such younger MFs (Suppl. Video 3). To compare these data to similar events in mature circuits *ex vivo*, we also monitored the dynamic behavior of a small sample of MFs in acute whole mount hippocampal preparations from P120 mice (Suppl. Fig. 5), an experimental system where all main inputs to the hippocampus are preserved, thus closely mimicking *in vivo* hippocampus (5 MFs; 5 distinct hippocampi; total of 760 μm; 10-15 min observation periods, see Suppl. Methods). Values for short-term dynamic activity in this *ex-vivo* system closely resembled the corresponding short-term dynamics data obtained with long-term slice cultures:12% of the epV (N = 25 epV) showed protrusive activity, and 33% of the filopodia (N = 15) exhibited extension-retraction activity (Suppl. Fig. 5). Taken together, these data provide evidence that mature MF exhibit sites of dynamic activity closely resembling those associated with synaptogenesis in developing axons. The frequency of these dynamic sites along mature MF was comparable to that of dynamic epVs, suggesting that these may represent sites of ongoing synapse formation/disassembly.

The short-term dynamics data described above, indicate that sites of appearing or disappearing epV along MFs may exhibit dynamic activity for protracted periods of time (at least 5 days), suggesting that they may represent axonal “hot-spots” with respect to synaptogenesis. To further explore this possibility, we systematically re-analyzed 80 MF segments of 40-50 μm in length over 3-5 different time points (over 3-5 days), scoring them for any evidence of dynamic activity. There was a marked tendency for disappearing epV to be either followed in time by filopodia, or by new epV at the same MF position (8 epV-

filopodia alternation events, and 4 epV disappearance and reappearance events at the same location out of 3440 μm of MF). In addition, we detected filopodial structures in association with 11.9% of the epV that were stable during the observation period, and with 21.4% of the epV that either appeared or disappeared during the observation period (for an example, see last panel in fifth row of **Fig. 3a**). These observations are consistent with the notion that in addition to stable epV, which do not undergo remodeling for long periods of time, mature MF exhibit a set of spatially defined sites ("hot spots") which are much more accessible to ongoing synapse formation/disassembly.

To search for molecular mechanisms that may regulate epV long-term dynamics, we tested the role of the cAMP-dependent pathway, which was shown to affect the behavior of developing axons, MF growth, and synapse formation in CA1 (Baranes et al., 1998; Ma et al., 1999; Bozdagi et al., 2000; Hatada et al., 2000; Mizuhashi et al., 2001). The cAMP analogue Sp-cAMPS (50 μM) had two major effects on epV: it nearly doubled the fraction of dynamic epV, and further accelerated their turnover rates (**Fig. 3d**). In contrast, the cAMP analog did not affect the total numbers of epV ($P > 0.99$, Mann-Whitney test). Therefore, stable epV can become dynamic within hours, and an agent that can persistently augment synaptic output (Baranes et al., 1998) also induces a substantial increase in presynaptic terminal dynamics. This regulation selectively affects the fraction of dynamic terminals and their turnover rates, but not the total number of terminals.

Dynamics of mossy fiber LMTfil

We next analyzed the other type of MF terminal contacting interneurons, the LMTfil. LMTfil exhibited substantial dynamics, with approximately 30% of them retracting/disappearing, extending/appearing or branching within a one-day observation period (**Figs. 4, 5**; see Suppl. Methods). Blocking actin dynamics with Cytochalasin D (5 μM) suppressed most of the LMTfil dynamics (from 0.28 ± 0.03 to 0.07 ± 0.02, over 6 h, $P = 0.0002$, paired t-test), indicating that this process is actin dependent (**Figs. 4c, 5a**). Individual LMTfil associated with any given LMT exhibited distinct dynamic properties (**Fig. 4a, b**), suggesting that dynamics may be regulated at the level of single LMTfil. While the total extent of rearrangements increased substantially over time for a sizeable fraction of LMTfil (the fraction of LMTfil with motility index greater than 0.6 (dynamic fraction) was 7% at 6h, and

36% at 1 day), a 50-60% fraction of them exhibited no overt motility for periods of up to1 day (the fraction with motility index < 0.4 (stable fraction) was 74% at 6h and 51% at 1 day). To determine whether the endings of dynamic LMTfil accumulate synaptic vesicles before and/or after remodeling, we repeatedly imaged LMTfil in slices from *Thy1-mGFP/spRFP* ^{s} mice, where axonal outlines and presynaptic vesicles can be imaged in the same living neuron. Dynamic LMTfil in living neurons were undistinguishable from more stable ones with respect to synaptic vesicle accumulation (**Fig. 4b**), consistent with the notion that they establish functional synapses. These findings suggest that, like for epV, there are stable and dynamic subpopulations of LMTfil (**Fig. 5b**), but that the fractions of dynamic terminals and their turnover rates differ significantly between the different types of MF presynaptic endings.

Regulation of LMTfil dynamics

The substantial dynamics of LMTfil allowed us to investigate the role of synaptic transmission in this remodeling. In a first set of experiments, we blocked action potential-induced transmitter release in the slice cultures for 1 day with TTX (1 μM). The toxin treatment did not influence LMTfil remodeling (**Fig. 5a**). We next determined whether Sp-cAMPS, which enhanced epV turnover, also enhanced LMTfil dynamics. This treatment greatly enhanced LMTfil remodeling (**Fig. 5a, b**). A detailed analysis revealed two types of changes induced by Sp-cAMPS: 1) virtually all (> 90%) LMTfil became dynamic (**Fig. 5b**); 2) average remodeling rates increased by approximately 50% (**Fig. 5a**).

We then mimicked increased network activity by adding Glutamate (100 μM) to the culture medium (see Methods). Glutamate destabilized LMTfil and enhanced their dynamics to an extent, and with kinetics comparable to those of Sp-cAMPS (**Figs. 4c, 5a, 5b**). We routinely reexamined granule cells and their presynaptic terminals, including LMTfil, one day after the end of these experiments, and found no evidence for a toxic effect of Glutamate in these experiments (see Suppl. Methods, and Suppl. Fig. 6). To identify the receptor pathway(s) through which Glutamate augmented LMTfil dynamics, we carried out experiments in the presence of specific Glutamate receptor agonists and antagonists. The specific AMPA-receptor agonist AMPA (400 nM) reproduced the effect of Glutamate (**Figs. 4c, 5a**). The presence of the NMDA-receptor antagonist AP-V (100 μM) in these experiments did not affect the stimulatory effect of AMPA (**Fig. 5a**), ruling out the possibility that activation was due to an indirect effect of AMPA-receptor activation on NMDA-receptor activity. In a

complementary series of experiments, the specific and non-competitive AMPA-receptor antagonist SYM2206 effectively blocked stimulation of LMTfil dynamics by Glutamate (**Fig. 5a**). AMPA-receptor activation is thus necessary and sufficient for Glutamate to enhance LMTfil dynamics.To define the pathway(s) through which cAMP and AMPA augment LMTfil dynamics, we first carried out experiments in the presence of both Sp-cAMPS and AMPA. However, combinations of the two agents or high doses of AMPA were toxic to the slice cultures (4 out of 4 slices, Suppl. Fig. 6), suggesting synergism between the two agents, but limiting the value of these agonist combination experiments. The specific inhibitor of PKA Rp-cAMPS (100 μM) completely and specifically blocked the effect of AMPA on LMTfil dynamics (**Fig. 5b**), providing evidence that PKA is downstream of AMPA-R activation in a pathway leading to enhanced LMTfil dynamics.

The stimulation of LMTfil remodeling by AMPA only became apparent after about 6 hours of treatment, suggesting that instead of acting directly on LMTfil, Glutamate may exert its effects indirectly. Treating slices for 6 hours with cycloheximide (60 μM) did not significantly affect basal LMTfil dynamics, but suppressed the stimulatory effect of AMPA (**Fig. 5a**), indicating that the mechanism leading from AMPA-receptor activation and PKA to enhanced LMTfil dynamics depends on the synthesis of new proteins. To search for further potential regulators of LMTfil dynamics acting upstream of protein synthesis, we carried out experiments with Brain Derived Neurotrophic Factor (BDNF), a neurotrophin that can induce LTP and destabilization of dendritic spines, and that can be released upon cAMP elevation to initiate a gene expression program in hippocampal neurons (Horch et al., 1999; Patterson et al., 2001; Poo, 2001). Short-term (6 h) application of excess BDNF (350 ng/ml) in the culture medium did not affect the fraction of stable LMTfil, but markedly enhanced the motility of dynamic LMTfil (36% LMTfil with motility indices > 0.8 within 6 hours, compared to 0% in untreated cultures). At 1d of treatment, BDNF had effects comparable to those of Sp-cAMPS and Glutamate, enhancing the fraction of dynamic LMTfil and their motility rates (**Fig. 5a, b**). This effect was blocked by an antibody against BDNF (**Fig. 5a**). These findings are consistent with the possibility that BDNF may be a downstream effector of enhanced excitation to induce alterations in synaptic connectivity.

The experiments described above raised the possibility that network activity may act through AMPA-R activation, PKA activation, protein synthesis, and possibly BDNF to enhance

LMTfil dynamics. To investigate this possibility, we stimulated identified MF either through a high-frequency protocol (four 1 sec 100 Hz bursts, spaced by 30s intervals), or a low-frequency protocol (15 min stimulation at 1 Hz). Such protocols have been shown to potentiate (high-frequency), respectively depress (low-frequency) transmission at MF synapses (Toth and McBain, 2000; Castillo et al., 2002). The 100 Hz local stimulation protocol enhanced LMTfil dynamics to an extent comparable to that produced by AMPA or Glutamate (**Figs. 4c, 5a, 5b**), whereas low-frequency stimulation did not (**Fig. 5a**). The effect of high-frequency stimulation was completely prevented by SYM2206, indicating that it involved AMPA-R activation (**Fig. 5a**). Upon 100 Hz stimulation, LMTfil dynamics were first enhanced at 6-10 h (not shown), peaked at 1day, and returned to control values at 2-3 days (**Fig. 5c**). Together, these results provide evidence that local high-frequency electrical stimulation enhances LMTfil dynamics through the activation of AMPA-R, followed by activation of PKA, and de novo protein synthesis. Enhanced LMTfil dynamics persists for 1-2 days, when it may mediate experience-dependent changes in synaptic circuitry.

The neural cell adhesion molecule NCAM has been implicated as a negative regulator of anatomical plasticity, and its expression in the hippocampus can be regulated by activity (Luscher et al., 2000). To determine whether nerve terminal dynamics can be altered permanently in the slice cultures, we compared LMTfil turnover in slices from *NCAM*$^{-/-}$ x *Thy1-mGFP*^{s} mice versus their *NCAM*$^{+/+}$ x *Thy1-mGFP*^{s} littermates. In the absence of NCAM (Cremer et al., 1994), the average motility of LMTfil was increased 3-fold (**Figs. 4a, 5a**), and the fraction of stable LMTfil was reduced by about half. The average number of LMTfil per LMT was increased 1.5-2-fold, and LMTfil were longer and more branched in the absence of NCAM (**Fig. 4a**). Average numbers of LMT and epV in slices from *NCAM*$^{-/-}$ x *Thy1-mGFP*^{s} mutant mice and wildtype *NCAM*$^{+/+}$ x *Thy1-mGFP*^{s} littermates were indistinguishable (not shown), suggesting that the absence of NCAM did not lead to a general increase in synapse numbers in these slices.

Presynaptic terminal dynamics in CA3a/b

To determine whether features of presynaptic turnover regulation in MF terminals can be generalized to other types of nerve terminals in the hippocampus, we analyzed the effects of

AMPA and Sp-cAMPS on the turnover of putative CA3a/b presynaptic structures in slice cultures from *Thy1-spGFP^{mu}* mice. AMPA + AP-V or Sp-cAMPS increased the fraction of dynamic synaptophysin-accumulating profiles from 7.9 to 17.2 %, respectively 16.9% (**Fig. 6**), suggesting that many types of presynaptic terminals can be converted from stable to dynamic ones through AMPA-receptor and PKA activation.

2.2.3. FUTURE PERSPECTIVES AND DISCUSSION

Genetic tools to visualize live synaptic dynamics

The analysis in this study was made possible by the development of new genetic markers to image the plasmamembrane and synaptic vesicles in living neurons in situ. Because it visualizes details of neuronal protrusions with high sensitivity (e.g. spine necks, or small filopodia), the plasmalemmal marker is superior to cytoplasmic forms of XFP to study neuronal plasticity.

The combination of the synaptic vesicle and the plasmalemmal marker allows monitoring stable and dynamic presynaptic terminals in the same living neuron. Combined with the possibility to express any combinations of transgenes in small subsets of mouse neurons, this approach provides a powerful tool for detailed, high-resolution non-invasive molecular imaging of individual neurons and their subcellular compartments in living tissue. This was a prerequisite to compare the dynamics of distinct types of presynaptic terminals of the same axon over long periods of time.

Presynaptic terminal dynamics in mature slices

Several reasons prompted us to focus on hippocampal circuits to investigate the dynamics of presynaptic terminals. First, the central role of the hippocampus in experience-related learning and memory makes it a prime candidate system to search for synapse dynamics and investigate their regulation. Second, postsynaptic site dynamics have been studied in most detail in this brain structure, where they are influenced by interventions that alter the efficacy of synaptic connections in vitro (LTP, see refs. (Antonova et al., 2001; Yuste and Bonhoeffer, 2001)), and behavior in vivo (for a review see (Nimchinsky et al., 2002)). Information about the dynamics of presynaptic terminals in hippocampal circuits can thus be related to corresponding data on postsynaptic spines. A further major reason was that the architecture of

the circuitry in the hippocampus is comparatively simple and well characterized, and that circuit architecture is well preserved in hippocampal slice cultures (Gahwiler et al., 1997). An extensive body of experimental data (Dailey and Smith, 1996; Gahwiler et al., 1997) supports the notion that long-term hippocampal slices are mature physiologically, suggesting that basic features of the dynamics detected in this study may also apply to hippocampal circuits in vivo. These unique advantages should thus allow extending this study to provide a detailed quantitative and mechanistic analysis of presynaptic terminal dynamics and its regulation in the hippocampus, and in other brain circuitry. It will for example be of particular interest to determine whether different types of axons and neuronal structures exhibit unique presynaptic dynamic properties, possibly related to local circuit architecture and specific plasticity requirements. In addition, complementary studies of accessible presynaptic circuitry in vivo will show whether and to what extent comparable presynaptic dynamics take place in the adult brain.

Dynamic properties of defined presynaptic terminals

Our results provide evidence that presynaptic terminal numbers in mature hippocampal slices are in a state of dynamic equilibrium regulated by AMPA receptor activation and cAMP. The baseline of presynaptic terminal dynamics in unperturbed slice cultures was not affected by chronic blockade of synaptic activity (TTX), specific blockade of AMPA receptors, or short-term blockade of de novo protein synthesis (cycloheximide), or specific inactivation of PKA, suggesting that it was an intrinsic property of the hippocampal circuits in these mature organotypic cultures. It is still open the possibility that a protracted (days) blockade of synaptic activity can affect the dynamics of pre-synaptic terminals. Alternatively, other extra-cellular signals (e.g. guidance molecules and neurotrophic factors still highly expressed in the adult brain or adhesion molecules) through regulators of the actin cytoskeleton (e.g. small GTPases) could mediate the basal dynamism that we report likewise for post-synaptic sites during development (Gahwiler et al., 1997). The analysis of individual MFs and their terminals over periods of up to two weeks revealed that there was a distinct tendency for short-term dynamics, filopodia and epV to reappear at sites of previous epV, suggesting that MF may exhibit specialized sites of ongoing synapse formation/disassembly (see also (Pennetta et al., 2002)). This possibility is further supported by the observation that new terminals seemed to have a substantially higher probability of disappearing during the following few days than the average population of epVs or LMTfil (data not shown). Taken

together, these findings suggest that while a fraction of new terminals may become stabilized, a majority of dynamic terminals turns over within periods of several days.

Due to the ways in which axons and dendrites are arranged in the brain, structural plasticity at the pre- or postsynaptic level can have distinct consequences for the connectivity of neuronal networks. Because presynaptic boutons are usually distributed at substantial distances (many tens of microns) from each other along axons, the presynaptic dynamics demonstrated in this study can profoundly affect the connectivity of neuronal networks, as individual axons may be synapsing onto different neurons at different times. The synaptic connections of individual axons exhibit a remarkable degree of anatomical specificity with respect to target type(s), topography, numbers of synaptic contacts and positions of these contacts on dendritic trees. Corresponding specificity in presynaptic dynamics may ensure that local rearrangements in circuitry exhibit comparable specificity with respect to information transmission, and its experience-related modification.

Mechanisms regulating presynaptic terminal dynamics

The experimental conditions in the slice cultures allowed us to investigate molecular mechanisms that may regulate presynaptic terminal dynamics in these mature networks. We found that brief local high-frequency stimulation of MF greatly increased the fraction of dynamic LMTfil and their turnover rates, without corresponding effects on total synapse numbers. LMTfil are thought to mediate feed-forward inhibition of CA3 pyramidal neuron activation through local interneurons. The transiently enhanced dynamics and rearrangements of LMTfil may contribute to a remodeling of the local circuitry in CA3 during a sensitive period after the initial stimulation event. Through such remodeling, event-related circuitry may be refined and consolidated for further transfer in the hippocampal formation and to other brain centers.

AMPA and Sp-cAMPS also enhanced the fractions of dynamic epV and presynaptic terminal populations in CA3b, suggesting that these regulatory mechanisms apply to many types of presynaptic terminals. This enhancement of presynaptic terminal dynamics is reminiscent of the stimulatory role of activity in synapse elimination (Lichtman and Colman, 2000), and in synapse turnover during the early phases of circuit formation (Cline, 2001). The features of this stimulation were also reminiscent of the conditions required to induce long-term

potentiation of synaptic transmission. Like in synapse elimination, synapse dynamics in mature neuropil may mediate and reflect a competition by synaptic inputs for innervation of postsynaptic territories. The relative efficiencies of synaptic transmission by individual terminals innervating the same postsynaptic territory, and the status of postsynaptic receptors at any individual synapse are key factors in synapse elimination and in synapse dynamics during development (Lichtman and Colman, 2000; Cline, 2001). In a similar manner, and like in LTP, selective stabilization and destabilization of synapses in mature neuropil may be controlled by coincidence detection mechanisms, coupled to the expression of postsynaptic components and receptor subtypes with distinct regulatory and trafficking properties (Okabe et al., 1999; Cline, 2001; Shi et al., 2001).

A further main finding of this study was that different types of terminals from the same neuron differed in their dynamic properties, suggesting that, as is the case for the functional plasticity of presynaptic terminals (Toth and McBain, 2000), presynaptic dynamics may be defined by intrinsic features of presynaptic terminals and by local signals from the postsynaptic neuron. This is reminiscent of the intrinsically different stability properties of neuromuscular junction subtypes (Pun et al., 2002), suggesting that, like at the neuromuscular junction, distinctions in postsynaptic receptor clustering and maintenance properties may contribute to differences in the dynamic properties of central synapses. The stabilization of subtypes of synapses for very long times may provide mechanisms for long-term storage of information in brain circuits, whereas the destabilization and specific rearrangements induced by coincident activity may allow for the refinement and modification of that information by subsequent experience.

2.2.4. MATERIAL AND METHODS

Generation of transgenic mice. Mice expressing GFP constructs specifically in adult neurons were generated using the mouse Thy1.2 expression cassette, as described (Caroni, 1997) mGFP consisted of the first 40 amino acids of the protein MARCKS, a plasmalemmal targeting sequence (Wiederkehr et al., 1997), fused to EGFP. The N-term of MARCKS was modified to include palmitoylation sites at residues 3 and 4; spGFP or spRFP consisted of full-length synaptophysin fused to EGFP (Li and Murthy, 2001) or RFP. The transgenic mice

had no detectable phenotype, and the expression of these transgenes did not affect neuromuscular junction physiology (quantal content, post-tetanic potentiation and depression) or anatomy (ultrastructure of pre- and postsynaptic terminal, paralysis-induced nerve sprouting). Neurons expressing different levels of transgene exhibited undistinguishable morphologies in slice cultures. Out of a total of 30 lines, ten transgenic lines expressed transgene in subsets of neurons (see also reference (Feng et al., 2000)). The experiments were approved by the Swiss Veterinary Office.

Immunocytochemistry. Hippocampal slice cultures (> 40 days *in vitro*, *Thy1-mGFP*^{s} and *Thy1-mGFP/spRFP*^{s}) in 6-well plates were fixed for 10 min at RT with 3.5% PFA-containing culture medium. Tissues were rinsed in PBS, solubilized in 1%Triton X-100 in PBS (2ml) overnight (ON, 4°C), blocked in 50 mM NH_4Cl and 20% horse serum, rinsed with PBS containing 1% horse serum (PBS + HS) (Marrs et al., 2001), and incubated ON (4°C) in PBS+HS, with 2 μg/ml affinity-purified anti-NR-1 mouse monoclonal antibody (Pharmingen) (*Thy1-mGFP*^{s} and *Thy1-mGFP/spRFP*^{s}), plus rabbit-anti-synaptophysin (DAKO, Denmark) (*Thy1-mGFP*^{s}). Tissue slices were then rinsed with PBS +HS, incubated for 10–16 hours (4°C) in Alexa-Fluor-546 conjugated goat-anti-rabbit and Oregon green-438 conjugated goat-anti-mouse (Molecular Probes, Eugene, Oregon), rinsed and analyzed. Argon and He, Ne-G lasers (488/543 excitation), with Rhodamine and GFP filter sets (560-600 and 505-525 barrier filters) were used to simultaneously visualize both synaptic markers in the same samples. Step sizes were 0.2 μm, for stacks of 9-30 μm. A 100X water immersion objective (NA = 0.1, Zeiss) was used for image acquisition. Synaptophysin and NR1 contents in MF terminals were scored in single optical planes and in 3D reconstructions.

In *situ* hybridization. In *situ* hybridization was carried out with digoxigenin-labeled cRNA probes corresponding to the entire EGFP gene. The brain was removed soon after cervical dislocation, frozen in Tissue-Tek (Sakura Finetek, Torrance, CA) and stored at – 80 C°. Sagittal section (12 μm thick) were prepared using a cryostat and thaw-mounted on glass slides. In *situ* hybridization for EGFP was carried out with cRNA probe corresponding to the entire EGFP coding sequence. The cDNA of interest was cloned into a vector such as a pBS+ or pcDNA3 that contained recognition sites for RNA polymerase (T3, T7 or SP6). 5

μg of plasmid DNA were digested with appropriate restriction enzymes to produce either a sense or an antisense RNA probe. pCDNA3-EGFP was linearised using NOTI and then we used T7 polymerase to generate the sense probe. To have the antisense probe the plasmid was cut with BstxI and the SP6 polymerase was used. The hybridized sections were treated with anti-digoxigenin sheep antibody (Boehringer) coupled to alkaline phosphatase. Anti-digoxigenin antibody and therefore cRNAs were visualized in a color reaction with BCIP-NBT (baumeister 97).

Propidium iodide assay for cell death. Cell death in the slices was assessed by Propidium Iodide (PI, Sigma) incorporation into the cells (Lahtinen et al., 2001). PI was added to the slices in tyrode's at a final concentration of 1 μg/ml for 30 min at RT. After a brief (5 min) wash in tyrode's, PI fluorescence images were acquired with an optimized filter set (530-585 filter; 2.5X objective connected to a Hamamatsu digital CCD camera). Images (512X512 pixels) were opened in Image software after the same mask to visualize the nuclei was applied in Photoshop (Suppl. Fig. 6h). Dead cells were counted with the function "analyze particles". For each experimental condition, data were compared (ANOVA) to those from untreated control slices, which exhibited a low level of spontaneously degenerating cells (Suppl. Fig. 6).

Live imaging in hippocampal slice cultures. The method of (ref. 13) was used to culture hippocampal slices because of its convenience for long term imaging in comparison to the "roller tubes" technique, which presented problems in preserving sterile conditions. Briefly, P8-9 pups were killed by decapitation, and hippocampi rapidly dissected out and placed in a MEM (Gibco) based ice-chilled medium. Usually, six to eight 400 μm-thick slices were selected from one hippocampus. They were then incubated in 5% CO_2 at 35 °C. For time lapse imaging, slices were taken out of the incubator in a physiological solution at RT (Gibco based). An Olympus set up (Bx61 LSM Fluoview) was used for confocal microscopy (see below). For conventional microscopy images were acquired with a Zeiss Axioskop equipped with a HBO 50 mercury lamp for fluorescence illumination, water immersion objectives (Achroplan 40X/0.75W, 63X/0.9W and 100X/1.0W), NDF (Neutral-Density Filters) (0.06, 0.25, 0.5, d = 18), and a Hamamatsu digital CCD camera (C4742-95) controlled by the QED Camera Plug-in for Power Mac G4 (QED Imaging Inc., Pittsburgh, PA). Due to the high expression levels in Thy1-transgenic mice, fluorescent images

exhibited high signal-to-noise ratios (Suppl. Fig. 7), and where either not, or only slightly contrasted, if not stated otherwise. Each imaging session, from the time the slice was taken out of the incubator to the time it was put back, lasted approximately 10 minutes. The following imaging conditions were used for *Thy1-mGFP*^{s} and *Thy1-mGFP/spRFP*^{s} slices: 40X objective, 0.25+0.5 NDF for up to 2 min to identify the proper axon (MF), 100X objective 0.25+0.5 NDF for 10-30 sec to identify the LMT (landmark); 100X objective, 0.25 NDF for 5-7 min to acquire images (20-70/session, 512X512 pixels). Live imaging was carried out in region CA3b (Acsady et al., 1998); imaging of CA3c was excluded to avoid photo damaging of sensitive neuronal cell bodies. Under these conditions no photo damaging was detected following up to five separate imaging sessions (see later). For time lapse recordings data set consisted of 36 different MF regions (N=4 MF) from >40 day-old hippocampal slice cultures, imaged for 3-6 minutes (10 sec frames). Measurements were performed with Image software, using a threshold function, by an observer blind to the experimental conditions. Where indicated, Sp-cAMPS (Biolog), Glutamate (RBI), Cytochalasin D (Sigma), TTX (Allergen AG, Switzerland), AMPA (RBI, 400 nM), AP5 (RBI, 100 μM), cycloheximide (Sigma, 60 μM), SYM2206 (Tocris, Bristol, 100 μM), and BDNF (serum starvation over night, followed by serum free conditions with the neurotrophin (Marty et al., 2000)) were added to the culture medium after a first imaging session. The treatment with Sp-cAMPS was limited to 20 min, when cultures were washed and then imaged at the intervals indicated in the figures. Glutamate was applied at concentrations of 10-100 μM directly into the culture medium after the first two time points were acquired (To and T6h). AMPA (with or without AP5) and cycloheximide were applied for 6h (24 h treatments were toxic). Basal values of LMTfil dynamics at 1d were not affected by a 6h treatment with cycloheximide (MI = 0.48 ± 0.05, unpaired t-test P = 0.9). When cycloheximide was combined with AMPA + AP5, the protein synthesis inhibitor was applied 1h before the Glutamate receptor agonists.

Hippocampal slice cultures were stimulated in the CA3 stratum lucidum region with monopolar glass electrodes. The electrodes were placed in the proximity of mGFP-positive MF axons, which were subsequently analyzed for LMTfil dynamics. Reliable stimulation of MF is achieved by this protocol (not shown). Two stimulation patterns were used: 1) High Frequency Stimulation (4 times 100 Hz for 1s each; interstimulation interval: 30 sec; single

stimulus duration: 100 μs); 2) Low Frequency Stimulation (1 Hz for 15 min; single stimulus: 100 μs).

Hippocampal whole mount preparation (Khalilov et al., 1997). Following decapitation, the brain was dissected in ice-cold medium in the presence of TTX and Mg^{2+} to prevent transmitter release-dependent toxicity. Cerebellum and frontal lobes were removed by coronal cuts, and brain stem, midbrain and striatum were separated from the hippocampus, using 2 spatulas. The entire procedure, from sacrificing the mouse to the whole-mount preparation, took less than 6 minutes. The right and left hippocampi, connected ventrally through the septum, were then exposed for direct imaging (continuous oxygenation with 95% O2, 5% CO2) under a fluorescent upright microscope. Only terminals belonging to granule cells in the free blade of the hippocampus could be imaged with this procedure.

Analysis of epV dynamics. Typically, axonal segments in CA3 (400-500 μm) were selected based on the presence of easily identifiable landmarks, such as LMT or characteristic axonal curvatures. Segments were then scored for the presence of swellings and/or filopodia. To be considered as epV, mossy fiber axonal swellings had to fulfill the following criteria: 1) The maximal diameter (perpendicular to long axis if epV is elliptical) had to be at least twice the width of the corresponding axon (the focal plane where a varicosity was most evident was used for size measurements); 2) swellings had to be visible in at least 2 focal planes to avoid potential image acquisition artifacts; 3) to exclude swellings reflecting axonal transport, epV had to be detectable at the same position along the axon throughout at least two separate observations. Data from 400-700 μm long continuous stretches of axons were aquired for all experimental conditions, and all terminal structures of a given type (epV, LMT, LMTfil) were included in the analysis. An experimenter blind to the experimental conditions performed all size measurements with Image software at 8:1 magnification, using a threshold function to a single level throughout each session. To control for possible artifacts that may have been introduced through image analysis, the experimenter blind to the experimental conditions also scored the raw data. No significant difference was detected between the two data sets (9.4% versus 8.6% dynamic epV). Values were averages of three measurements.

Quantification of LMTfil dynamics. LMTfil were defined as any axonal extension unequivocally traced back from a swelling larger than 3 μm (LMT) in diameter. Individual images were superimposed in Adobe Photoshop, and rotated to correct for x-y shifts. Single layers were then opened with Image software, "Threshold" and "Make Binary" tools were used to standardize measurements within one imaging session, and filopodial areas were calculated. Measurements were carried out by an observer blind to the experimental conditions. A motility index (MI) based on accumulated filopodial areas while the filopodia move over time was derived as described (Dunaevsky et al., 1999; Chang and De Camilli, 2001). Two filopodium configurations exhibiting equal length, and a 50% overlap in area lead to an MI value of 0.5. By only considering as dynamic LMTfil with MI values larger than 0.6, we excluded the possibility of including variations due to local tissue distortions. This possibility was further excluded by analyzing 3D reconstructions of LMTfil configurations. Ranges of LMTfil retraction/elongation rates were as follows: untreated slice, average value: 2 μm/4 h; max. value: 4 μm/4 h; BDNF treated slices: average value 4 μm/4 h; max. value 8 μm/4 h; $NCAM^{-/-}$ slices: average 5 μm/4 h; max. value 10 μm/4 h. Stat view (for Mac) was used for all the statistical analysis.

Time-lapse imaging and analysis of slices from *Thy1-spGFP*^{mu} mice. To visualize the dynamics of synaptic puncta, imaging fields were about 80 μm^2. To maximize the discrimination of puncta from background, parameters were set as follows: argon laser 488 nm (GFP imaging); barrier filter 505-525; intensity minimized to 5% with C.A. 100μm; PMT 800; gain 5.3; offset 0%. Initial scanning of the slice was carried out using neutral density filters (fluorescent mode). Stacks included all puncta within a given range of z-axis, and were projected onto one plane for analysis (horizontal view). Background was subtracted using an option of the Fluoview software, and "Metamorph 4.6r7" was used for the subsequent steps. All images acquired during the same session were thresholded equally, and superimposed correcting for x-y shifts. To try to standardize fluorescent signals among different confocal sessions, at the beginning of each session we set the gain and offset to ensure that the same saturation levels were obtained (i.e. most intense signal just below saturation, and background adjusted just above detection limit). Sizes of puncta were calculated with an Integrated Morphometric Analysis tool. Only puncta between 1.5-3 μm and/or 50-300 pixel area (0.14667 pixel/ μm) were included in the analysis. This range was

chosen to exclude transport packets and LMT. To exclude ambiguities due to sub-micron (0.1-0.5 μm) shifts in the position and shape of puncta, only gain/loss events with no detectable fluorescence in the surrounding 0.5 μm were included in the analysis. Changes in the size and/or shape of puncta were not scored as gain/loss events. The size of boutons in the CA3 region was in accordance to previous in vivo data (1-10 μm), and subsequent immunocytochemistry for synaptic vesicle markers yielded labeled structures undistinguishable from those previously detected in the living cultures (data not shown).

Controls for photo damage. All slices and structures included in the analysis were assessed for signs of photo damage one day after the last imaging session. Characteristic signs of damage (mGFP marker) include: drastic weakening of fluorescent signals; swelling and breakdown of axons into a chain of beads; blurred GFP signals around membranes due to degradation and leakage; formation of large blebs on cell bodies and dendrites; loss of dendritic spines (Bastmeyer and O'Leary, 1996). Using Neutral Density Filters, objectives with high NA, laser intensity <5%, and minimizing exposure and picture acquisition times (one imaging session lasted around 10 min overall), axonal segments of up to 500 μm could be imaged repeatedly (at least 4 different time points), without inducing photo damage. These imaging conditions did not influence dendritic motility and short term axonal dynamics or axonal transport (data not shown). In a further set of control experiments, we determined the possible influence of fluorescent light on the translocation rates of transport packets (spGFP marker). Translocation rates were 0.08 ± 0.05 μm/sec (in the vicinity of stable clusters; N = 24, 6 slices), and 0.3 ± 0.1μm/sec (>10 μm away from stable clusters; N = 37, 9 slices). These values are in good agreement with those reported from dispersed culture studies (Li and Murthy, 2001), and were not affected by the imaging conditions used in this study (no detectable changes between sessions, or up to 2 days after the last session, when up to 3 fields of ca. 150 μm^2 were imaged repeatedly).

Acknowledgments

We thank the members of the Caroni group for helpful discussions, Y. Barde and D. Muller for comments on the manuscript, M. Moosmayer (D. Muller lab, Geneva) for introducing us to the slice culture technique, the Matus lab for valuable technical help, L. Xu for help with electrophysiology, and I. Dodevsky for help with quantifications. We are very grateful to M. Abegg and M. Scanziani (ETH, Zurich) for generous help with the electrophysiology experiments. SA was supported by the Swiss National Science Foundation and the Kanton Basel-Stadt. The Friedrich Miescher Institute is a branch of the Novartis Research foundation.

2.2.5. FIGURES

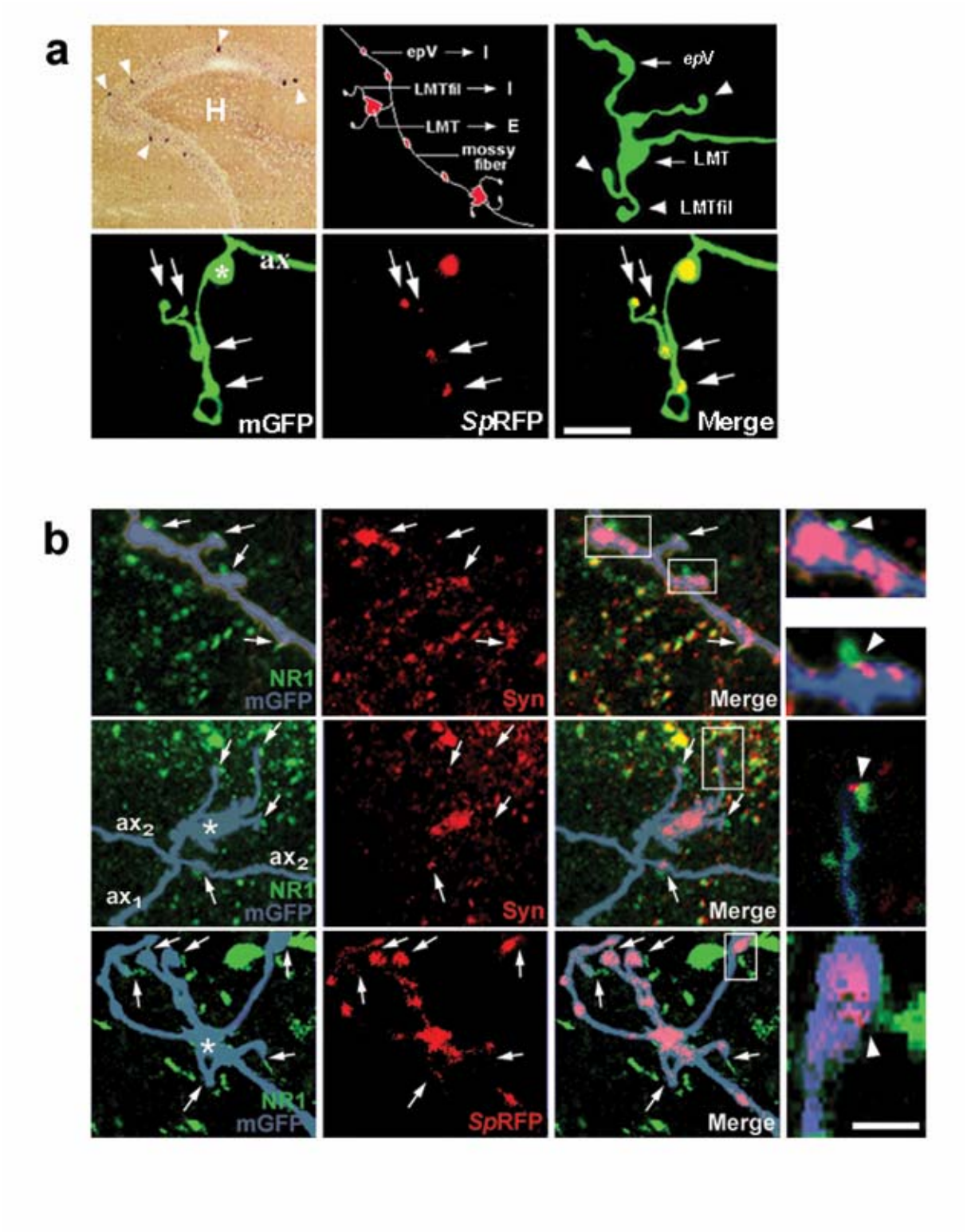

FIGURE 1

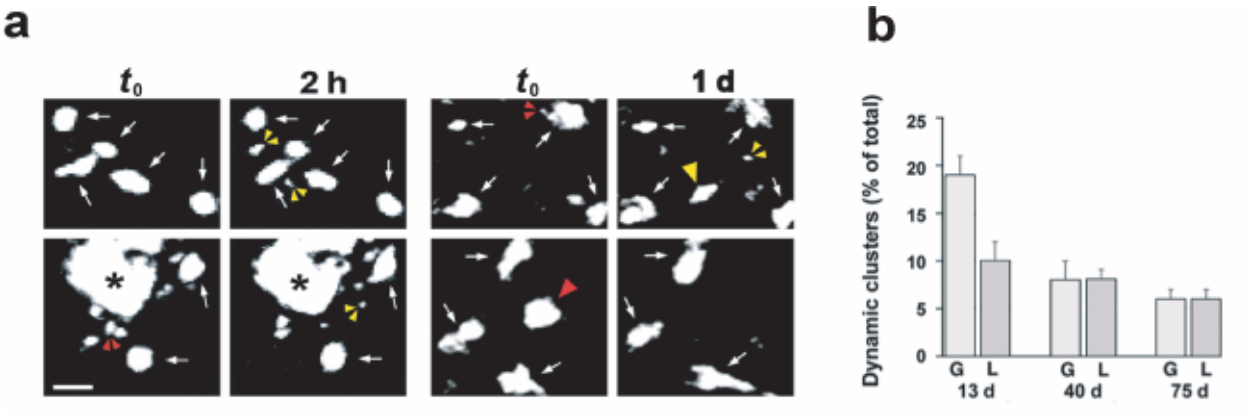
a
t_0
2 h
t_0
1 d
b
Dynamic clusters (% of total)
25
20
15
10
5
0
G L
13 d
G L
40 d
G L
75 d

FIGURE 2

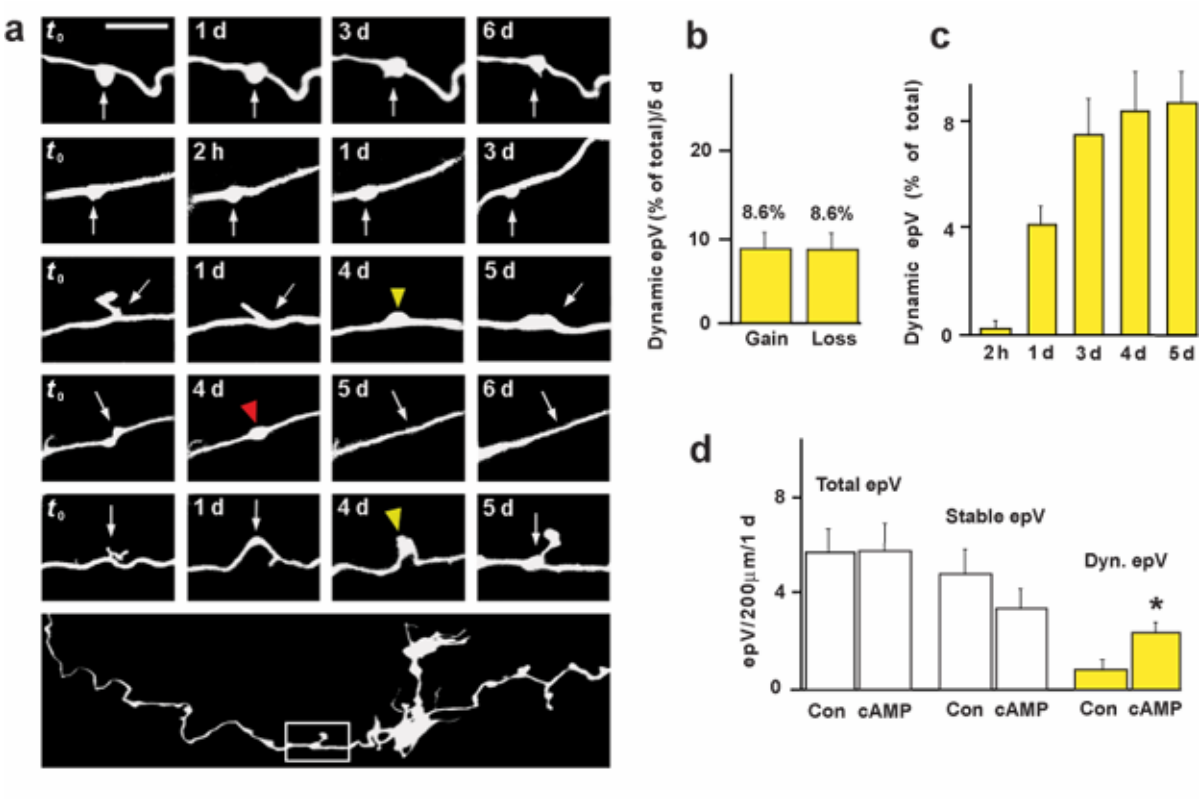
a
t_0
1 d
3 d
6 d
t_0
2 h
1 d
3 d
t_0
1 d
4 d
5 d
t_0
4 d
5 d
6 d
t_0
1 d
4 d
5 d
b
Dynamic epV (% of total)/5 d
20
10
0
8.6%
8.6%
Gain
Loss
c
Dynamic epV (% of total)
8
4
0
2 h
1 d
3 d
4 d
5 d
d
epV/200µm/1 d
8
4
0
Total epV
Stable epV
Dyn. epV
*
Con
cAMP
Con
cAMP
Con
cAMP

FIGURE 3

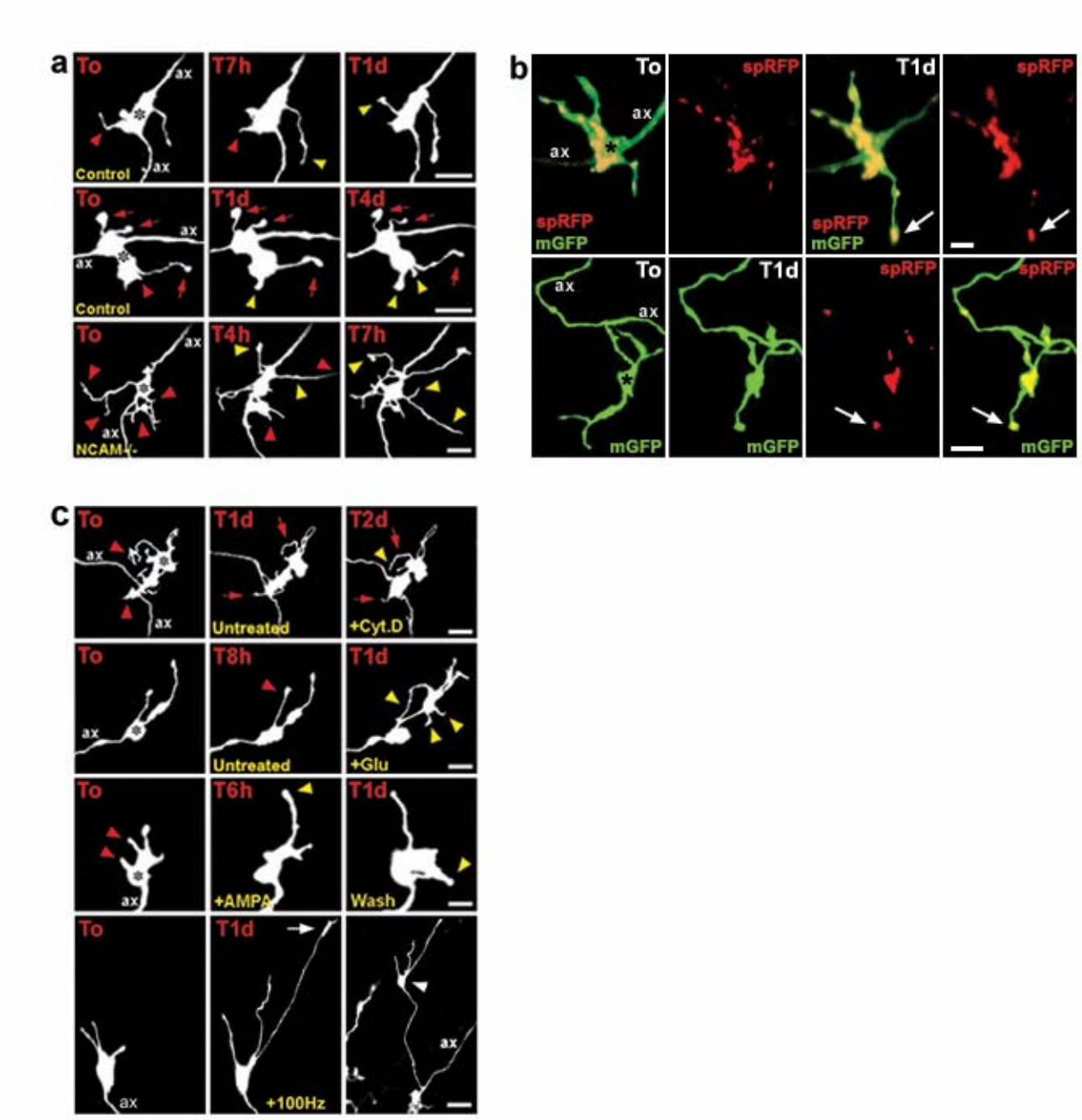
a
To
T7h
T1d
ax
Control
To
T1d
T4d
ax
Control
To
T4h
T7h
ax
NCAM+/-
b
To
spRFP
T1d
spRFP
ax
spRFP
mGFP
spRFP
mGFP
To
T1d
spRFP
spRFP
ax
mGFP
mGFP
mGFP
c
To
T1d
T2d
ax
Untreated
+Cyt.D
To
T8h
T1d
ax
Untreated
+Glu
To
T6h
T1d
ax
+AMPA
Wash
To
T1d
ax
+100Hz
ax

FIGURE 4

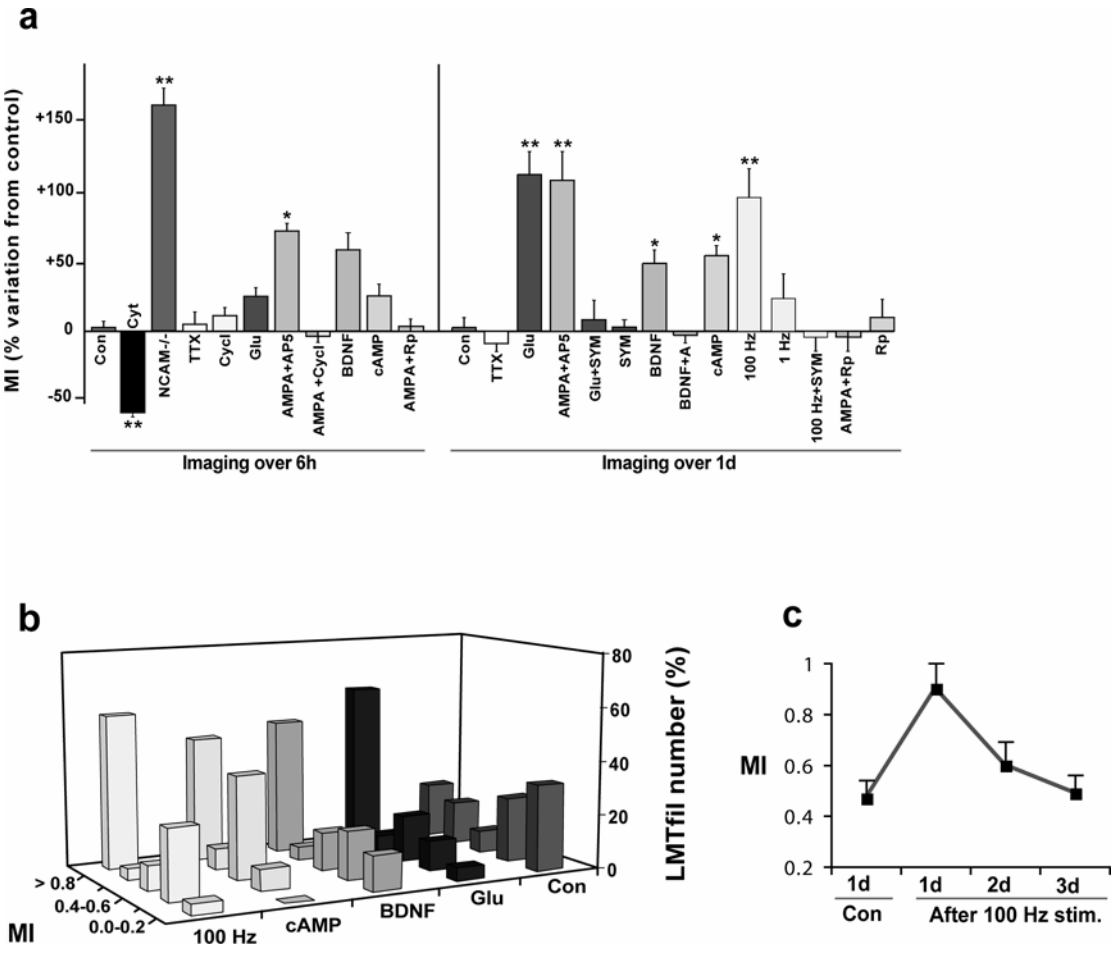
a
MI (% variation from control)
+150
+100
+50
0
-50
Con
Cyt
NCAM-/-
TTX
Cycl
Glu
AMPA+AP5
AMPA +Cycl
BDNF
cAMP
AMPA+Rp
Con
TTX
Glu
AMPA+AP5
Glu+SYM
SYM
BDNF
BDNF+A
cAMP
100 Hz
1 Hz
100 Hz+SYM
AMPA+Rp
Rp
Imaging over 6h
Imaging over 1d
b
LMTfil number (%)
80
60
40
20
0
> 0.8
0.4-0.6
0.0-0.2
MI
100 Hz
cAMP
BDNF
Glu
Con
c
MI
1
0.8
0.6
0.4
0.2
1d
Con
1d
2d
3d
After 100 Hz stim.

FIGURE 5

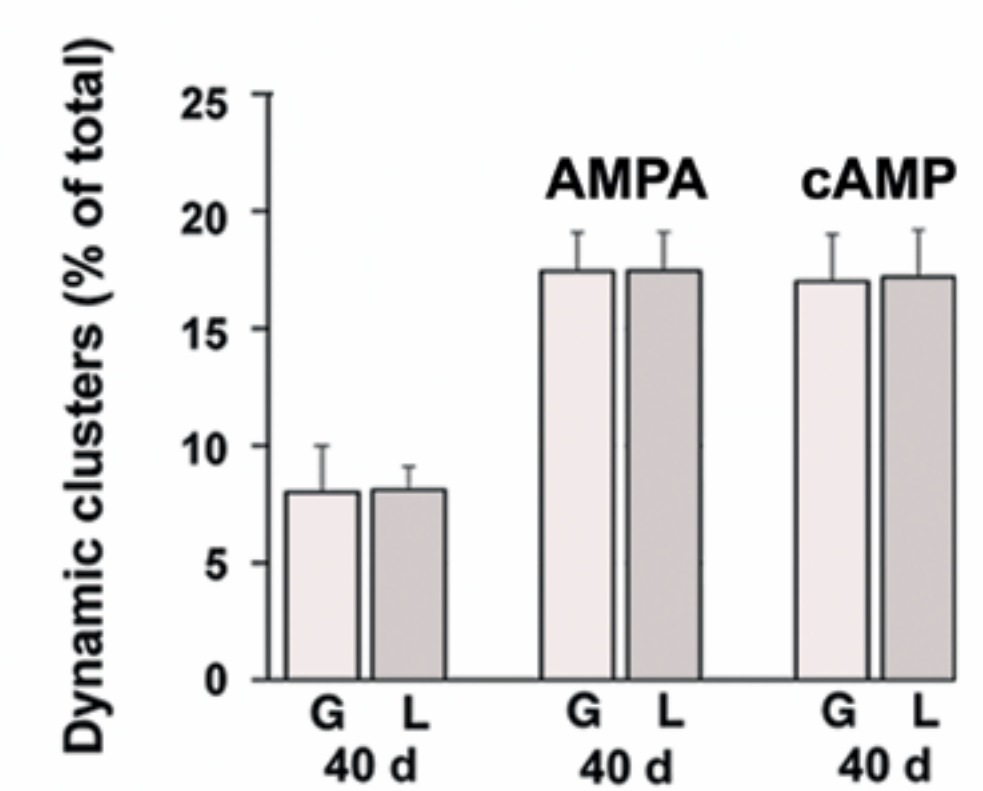
Dynamic clusters (% of total)
25
20
15
10
5
0
AMPA
cAMP
G L
40 d
G L
40 d
G L
40 d

FIGURE 6

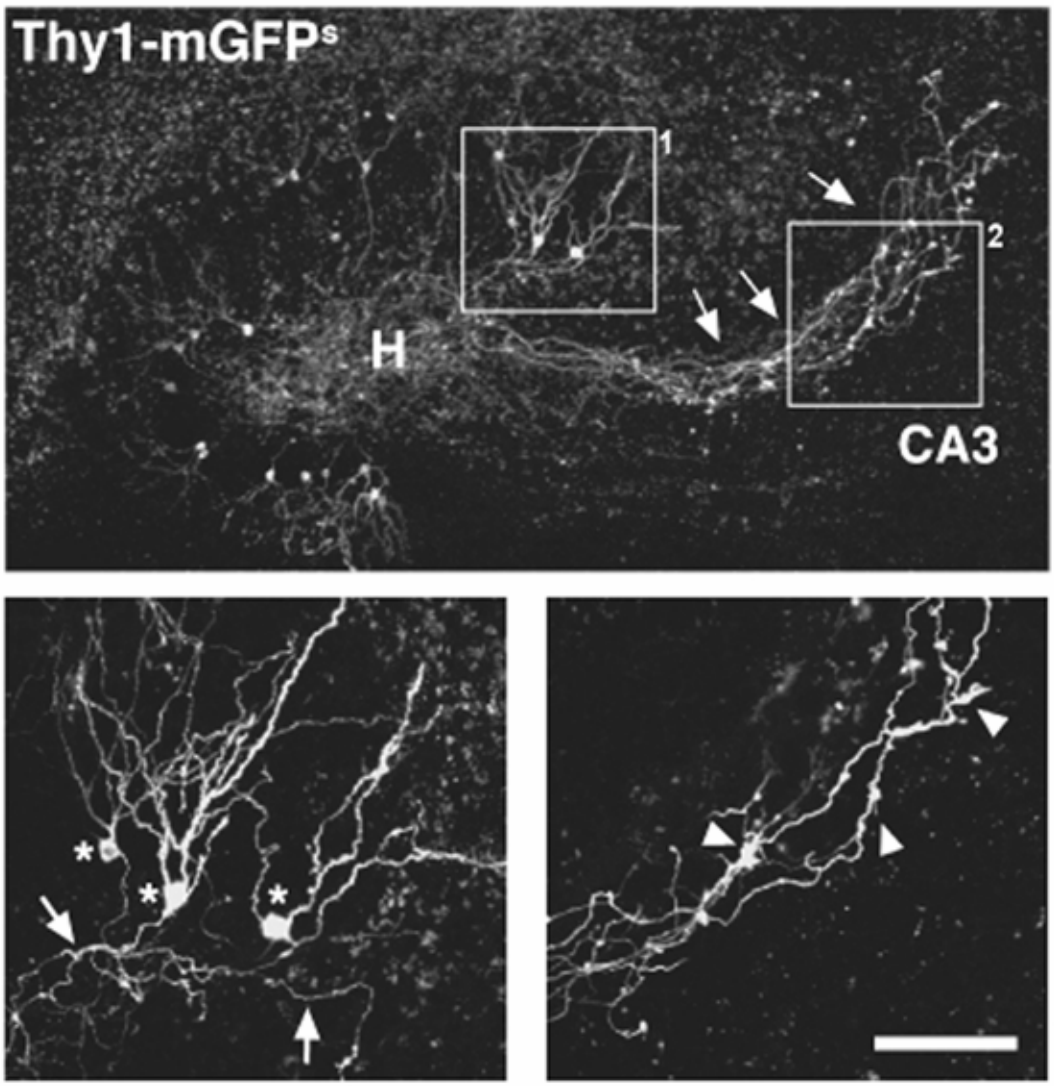

SUPPL. FIGURE 1

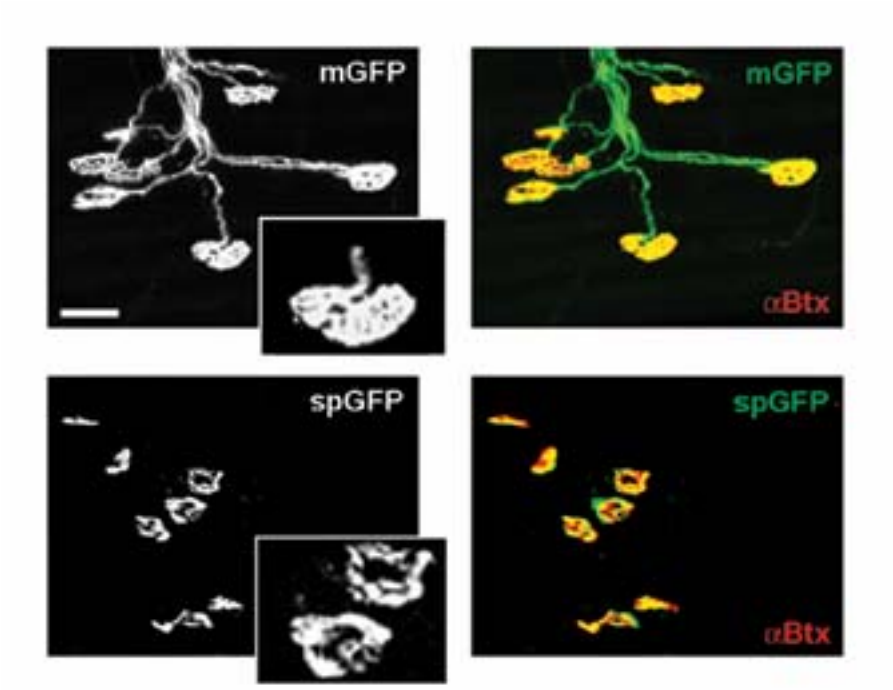

SUPPL. FIGURE 2

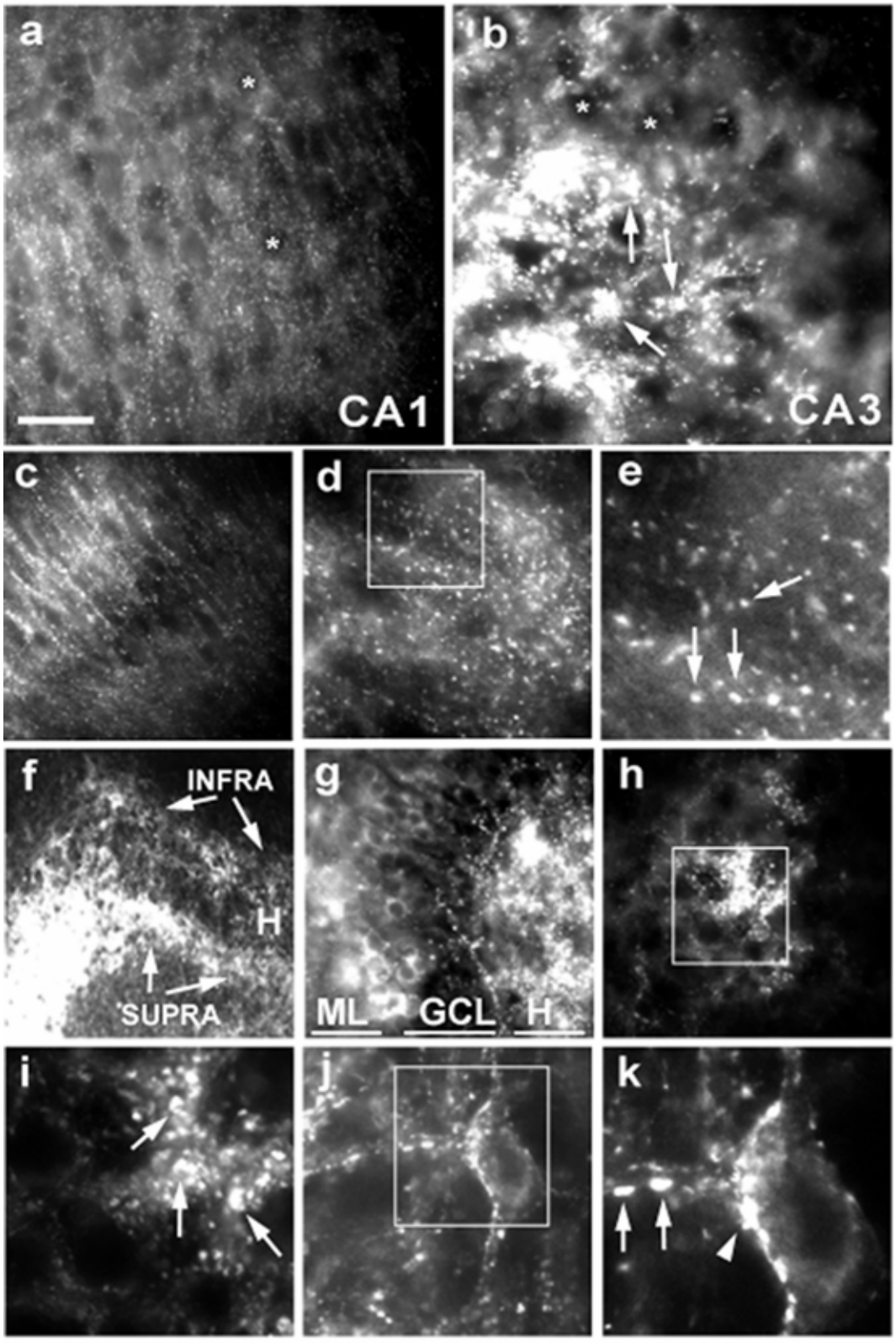

SUPPL. FIGURE 3

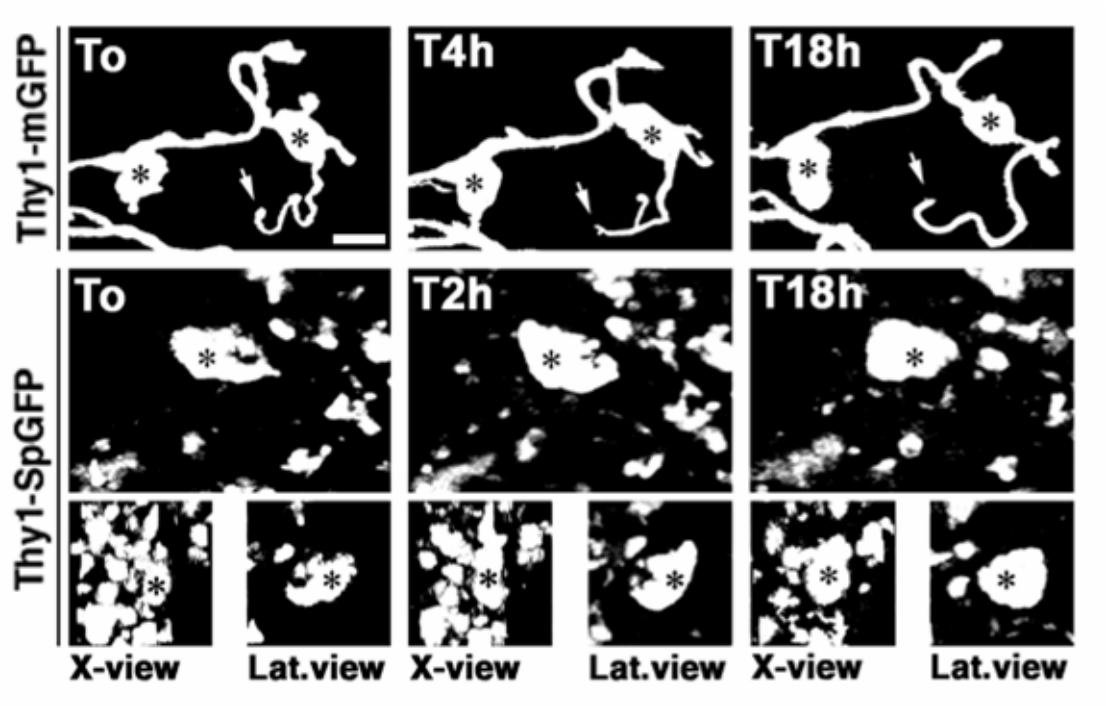

SUPPL. FIGURE 4

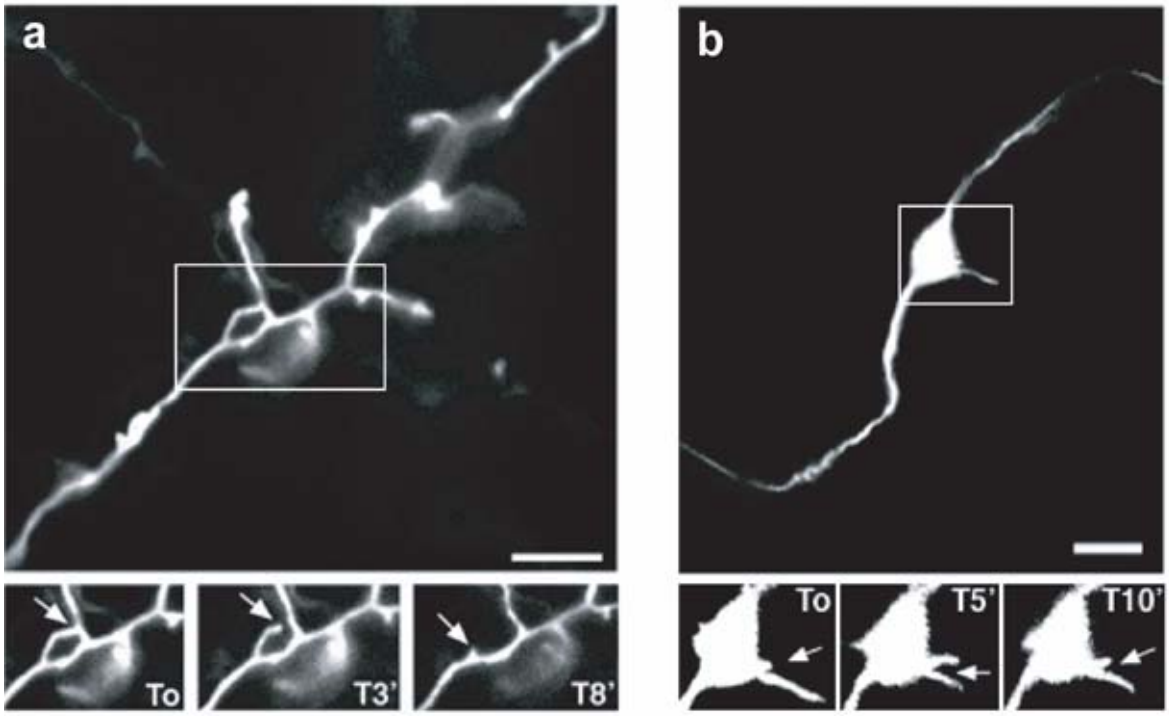

SUPPL. FIGURE 5

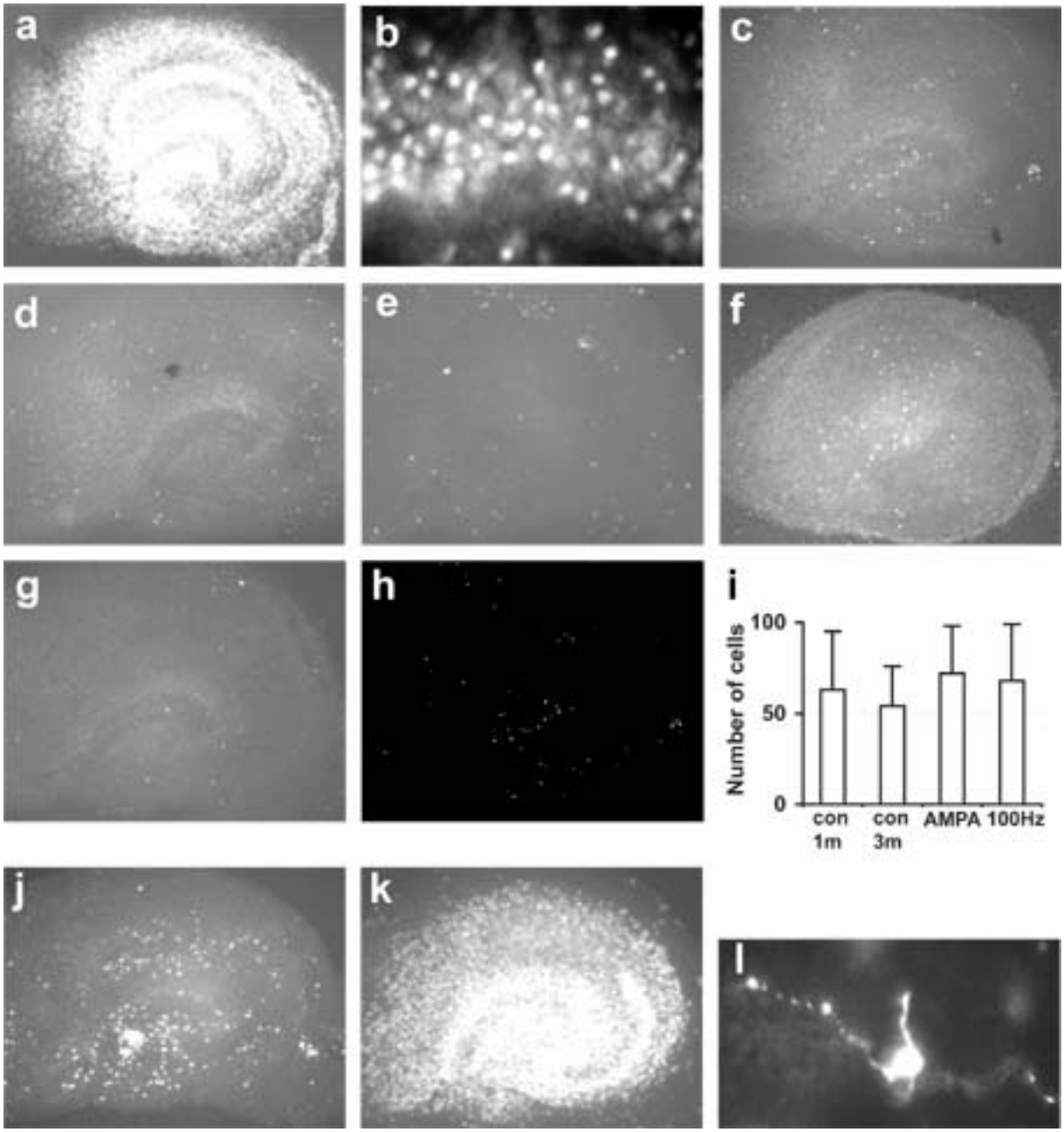

SUPPL. FIGURE 6

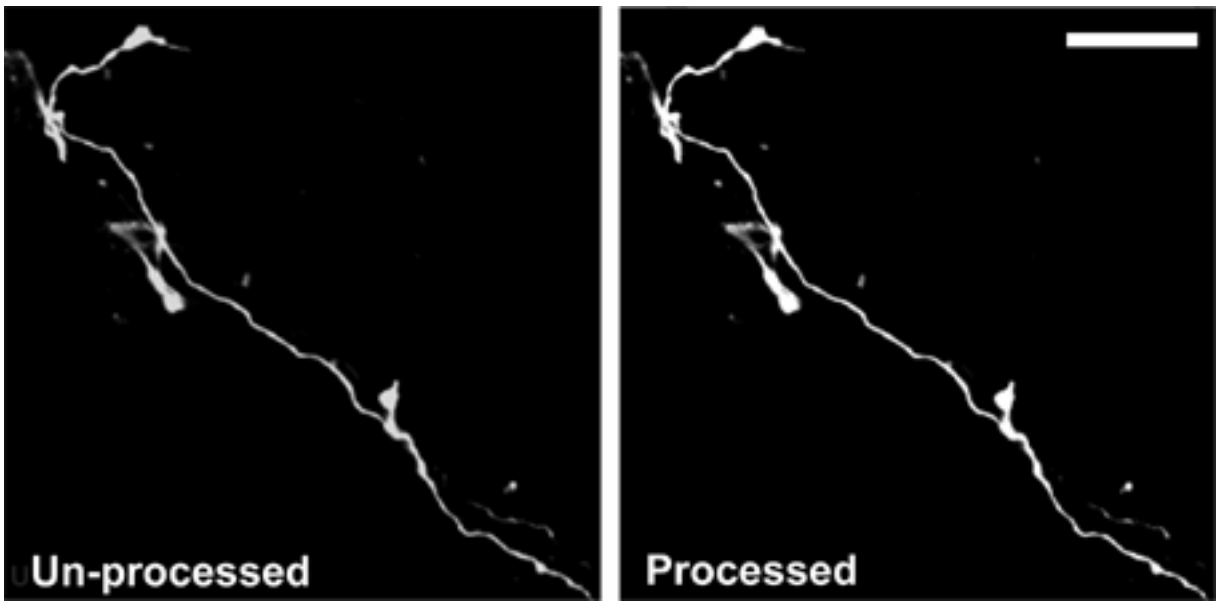

SUPPL. FIGURE 7

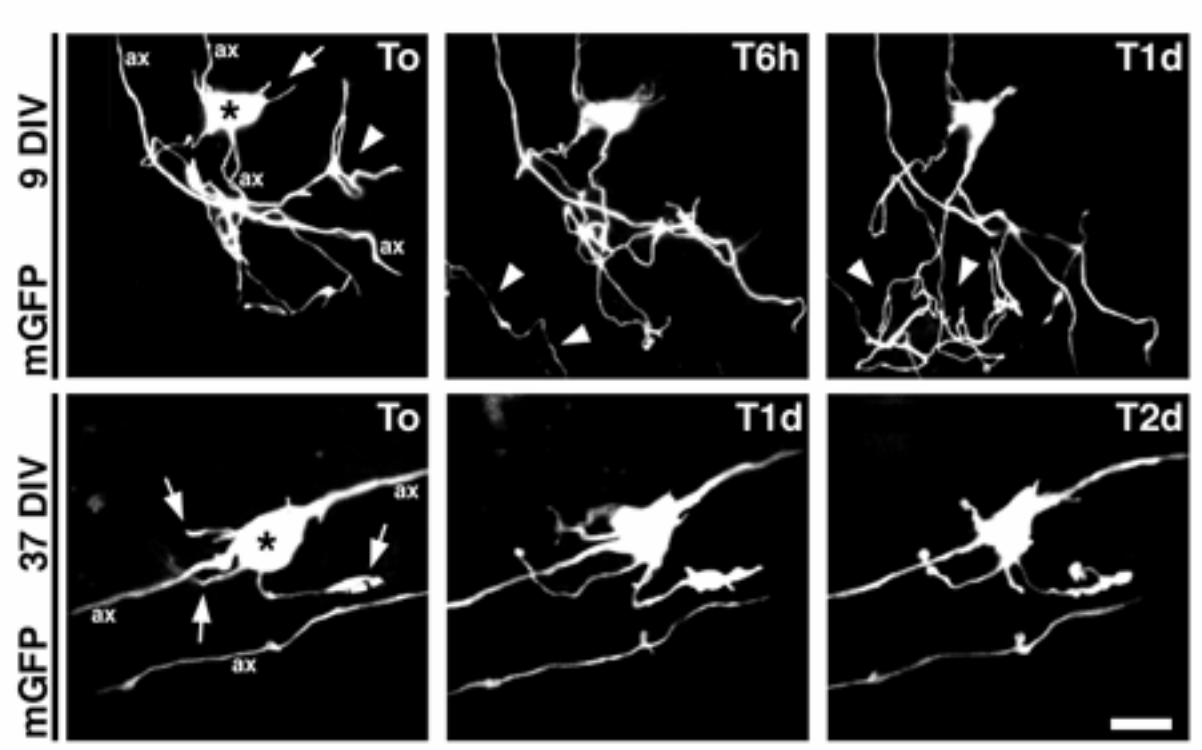

SUPPL. FIGURE 8

2.2.6. FIGURE LEGENDS

Fig. 1. Visualization of mossy fiber arborization and presynaptic endings using transgenic lines expressing membrane- and/or synaptic vesicle-targeted spectral variants of GFP in subsets of neurons.

(**a**) First row, first panel: Expression of mGFP mRNA in small subset of hippocampal neurons of *Thy1-mGFP*^{s} mouse. The in situ hybridization panel shows single dentate gyrus granule cells expressing transgene (dark color reaction (arrowheads); 8 positive neurons are shown on the section). H, hilus. First row, second panel: Schematic representation of presynaptic terminal distribution along granule cell axon (mossy fiber). EpV and LMTfil synapse onto inhibitory interneurons (I), whereas LMT form complex synapses with excitatory CA3 pyramidal neurons (E). First row, third panel: Visualization of MF axon expressing mGFP. The high-magnification panel shows details of the axon in CA3b, with one LMT (asterisk), three LMTfil (arrowheads), and one epV (arrow).

Second row: Accumulation of synaptic vesicle clusters in LMT (asterisks), and at LMTfil endings and varicosities (arrows). Live imaging of slice culture from *Thy1-mGFP/spRFP*^{s} mouse; ax: axon. Bar: 12 (first row, third panel), and 14 μm (second row).

(**b**) Synaptophysin (presynaptic marker) and NR1 (postsynaptic marker) at anatomically identified (mGFP fluorescence) epV, LMT and LMTfil. Slice cultures were fixed and stained with anti-synaptophysin (syn, red; first two rows) and anti-NR1 antibody (green; all rows). The axon has been pseudo-colored (purple mask). First row: z stack projection (121 images) of mGFP-expressing mossy fiber (*Thy1-mGFP*^{s}), with 4 synaptophysin and NR1-positive epV (arrows). Inserts on the right: detailed views of single confocal images from two boxed regions, demonstrating co-localization of the two synaptic markers at epV (arrowheads). Second row: z stack projection (27 μm) from a *Thy1-mGFP*^{s} culture. Note co-localization of both synaptic markers at LMTfil (arrows, ax_1). Panel on the right: single confocal image from the boxed region, showing co-localization of both synaptic markers at one LMTfil (arrowhead). Third row: z stack projection (52 images, 10.4 μm) across one LMT (asterisk) and its LMTfil from a *Thy1-mGFP/spRFP*^{s} culture. Note co-localization of SpRFP fluorescence and NR1 at LMTfil (arrows). Panel on the right: single confocal image from the boxed region, showing co-localization of both synaptic markers at one LMTfil (arrowhead).

Bar: 3/1.4 (upper row / single plane images on the right), 5/2.7 (middle row / single plane image on the right), 4/0.7 μm (lower row /single plane image on the right).

Fig. 2: Matched frequencies of synaptophysin puncta appearance and disappearance events in mature hippocampal slice cultures.

(**a**) Dynamics of spGFP puncta. Two examples each of confocal time-lapse imaging in CA3b over 2 hours (panels on the left) and 1 day (panels on the right). Figures are projections of 43 images, spanning 7.6 μm in the z-dimension. Arrows/arrowheads point to clusters larger than 1.5 μm, which stayed (white), disappeared (red), or appeared (yellow) during the observation time. Double-arrowheads point to examples of transport packages (< 1μm). Note rapid translocation of transport packages. While exhibiting alterations in shape, the majority of puncta were maintained. Asterisk: LMT. Bar: 3 μm.

(**b**) Turnover of spGFP puncta in CA3b in hippocampal slice cultures at 13, 40 and 75 days in vitro (*Thy1-spGFP*^{mu} mice). G: gain events; L: loss events. Note higher frequency of turnover with net increase of puncta in the young slice culture, and balanced appearance/disappearance events in the older cultures. Time between observations: 1 day. The values are means and SEM from 5 representative fields (at least 50 puncta per field).

Fig. 3. EpV dynamics in mature hippocampal slice cultures.

(**a**) Time-lapse imaging series in 1.5 months cultures. The two top panels show examples of epV (arrows) that were stable over 6 (first row) and 3 days (second row). The four bottom panels show examples of dynamic epV. The varicosities in the third and fifth row appeared during imaging (yellow arrowhead), whereas that in the fourth row persisted for four days (red arrowhead), and then disappeared. The bottom panel shows a low magnification view of the axon in the fifth row (at 5d); the epV imaged during the experiment is boxed. Note the presence of landmark structures (e.g. LMT, asterisk) along the axon, allowing for unambiguous relocation of imaged epV at subsequent imaging sessions. Bar: 5 μm.

(**b**) Dynamics of epV in one month-old slice culture (*Thy1-mGFP*^{s} *mice*). Note equal frequencies of appearance and disappearance events. Time between observations: 5 days. Values are means and SEM (12 mossy fibers).

(**c**) Frequency of dynamic epV as a function of the time elapsed between repeated observations (N = 8, 146 epV).

(**d**) Sp-cAMPS increases the fraction of dynamic epV and their turnover rates, but not their total numbers. Time between observations: 1 day; N = 4, 1395 μm of total axonal length each. The fraction of dynamic epV was significantly increased (P = 0.01, Mann-Whitney test).

Fig. 4. LMTfil dynamics in mature hippocampal slice cultures.

(**a**) LMTfil dynamics under basal conditions. Time lapse imaging of *Thy1-mGFP*^{s} 1.5 month-old slice cultures. Imaging of LMTfil over 1 and 4 days (wildtype; first and second rows), and 7 hours (*NCAM-/-*, third row). Red arrowheads: lost or retracted filopodia; yellow arrowheads: new or extended filopodia; asterisks: LMT. Note presence of stable and dynamic LMTfil on same LMT (second row), and enhanced dynamics in the absence of NCAM. Bars: 5μm.

(**b**) Dynamic LMTfil contain synaptophysin in living tissue slices. Examples of two repeated observations over 1 day in 45 (top row) and 53 day-old (bottom row) Thy1-mGFP/spRFP^s tissue slices. Remodeling of LMTfil at both the membrane (mGFP) and synaptic vesicle (spRFP) level is evident in living terminals over 1d (arrows, top row). Note the presence of spRFP signal at dynamic LMTfil endings (arrows). Asterisks are LMT. Ax: axon. Bar is 5 μm in top row and 4.2 μm in bottom row.

(**c**) Effects of Cytochalasin D, Glutamate, AMPA, and 100 Hz stimulation on LMTfil dynamics. Experimental conditions as described above. Cytochalasin D (5 μM; arrows point to LMTfil that were dynamic before, but not after Cytochalasin D) and Glutamate (100 μM) were added immediately after the second observation. AMPA was added for 6h, immediately after the first observation. The high-frequency stimulation protocol was applied immediately after the first observation (panel on the right: 1d, lower magnification image to show the position of the LMT, arrowhead). Note substantial change of LMTfil arrangement 1d after 100 Hz stimulation. The unusually long LMTfil on the right also ends with a swelling (arrow), suggesting the presence of a presynaptic terminal. Bars: 5μm.

Fig. 5. Regulation of LMTfil dynamics through high-frequency stimulation, AMPA-receptor activation, Sp-cAMPS and BDNF in mature hippocampal slice cultures.

(**a)** Average motility indices (MI) of LMTfil without (Con), or with treatments, as indicated. The graph shows deviations of MI values from those under control conditions. Absolute values for MI under control conditions were 0.28 ± 0.03 (6h) and 0.47 ± 0.05

(1d). Sample sizes for each experimental condition: 24-36 LMTfil, 10-15 LMT, 4-6 mossy fibers, 4-6 independent experiments; values are means, and SEM. Cytochalasin D induced a significant reduction in MI (P = 0.0002, paired t-test); MIs in the absence of NCAM were significantly higher than control (P = 0.0007, ANOVA, Fisher's test); Glutamate, AMPA and BDNF, Sp-cAMPS and 100 Hz stimulation enhanced average MI values at 1 day (P = 0.005, 0.004, 0.02, 0.02, 0.01, respectively, unpaired t-test), whereas TTX, Glutamate + SYM2206, SYM2206 alone, BDNF + anti-BDNF (kind gift of Y. Barde, BDNF+A), low-frequency stimulation (1 Hz), 100 Hz + SYM2206, AMPA + Rp-cAMPS, and Rp-cAMPS alone were not significantly different from control (P = 0.3, 0.7, 0.95, 0.9, 0.35, 0.6, 0.6, 0.4 respectively).

(**b**) Long term (1 day) regulation of LMTfil dynamics. The histogram shows the distribution of MI values for each experimental condition. MI values are grouped as follows: < 0.2, 0.2-0.4, 0.4-0.6, 0.6-0.8, >0.8. Treatments and sample sizes were as described in (**a**). Glutamate, Sp-cAMPS, BDNF, or high-frequency stimulation reduced the fraction of stable LMTfil, while increasing the incidence of LMTfil with high dynamics (MI > 0.8).

(**c**) Transient enhancement of LMTfil dynamics by high-frequency stimulation protocol. Sample size: 35-42 LMTfil, 10-15 LMT, 3 mossy fibers, 3 independent experiments for each time point. Each average MI value was measured for 1 day. MI values at 2d after stimulation had nearly reversed to control values.

Fig. 6. Stimulation of spGFP puncta dynamics by AMPA or Sp-cAMPS (*Thy1-spGFP*^{mu} mice) and proposed model of presynaptic terminal dynamic regulation.

40 days hippocampal slice cultures analyzed in CA3b. G: gain events; L: loss events. Drug treatments were for 20 minutes (Sp-cAMPS) and 6 hours (AMPA+AP-V). Time between observations: 1 day. The values are means and SEM from 5 representative fields (at least 50 puncta per field).

Supplementary Figure 1: Hippocampal slice cultures from *Thy1-mGFP*^{s} mice allow the visualization of the terminal arborization of subsets of Dentate Gyrus (DG) granule cells. Images are projections of confocal stacks spanning 51.15 (large panel), 33.17 (left bottom panel), and 11.04 μm (right bottom panel) in the z-dimension. Large panel shows at low magnification the DG-CA3 area of the hippocampus. Note mossy fiber axons originating

in the granule cell layer (boxed region 1), exiting the hilus (H), and coursing in the CA3 region (arrows), where their terminals were imaged. Left bottom panel is a high magnification image of the boxed region 1. Note granule cells bodies (asterisks), basal dendrites and the initial part of MF axons (arrows). The right bottom panel is a higher magnification confocal stack through the boxed region 2. Note the relatively few MF that allow high resolution imaging of their terminals. Three examples of LMTs are indicated by the arrowheads. Arrow bar is 130 μm in the large panel and 45 μm in the two small ones.

Supplementary Figure 2. Visualization of terminal arborization with mGFP, and of presynaptic terminals with spGFP. Imaging of acute whole mount gluteus muscle preparations from *Thy1-mGFP*^{mu} and *Thy1-spGFP*^{mu} mice. Neuromuscular junctions were counterstained with α-Bungarotoxin to visualize postsynaptic Acetylcholine receptors (αBtx; merged images). The characteristic arrangement of pre- and postsynaptic elements at the neuromuscular junction allows for a detailed validation of the subcellular compartment markers used in this study. The mGFP membrane marker visualizes motor axons and the details of their arborization at the neuromuscular junction, whereas spGFP selectively visualizes presynaptic terminals (see also (Li and Murthy, 2001)). The inserts show higher magnification views of individual neuromuscular junctions. Bar: 50 μm.

Supplementary Figure 3: Characteristic presynaptic patterns visualized by spGFP in slices from *Thy1-spGFP*^{m} mice. (a-k): un-processed fluorescence images of CA1 (a, c, d, e) and Dentate Gyrus (DG)-CA3 (b, f-k) regions from living hippocampal slice cultures. (a) and (b) are low magnification examples from CA1 pyramidal layer and CA3b regions shown at the same magnification. Note punctuate synaptic pattern of expression of spGFP; larger spGFP clusters in CA3 presumably correspond to MF terminals (arrows). Asterisks mark cell bodies. An example of region CA1 stratum radiatum at low magnification is shown in (c). In (e) a high magnification of the boxed region from (d) is displayed. Note clear puncta in CA1 stratum radiatum (arrows). Low magnification of the DG-CA3 border is shown in (f). The infrapyramidal (INFRA) and suprapyramidal (SUPRA) mossy fiber terminal layers are indicated. A low magnification image of the DG Molecular Layer (ML)- Granule cell Layer (GCL)- Hilus (H) boundaries is shown in (g). Note larger spGFP

clusters in the hilus, where MF terminals are also located. A high magnification image of the boxed region in (h) is shown in (i). Note the prominent accumulations of spGFP, corresponding to the large MF terminals (arrows); these are never observed in region CA1 (see (e) for a comparison at the same magnification). In (k) the high magnification picture from boxed region in (j), shows presynaptic puncta on a CA3 pyramidal neuron dendrite (evident from background signal) (arrows) and cell body (arrowhead). Bar is: (a, b) 45, (c) 70, (d) 30, (e, i) 8, (f) 145, (g) 65, (h) 55, (j) 12, (k) 6 μm.

Supplementary Figure 4: LMT undergo spatial rearrangement in shape, but do not change their numbers or position over many hours in mature hippocampal slice cultures. Top panels show an example of confocal time-lapse imaging on two LMTs (asterisks) in a *Thy1-mGFP*^{s} slice. Arrow points to an LMTfil. Each of the 3 un-processed panels is a projection of 63 images spanning 11 μm in the *z*-dimension. Bottom panels are frames from a representative confocal series from a *Thy1-spGFP*^{m} slice. Each panel represents a projection of 36 images spanning 6.3 μm in the *z*-dimension of a representative field containing the LMT indicated by the asterisk in its entirety. Note shape alterations over 18h period. The smaller panels show the same LMT (asterisk) from different angles. Bar is 3 μm for top panels and 2 μm for bottom ones.

Supplementary Figure 5: Mossy fibers are characterized by a dynamic activity at axonal filopodia and varicosities in the adult hippocampus ex vivo. (a, b) The panels are fluorescent un-processed pictures of mossy fibers from a 120d whole mount hippocampal acute preparation. (a) shows at low magnification a mossy fiber coursing from bottom left to top right. The three panels at the bottom represent the boxed region imaged over 8 minutes. Note the retraction of a filopodium indicated by the arrow. (b) The panel shows a low magnification of a MF bearing an epV (boxed region). The same epV is shown in the three bottom panels imaged over 10 min. Note a rapid phase of filopodial extension-retraction from the epV, indicated by the arrow. Bar is 3.7 in (a) and 1.5 μm in (b).

Supplementary Figure 6: Propidium Iodide (PI) assay for cell death in long term hippocampal slice cultures. Control and treated slices were analyzed for the presence of cell death (see methods) 1 and 2 days after treatments. All hippocampal slices are

positioned in the same orientation, with the CA3 region on the right. (a) Positive control: a slice left for 4 days without nutrients and O_2 is degenerating. Note in (b) at high magnification the fluorescent nuclei (arrows). (c) Control slice, 1 month-old. A broken glass electrode was used to kill cells locally (arrow), and investigate their removal kinetics. After 2 days they were still detectable indicating that PI incorporation is an appropriate tool to investigate the possible toxicity of our treatments. (d) Further example of untreated 1month slice culture. Note variability, but relative paucity in the number of dead cells, when compared to (c). (e) Example of a slice kept for 3 months in vitro, without further treatments. (f) Example of a 34 day old AMPA+AP5 treated slice, 2 days after application of the drugs. (g) 1 month slice stimulated with 100 Hz protocol and assayed for PI incorporation 2 days later. (h) Example of the digital mask applied in this case to the raw image in (c), to count number of cells with Image software. (i) Quantification of dead cells in 1month and 3 month cultures. Data from each condition are mean±SD from 4-6 slices, 3 independent experiments. There was no significant increase in the number of dead cells 1 day after the treatments (P = 0.7 and 0.8 for AMPA+AP5 and 100 Hz respectively, versus control group). Same results were obtained for Glutamate, TTX, BDNF and cAMP under the conditions used in our experiments. Moreover, all the drugs were tested at higher concentrations and for longer times in cell death assays, and used at lower concentrations and for shorter times than those that proved to be safe for the presynaptic dynamics experiments. (j-l) Simultaneous AMPA-R and cAMP–dependent pathway activation leads to extensive cell death in hippocampal slice cultures. We obtained the same results with high doses of AMPA. (j): 1 day after treatment, (k): 2 days after treatment. (l) Degenerating MF in the slice shown in (j). Arrows point to beaded areas indicating a degenerating axon.

Supplementary Figure 7: Representative unprocessed data from mGFP imaging sessions of slice cultures used in this study, exhibit high signal to noise ratios. (see also Suppl. Figs. 1, 3, 4, 5 for other examples of unprocessed data). The processed picture representing a MF axon, was slightly contrasted in Photoshop.

Supplementary Figure 8: Remodeling of mossy fiber axons in young, but not mature hippocampal slice cultures. Note the dramatic change in axonal branching and growth pattern

over 1 day in the representative example of young tissue (9 DIV, Days In Vitro, arrowheads, top panels). Arrows indicate LMTfil originating from LMT (asterisks). Ax, axon. Bar is 6 μm.

Supplementary Video 1: There are 2 distinct classes of *Thy1-spGFP*^{m} expressing clusters in mature slice cultures. The video illustrates the difference between small clusters (size range of transport packets, arrows) and larger ones (> 1.5 μm) in their dynamic behavior over a few minutes. Clusters in the size range of transport packets (0.3-0.6 μm, long axis; 0.2-0.4 μm, short axis) were seen moving rapidly back and forth along the axon (arrows). Larger clusters (> 1.5) did not move over minutes. Three stable clusters are indicated by the arrowheads. Frames were captured at 10 sec intervals, and the video sequence is shown at 15 frames/second.

Supplementary Video 2: Mature MF are characterized by foci of dynamic activity. The video shows a MF axon from a *Thy1-mGFP*^{s} slice (40div) imaged over a few minutes. The arrow points to an epV, where protrusive activity (rapid filopodia extension-retraction events) is evident. On the same axon an LMT is out of focus (asterisk), and 2 of its filopodia are marked by the arrowheads. Frames were captured at 10 sec intervals; the video has been time-compressed, and is shown at 15 frames/second.

Supplementary Video 3: Young MF are characterized by more frequent and prominent dynamic activity than mature ones. The video shows a young MF axon from a *Thy1-mGFP*^{s} slice imaged over a few minutes (same slice culture as Suppl. Video 2). The corresponding granule cell exhibited the characteristic features of young granule cells: including the location in the DG GCL, a granular shape of cell body, one basal dendrite, no real spines on the dendrite but highly motile filopodia-like spines and highly motile growth cone filopodia at the end of axonal branches. Note an epV (arrow), where multiple events of filopodial extension-retraction are visible. A dynamic filopodium is evident towards the left (arrowhead). Frames were captured at 10 sec intervals, and the video is shown at 15 frames/second.

3. DISCUSSION AND FUTURE PROSPECTS

3.1. OVERVIEW

The main efforts of my PhD thesis work focused on two lines of research: 1) to develop, characterise and demonstrate the value of novel genetic tools for the analysis of synaptic structure and dynamics and 2) to use these tools to investigate the plasticity of presynaptic terminals in mature networks at a cellular and molecular level.

I will briefly summarise the main results of these studies, and discuss their relevance especially with respect to the current status of the field, and with respect to future lines of research that may follow these studies. Concluding remarks follow each of the two subsections.

3.2. GENETIC TOOLS TO STUDY LIVE SYNAPTIC DYNAMICS AND FINE DETAILS OF NEURONAL MORPHOLOGY

3.2.1. Main achievements and relevance of results

Since one of the main interests in the laboratory concerns structural synaptic plasticity, we have generated three independent targeted-GFP mouse lines with neuron-specific expression with the aim of targeting the neuronal membrane and the presynaptic site specifically. Three different constructs were designed which resulted in the expression of three GFP fusion proteins in transgenic mice: a plasmalemmal-targeting domain fusion with GFP (mGFP), a synaptophysin-GFP fusion protein (spGFP), and a combination of the two (mGFP/spRFP).

The correct targeting of the fusion proteins was tested in cell culture experiments as well as in intact tissue specimens from the transgenic mice. Since this approach could have a number of practical general applications we carefully studied any possible phenotype of the mice with regard to morphology and physiology of the expressing neurons. We found no evidence of pathological or abnormal features in the transgenic neurons, or in their processes and synapses, in either normal or in challenged experimental conditions. This is an important finding because it validates the use of these mice as novel genetic tools for the study of synaptic plasticity. The remarkable feature of the Thy.1 promoter of driving expression in a great variety of neuronal types is both a strong and a weak point. A strength because as we show in the study, due to

occasional striking patterns of expression, visualization of the connections between many different types of neurons in different neuronal circuits becomes possible. This therefore permits the study of their plasticity *in vivo* or in whole mount preparations. On the other hand, it is not possible to predict and thus select the expression patterns, and a careful analysis of transgenic lines has to be performed in order to find patterns of interest. We have illustrated in three experimental systems the unique advantages of these mice for the study of synaptic plasticity in both the CNS and PNS.

First, using mGFP mice we have studied the morphology of dendritic spines in adult brain tissue with high-resolution confocal microscopy and compared it in cGFP mice. A main result is that for complex dendritic branches, cGFP expression does not allow single spines to be resolved. The strong shaft fluorescence signal, in fact, masks the one from the little dendritic protrusions. Moreover the outline of spines is completely absent in cGFP expressing dendrites. Finally, the lack of diffusion of cGFP in distal basal dendrites precludes the study of this region using cGFP mice. The existence of complex spine regions (i.e. protrusions emerging from the tip of spine heads) along dendritic branches is demonstrated with mGFP mice (Fig. 3, 4). These data, together with the comparison with cGFP markers, establish our approach as the method of choice when high resolution imaging of small structures matters.

Second, using spGFP mice we studied Synaptic Vesicle (SV) dynamics at mammalian NMJs *in vivo*. Previous studies documented that the configuration of the nerve terminal endings at NMJ does not change shape during development, but it is instead confined to expansion of a conserved pattern (Balice-Gordon and Lichtman, 1990). How do SVs mature in presynaptic terminals of peripheral nerves? Do they also expand during development, maintaining a conserved pattern? From our studies it does not seem to be the case. We observed a reorganization of developing SV clusters. This dynamic behavior at developing NMJs adds a new important level to the investigation of presynaptic maturation. It will be interesting to study the role of synaptic activity in this SV maturation process. The elegant experiments of synaptic competition at single nerve terminals (Balice-Gordon and Lichtman, 1994) can thus be extended to study how SVs are reorganized upon this impaired activity at single NMJs. For example, when only one side of the NMJ vesicle pool is blocked with BotA, how are the SVs from the blocked side going to be eliminated? And do the active SV clusters reorganize accordingly? Moreover, a characterization of the dynamics of SVs during synapse elimination at developing NMJ is currently lacking. How are SVs reorganized upon synapse takeover and elimination at postnatal developmental stages? Answers to these questions will add a molecular mechanistic

view on the amount of data already existing regarding dynamics of axon terminals at developing NMJs. Our data based on the use of spGFP mice, although preliminary, constitute an important starting point in this direction.

Third, using mGFP mice in a slice culture experimental system, we studied the behavior of young granule cells while they developed in a mature network. We discovered that the Thy.1 promoter drives expression in young, presumably newly born, cells in the DG. These young granule cells were followed in the mature network with respect to their short-tem process dynamics and axonal development. Our results are consistent with the hypothesis that axonal as well as dendritic short-term dynamics are a cell autonomous phenomenon and not a function of the maturity of the neuronal network. Moreover they indicate that these newly born cells might use similar mechanisms to developing granule cells, to integrate into adult networks. Our understanding of young granule cell axon guidance biology could greatly profit by molecular and cellular studies using this system. In fact, nothing is known about possible guidance cues that direct new neurons in the adult network. Since molecules used by the developing nervous system are still present in adult animals, they are good candidates to mediate this process. Our simple in vitro system that relies on the mGFP marker to label the neuronal membrane effectively, promises to be helpful in the characterization of the molecular mechanisms underlying this fascinating aspect of neuronal biology. Furthermore, the molecular mechanisms of young granule cell development, notably activity-dependent regulation of synapse formation and plasticity, can also be investigated using our approach.

3.2.2. Future applications of the genetic tools

A number of transgenic mice that express multiple forms of cytosolic GFP (cGFP) in the nervous system are currently available. These transgenic mice have had a great impact in the study of synaptic dynamics especially in the PNS, but recently also in the CNS (Grutzendler et al., 2002; Trachtenberg et al., 2002; Walsh and Lichtman, 2003). One great advantage over other methods of visualization of neuronal morphology that also use mice and fluorescent markers (e.g through viral infection, gene gun or DiOlistics), is the possibility of following at any time the fluorescent signal in intact tissues without invasive manipulations. This is remarkable because it allows the study of synaptic dynamics *in vivo*, making little, if any assumptions. Our approach of GFP-fusion protein expression in neurons of transgenic mice, while holding this decisive advantage for the study of neuronal morphology, constitutes an evolution and a major improvement over the last generation of GFP transgenic mice. Our new generation of “green” mice provides the following advantages: first, it allows the visualization

of the entire neuronal membrane (mGFP) thus enabling the detailed study of both axonal and dendritic dynamics with higher resolution for thin structures like filopodia and spines. This can be very useful when the detail of the analysis is central, as is for *in vivo* imaging of synapse dynamics or for the analysis of subtle structural phenotypes in mutant mice (e.g. FMRP knock out). Second, it allows monitoring of SV dynamics (spGFP and mGFP/spRFP) both at the NMJ and at central synapses *in vivo*. This possibility will certainly contribute to the progress of our understanding of presynaptic development and plasticity. Third, the simultaneous visualization of the neuronal membrane and the SV inside is now possible (mGFP/spRFP). This is the prototype of a next generation of transgenes that will permit the study of the relationships between two different subcellular compartments in real time (De Paola et al., 2003). Thus our approach promises to bring a new impulse to the study of synaptic plasticity.

Further examples of the use of selective neuronal expression of GFP fusion proteins in transgenic mice are: 1) the possibility of preparing neuronal cultures that express the three GFP-reporter genes from these mice. A dispersed hippocampal neuron co-culture approach has been already tested in the lab to investigate the properties of genetically modified terminals (e.g. in CAP23 knock out animals; Frey, Wacha, De Paola and Caroni, unpublished data). In particular the selective labelling of wild type (wt) neurons using a ubiquitous expressing line of mGFP (L17) enabled us to distinguish between CAP23 knock out (no green fluorescence) and wt terminals (green) in the co-culture system. This approach is useful when investigating mechanisms of synapse formation and maintenance because in the co-culture dish diverse arrangement of pre- and post synaptic sites coexist. Namely, wt presynaptic terminals can be faced by knock-out postsynaptic sites and/or vice versa, thus allowing determination of the sites and modes of action of a synaptic protein.

2) The possibility of studying relevant models of nervous system diseases and mutant mice. I will briefly outline here but two of the more compelling examples to illustrate this point.

We crossed our spGFP and mGFP/spRFP mice with a mouse model of Amyotrophic Lateral Sclerosis (ALS) (Gurney et al., 1994), a devastating progressive disorder that affects motor neurons. ALS mice die at around 140 days of age and display a number of defects in NMJ physiology and function. However, the precise sequence of events that leads to synaptic loss is unknown. This information is important because it will direct potential therapeutical strategies. SpGFP and mGFP/spRFP mice might be very helpful in this context. Our hope is to characterise the defects in ALS NMJs at the level of SV organization and dynamics at different developmental stages, including those stages when there is no detectable phenotype. Thus our

tool may introduce a new level of investigation in the study of ALS.

The second example regards the full NCAM KO mouse. The role of Neural Cell Adhesion Molecule in presynaptic function is far from being understood and important questions relate to the roles of each of the three different NCAM isoforms present in mammals. However, given the defects in synaptic vesicle mobilization and recycling at NMJ (Polo-Parada et al., 2001) we have crossed NCAM KO mice (together with different NCAM isoform mutations in transgenic mice; Hund and Caroni, unpublished data) with spGFP and mGFP/spRFP mice with the aim of studying SV dynamics in a mouse model with impaired neurotransmitter release. Hopefully this approach will give us further insight into the role of NCAM in presynaptic function and in the role of SV dynamics at mammalian NMJs.

3) The study of the plastic (upon reinnervation or sprouting) properties of single motor units. BotA-mediated paralysis triggers a plastic response of the nerve terminal called sprouting. We used a mGFP line with expression in single motor axons (L21) to follow the sprouting behaviour of NMJs belonging to the same motor unit. This analysis revealed, unambiguously, that sprouting competence is not determined by the motor neuron, since NMJs belonging to the same motor axon exhibited different extents of responses to the paralysis (Santos, De Paola and Caroni, unpublished observations, Discussion figure 1). A recent study also describes the benefit of single neuron transgenic GFP lines (Livet et al., 2002). Moreover, in this system the long-term behaviour of presynaptic terminal apparatuses in response to this activity blockade can be related to the correspondent status of the postsynaptic complex. Recent data in the lab using both mGFP and spGFP mice, point to differences in plastic responses of NMJs among different muscles but also among subregions within the same muscle (Santos, Pun, De Paola and Caroni, unpublished data). These differences might be due to the local environment and to intrinsic differences in nerve terminals. Repeated observations of mGFP and spGFP expressing NMJs upon synaptic silencing and upon pharmacological manipulations in living animals will allow us to follow, in real time, nerve terminal responses and therefore to gain a deeper understanding of their mechanisms of action. At the same time, it would be interesting to establish a parallel in the CNS. The ability to monitor the behaviour of different types of terminals along the same axon for extended periods of time in hippocampal slice cultures, will reveal to which extent similar phenomena occur at central synapses.

Ideally, one would prefer to label functionally connected neurons. The next generation of reporters could have the capacity to label neurons transynaptically allowing direct visualization

of neuronal circuits. For example tetanus toxin C fragment (TTC) fusion proteins are transported retrogradely and transynaptically within the CNS (Maskos et al., 2002). These, as TTC-targeted-GFP fusions, might be used in transgenic animals (e.g. under the Thy.1 promoter) to label specific classes of interconnected neurons and enable their visualization in a non-invasive manner.

3.2.3. Conclusions

As outlined above, the potential use of targeted-GFP expression in neurons of transgenic mice is only at its dawn. Here we have demonstrated the distinctive features of this tool and presented three experimental examples of potential applications that open the way for future studies. We anticipate that targeted-GFP expression in adult neurons of transgenic mice will constitute a widely used tool to study morphological and dynamic aspects of both CNS and PNS synapses. Noteworthy is the possibility of employing this new generation of reporter-based method to study synapses in mammalian intact specimens. SpGFP and mGFP/spRFP mice will be an invaluable tool to investigate SV dynamics in living terminals, especially in the mammalian cortex with the aid of two photon *in vivo* imaging technology. The possibility of crossing these mice into the appropriate genetic models (mutant mice) will also strongly increase their value, allowing investigation of the molecular mechanisms of synaptic plasticity and nervous system diseases with previously impossible experimental assays.

3.3. PRESYNAPTIC TERMINAL DYNAMICS IN THE HIPPOCAMPUS

3.3.1. Main findings, open questions and follow-ups

While the growth and retraction of axons and dendrites, as well as that of presynaptic terminals and postsynaptic spines have been well-studied processes in the developing nervous system, there is increasing interest in monitoring synaptic dynamics in the adult brain. Profuse hints for the relationship between structural changes and cognitive changes already exist in the adult brain. Thus even if the cellular mechanisms for processing memory in the brain are not known, current theories include the possibility of changes in synapse number and/or structure and not just modification of their strength. In a variety of systems as well as in dissociated cells and brain slices there is evidence that modulation of activity, including long-term potentiation, involves structural changes of postsynaptic dendritic spines. In contrast, axonal dynamics of mature CNS neurons have not been studied extensively, and very little is presently known about

the stability of presynaptic terminals. Open questions include whether there is any turnover, whether such turnover is measured in hours, days or years, and how it is regulated. To address these important issues, we generated transgenic mice over-expressing different types and combinations of GFP-fusion proteins specifically in subsets of neurons in the adult (see above). Our experimental plan was based mainly on two tissue-organized specimens prepared from these mice. Because of its prominent role in learning and memory we chose the hippocampus as a model system, thus hippocampal whole mount acute preparations from adult mice and mature organotypic slice cultures (4-8 weeks) were used. This latter one is the only tissue-based technique that allows long-term imaging in the hippocampus.

We developed then a method for prolonged (days and weeks) imaging at the level of single synapses. The possibility to follow, for the first time, the behavior of terminals in real time for such extended periods of time enabled us to discover a surprising degree of plasticity of pre-synaptic terminals. The molecular mechanisms, in particular with respect to the role of activity, were also investigated. Our main findings are:

1) Pre-synaptic terminal numbers in mature hippocampal networks are in a state of dynamic equilibrium

2) Distinct types of terminals of the same neuron exhibit unique dynamic properties

3) Stable terminals can be reversibly converted into dynamic ones by patterned electrical activity

According to our proposed model (Discussion Fig. 2), activation of AMPA receptors by synaptically released glutamate leads to an increase in presynaptic terminal dynamics through PKA activation and de novo protein synthesis. These enhanced dynamics are transient: they are first detectable at 6h after stimulation, and revert to control values 2 days after stimulation. BDNF release may occur downstream of PKA activation, to stimulate de novo protein synthesis. Reversible enhancement of dynamics may involve transient elevation in the levels of critical protein(s), e.g. actin-regulating proteins or alternatively, negative regulators of NCAM.

The exact location of the proposed regulatory cascade of events is yet to be determined. Does it take place in the pre- or postsynaptic cell?, this is a very difficult task to be solved in brain tissues. In fact it would require, in the simplest case, specific modulation of pre- or post-synaptic glutamate receptors. Injections of glutamate receptor blockers specifically in pre- or post-synaptic cells could, in principle, help to elucidate this issue. Alternatively a granule cell-enriched dispersed culture system (Baranes et al., 1996) could permit us to determine if the cascade of events that regulate MF terminal dynamics is purely a presynaptic phenomenon.

Another unresolved issue concerns the gene expression requirements. We suggest that new protein synthesis is necessary for the enhancement of presynaptic terminal dynamics. However, the relatively long time-scale of presynaptic terminal dynamics (several hours to days) does not preclude a gene transcription requirement. Further experiments with gene transcription blockers will answer this question. Nevertheless, the recent discovery that axons are, like it is already established for dendrites, sites of local protein synthesis (Brittis et al., 2002), will constitute an exciting field for future studies regarding presynaptic terminal dynamic regulation mechanisms.
Further investigations will also be needed to gain a more complete mechanistic view of presynaptic terminal dynamic regulation. These include:
How does AMPA-R activation lead to PKA activation? Since NMDA-Rs were blocked in these experiments, the possibility of NMDA-R-dependent Ca^{2+} entry and consequent activation of adenylyl cyclase and rise in cAMP levels is excluded. However, Ca^{2+} entry through voltage-gated-calcium channels is still possible. This possibility can be tested using specific inhibitors for these channels while AMPA-R are activated.
Is the BDNF mediated increase in LMTfil motility dependent on new protein synthesis? The answer to this question will more clearly define the relationship between BDNF and PKA effects.
Downstream candidate effectors of activity in mediating the dynamics of presynaptic terminals are, as already mentioned, actin-regulating proteins and actin itself, but we cannot exclude a role for other cytoskeletal components like microtubules and neurofilaments. A further effector could be the tissue plasminogen activator, an extracellular serine protease that can be induced by LTP and mediate morphological synaptic plasticity (Baranes et al., 1998).

Another promising subject for future investigations is constituted by the regulation of the basal dynamism that we reported. About 4 % of epV and 30 % of LMTfil are dynamic over a 1-day observation period in untreated conditions. We suggested that this was an intrinsic property of the hippocampal circuits in these mature organotypic cultures. It is still an open possibility that a protracted (days) blockade of synaptic activity can affect the basal dynamics of pre-synaptic terminals. Alternatively, other extra-cellular signals through regulators of the actin cytoskeleton (e.g. small GTPases) could mediate the basal dynamism that we report likewise for post-synaptic sites during development (Cline, 2001). Guidance molecules and neurotrophic factors are still highly expressed in the adult brain, thus together with adhesion molecules and estrogen-mediated pathways, are among other plausible candidates.

This study could open exciting future areas of research. We have discovered that in late developmental stages there is a fine equilibrium of presynaptic terminal gains and losses. This is more important than it may seem at first glance. In fact although synaptic density cannot grow indefinitely in the adult brain, and thus synaptic turnover is expected, it does not necessarily mean that presynaptic terminals are involved. Indeed, so far, synapse turnover has always been explained by the formation of multiple synapse boutons between new spines and pre-existing pre-terminals (Luscher et al., 2000). Therefore, in developing networks there seems to be an alternative program that leads to the increase in synapse number. What factors are responsible for the shift towards homeostasis in mature neuronal networks? The understanding of how a mature neuronal network achieves the kind of homeostasis we report with regard to synapse number should be a fruitful area of research. It is interesting to note that recent data point to the existence of a similar mechanism regulating spine turnover in adult cortical regions (Knott et al., 2002; Trachtenberg et al., 2002). In both hippocampal and cortical networks, remarkably, enhanced synaptic activity leads to an increase in synapse turnover rates without an actual increase in number, suggesting that this activity-dependent regulation of homeostasis of synapse numbers can be a general distinctive feature of adult brain function. Our study provides a useful starting point for the investigation of the molecular mechanism underlying this homeostatic regulation.

It is generally thought that the synaptic distribution patterns along an axon are determined by connectivity rules that likely depend on the length of the axon (Shepherd et al., 2002), but in fact the input to a neuron is also a determining factor. On the other hand, the input onto a single neuron is determined by the integration of the strength of the numerous synapses impinging on the correspondent cell body and dendritic tree (Hausser et al., 2000). This raises the intriguing problem of how a single GC differentially regulates the turnover of its three distinct MF presynaptic terminals. How are the plastic properties of presynaptic terminals determined? our data on the fine equilibrium in gains and losses suggest a regulation at the circuit level, possibly mediated by the local postsynaptic environment. However it would be of great significance to know if a similar regulation exists at the level of single axons. That is to say if the balance in gains and losses is maintained for a single mature axon. Our data over a 5-day observation period for epV, although to be used for statistical analysis they would need to be extended with a higher number of terminals per axon, indicate that this may indeed be the case. Similarly, cell-autonomous phenomena might intervene in the activity dependency of pre-terminal turnover. To determine whether synaptic activity can act on MFs in a cell-autonomous way will require

changing the activity patterns of single GCs and then relating these impaired activity patterns to the dynamics of the correspondent presynaptic terminals. The recent development of sophisticated mutant K^+ channels could be of use in this context (Paradis et al., 2001).

Further areas of future research may include: the regulation of short-term axonal dynamics, particularly with respect to the role of activity (see for example (Chang and De Camilli, 2001). Our data on the short term dynamics of MF in whole mount preparations in the presence of activity blockers (i.e. TTX), suggest that activity is not required for short-term axonal dynamics. However, experiments designed specifically to address this purpose are necessary. They will require, for example, repeated monitoring of identified stretches of axon using mGFP mice without and with blockers of synaptic activity.

The third type of MF terminal types, the large multisynaptic complexes on CA3 pyramidal neurons (LMTs), seems to be remarkably stable as a whole. This is in a way expected given their large size and the extreme complexity of their arrangement, and supports the idea that these terminals convey a different type of information to the CA3 network than epV and LMTfil (Toth et al., 2000). However, the possibility of the regulated remodeling of individual active zones on LMTs (Suppl. Fig. 4, Pag. 92), will certainly be the subject of further studies because of the prominent role of this synaptic complex for understanding mechanisms of LTP (Geiger and Jonas, 2000; Castillo et al., 2002).

Finally, it will be interesting to know under the same experimental conditions how postsynaptic sites behave over such long time frames. This knowledge will tell us to which extent anatomical rearrangements of presynaptic terminals reflect functional changes in the neuronal circuit. Of course a more direct and informative, yet so far poorly explored (but see (Colicos et al., 2001)), approach would be to monitor both pre- and post-synaptic site dynamics contemporaneously. The few data in the literature in this regard support a functional role for presynaptic terminal dynamics. Thus turnover of postsynaptic sites has been studied in neurons in dispersed cultures, and seems to be happening at comparable rates to the one reported by us (Okabe et al., 1999). This study, observed PSD-95 tagged with GFP in cultured hippocampal neurons for periods of up to 1 day. Most of the PSD-95 clusters were stable but more than 20 % were eliminated within 1 day. Moreover, similar findings on active presynaptic terminals (~ 20 % turnover of FM4-64 structures in 24 hours) were obtained in experiments performed in long-term primary cultures of rat hippocampal neurons (Y. Ramati and N. Ziv, personal communication). Turnover of synapses has been recently demonstrated in the intact adult cortex, with a remarkable quantitative (40 % of dynamic spines over 1 day) and qualitative (e.g. the subdivision of spines

in distinct classes with different turnover rates, some very stable others less or the stability of dendritic branches) correspondence to our data (see also above) (Trachtenberg et al., 2002). So it seems likely that the pre-synaptic turnover we report reflects a turnover of synapses and thus has functional impact on neuronal networks.

How synapse formation and elimination occur in mature brain circuits is not clear. Our data, with the involvement of AMPA-R and PKA activation, BDNF and protein synthesis, provide the first mechanistic details of possible scenarios. They support the idea that presynaptic complexes are assembled prior to post-synaptic ones during synapse formation in developing networks (Friedman et al., 2000). In fact a higher percentage (> 93 %) of MF terminals contained synaptophysin in living tissue including the dynamic ones (Fig. 4b), whereas postsynaptic receptors were apposed to MF terminals with lower percentages (~ 60-70 %), suggesting that the assembly of presynaptic sites also in these mature networks precedes that one of postsynaptic sites.

In summary, for most future studies, be they at the MF pathway or at different pathways, the possibility of coupling imaging techniques to more sophisticated electrophysiological recordings or electron microscopy will be crucial for monitoring the functional effects of anatomical rearrangements of presynaptic terminals.

3.3.2. Biological relevance of pre-synaptic plasticity

By far the most interesting open question is the extent to which the presynaptic terminal dynamics demonstrated here in this study in the hippocampus also apply for axons in living animals. If this were the case, the implications would be considerable. In fact, the instability of presynaptic terminals would have far more drastic consequences for the connectivity of neuronal networks than rearrangements in postsynaptic spines. If specific sites along axons undergo constant changes including disassembly and formation of new terminals it is reasonable to assume that also the connectivity of the network will be, in turn, frequently altered. This challenges, in a way, the common understanding of long-term memory that is thought to rely on the long-term stability of brain structure. However, stable structures were indeed detected in our study (the LMTs) and thus this apparent paradox can be unravelled hypothesizing that memory is stored in these long-lasting synaptic sites. The question raised above will probably find an answer in the near future thanks to the development of imaging techniques, together with established paradigms for studying experience-dependent plasticity in cortical regions like in the barrel cortex (Trachtenberg et al., 2002). In vivo imaging of plasmamembrane-targeted GFP

expressing single cortical axons, and synaptophysin-GFP containing presynaptic terminals, or both simultaneously in the intact mouse cortex could constitute a further means to study this important, yet elusive question.

The study of the activity-dependency of structural changes is critical in determining their physiological relevance. The finding that enhanced electrophysiological activity can regulate the structural plasticity of hippocampal presynaptic elements can be interpreted in functional terms only once we know more about the normal patterns of activity and how they relate to cognitive processes like learning and memory in the intact brain (and in particular in the hippocampus). It is possible that the frequency of electrical stimulation used by us (100 Hz for few minutes), which enhanced the turnover rates of presynaptic terminals, does not correspond to frequency patterns normally recorded in the intact brain. Nevertheless, the discovery that the synaptic-activity-dependent enhancement in presynaptic dynamics is transient, strongly argues for a physiological role of activity in the regulation of presynaptic terminal plasticity.
In NCAM KO slices, interestingly, terminal turnover rates seemed to be permanently increased (at least for one type of terminal, the LMTfil) with respect to control values (3-fold increase). It will be interesting then to know whether high frequency stimulation can reversibly enhance these dynamics. A failure to do so would be significant because it would mean that NCAM plays a key role in the reversible increase of terminal turnover rates. Furthermore, indirect *in vitro* studies employing targeted-GFP mice crossed with mouse models of enhanced or impaired learning could provide informative insights into the physiological relevance of presynaptic terminal dynamics.

The MF to CA3 pathway represents an ideal system to study the relationship between excitation and inhibition in a neuronal network. The anatomy of this relatively simple network is to a large extent (but see later) defined and the cell types involved have been characterized in their electrophysiological properties. Moreover, inhibitory interneurons are excited by the same input (the MF epV and LMTfil) that also excites pyramidal neurons (LMT-to thorny excrescence-synapses) in the same network. This property of cortical networks whereby the same excitatory input excites both GABAergic interneurons and principal cells is called feed forward inhibition (Pouille and Scanziani, 2001). The discovery that two subtypes of excitatory presynaptic terminals that contact interneurons (LMTfil and epV) are anatomically plastic in normal circumstances, opens the possibility that feed forward inhibition could be mediated by a structural change involving specific terminal types (the LMTfil and epV). It also raises the

question of how these anatomical dynamics may influence the degree of inhibition in the CA3 network. Do dynamic filopodia and epV maintain their target selectivity for the same interneurons? And more importantly what is the impact of the enhanced anatomical changes upon increased activity that we describe in this study for feed forward inhibition phenomena in the CA3 network?. The evidence that also dynamic filopodia contain synaptophysin, suggests that they could actively participate in the excitation-inhibition balance of the CA3 network. Further experiments involving imaging of mGFP-positive MF terminals and electrophysiological recordings (e.g. recordings from CA3 pyramidal neurons in voltage clamp-configuration, while stimulating the "green" MF to record the average inhibitory response on single principal cells) in acute slices, however, are needed to solve these issues. As I pointed in the introduction (pag. 23), answers to these questions will be greatly illuminated once we learn more about the connectivity of the CA3 network. It is crucial to know whether the interneurons contacted by a single MF also contact the same pyramidal neurons that are postsynaptic to that MF or if neighbouring granule cells contact the same interneurons. At present it is simply not known whether a strong activation of the MF pathway leads to an excitation or inhibition of the CA3 network. This knowledge will be important to better interpret the role of presynaptic structural plasticity for hippocampal function.

We studied presynaptic terminal dynamics in hippocampal area CA3. To what extent can we generalize our findings? The MF is a special axon. It bears three functionally and morphologically different terminals, one of which has a unique anatomical complexity in the hippocampus (the LMT). It also contains unusually high levels of actin (Capani et al., 2001) that could explain its dynamic properties. This made us concerned about the generalization of these findings for other classes of axons and terminals. However, two lines of evidence make us confident that, although likely with different kinetics, other axons and terminals may also be plastic in mature networks. First, when we looked at the general population of spGFP-positive terminals in CA3 that comprise also CA3 pyramidal neuron and GABAergic terminals, we found similar dynamic properties to MF terminals including aspects of regulatory mechanisms (Fig.2 and 6). Second, prominent axonal short-term dynamics (ranging from sec. to minutes), a phenomenon that we document in detail for mature MF (Suppl. videos 2, 3 and suppl. Fig. 5), also characterize CA1 axons in mature hippocampal slice cultures (Discussion video 1). Repeated observations every ten seconds over 5-10' show that varicosities from CA1 pyramidal neuron axons in the stratum oriens or subiculum are characterised by frequent shape changes (42 % of them, n = 31) closely resembling spine motility. Protrusive activity (filopodial extension

retraction) from the varicosity, which can last from tens of seconds to minutes, is also a recurrent phenomenon (24 % n = 25). This dynamic behaviour can alternate, also producing periods of no detectable movement (up to 20 minutes of no movement). Also filopodia emerging from the shaft can rapidly elongate or retract alternating with periods of no detectable movement (56 % n = 45). Moreover, we detected one varicosity loss event out of 10 total varicosities followed over 1 day observation period. Finally, dynamic activity of varicosities seem to be retained in Botulinum A treated cultures (n = 4 slices, 4d treatment). Thus these axonal dynamic behaviours characterise different types of axons in mature hippocampal networks suggesting that they can be general features of non-developing axons.

Nevertheless, to gain a comprehensive view on CNS presynaptic terminal turnover and regulation, different axons in different brain areas need to be studied, as properties could vary according to the specific role of the axon in that specific brain area.

Are inhibitory terminals also turning over? If so, the mechanisms underlying the regulation of these dynamics could be different as AMPA receptors cannot be directly activated by the neurotransmitter GABA.

Given the high specificity of terminal location sites along axons (Shepherd et al., 2002), it would be interesting to know whether terminal dynamics are also characterized by similar specificities. For example knowing whether they take place only at restricted axonal regions or, in contrast, if they take place throughout the entire axonal arbor, would be important information. As I already mentioned, even though we asked whether terminals other than the mossy fibers turned over, we tested only a relatively restricted brain region and axonal sub region for presynaptic dynamics, that is the hippocampal CA3 region. This includes only the final part of the mossy fiber axons. Within the different axonal segments that we studied in area CA3 (i.e. proximal or distal to the DG) we found no indication that terminals could behave differently with respect to their position along the axon. However, a comprehensive understanding of axonal synaptic plasticity awaits in experiments where different regions, with respect to postsynaptic target circuitry, of the same axonal arbor can be compared in their terminal dynamic properties.

3.3.3. Conclusions

The brain’s ability to form and store memories and to change (learning) in response to everyday experience has attracted several generations of biologists. A major area of research in neuroscience seeks to understand to what extent this ability is due to alterations in synaptic connections. While previous attempts to relate experience-dependent changes in synaptic

activity and anatomical modifications documented only post-synaptic site dynamics, our data provide evidence for the existence of an activity-dependent pathway that acts on the stability of presynaptic terminals in mature circuits. Furthermore, our data establish pre-synaptic terminals as possible substrates to translate experience into long-term changes of network connectivity.
Our data provide an important starting point for future studies that will test plastic properties of presynaptic terminals in a variety of brain regions and under different experimental conditions.

3.4. DISCUSSION FIGURES

DISCUSSION FIGURE 1

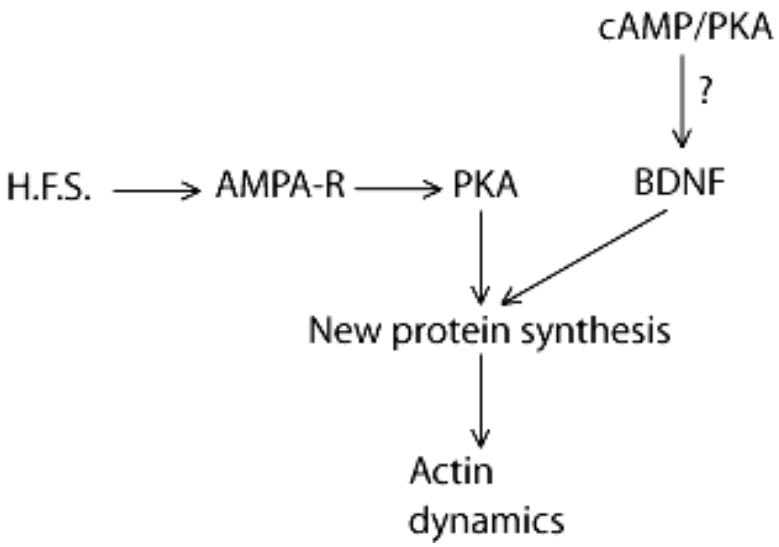

DISCUSSION FIGURE 2

FIGURE LEGENDS

Discussion Figure 1: Sprouting competence is determined by the local environment and not by the motor neuron. mGFP expressing motor unit in the gastrocnemius muscle upon paralysis. Note that three different end plates (arrows) on the same motor neuron exhibit different extents of sprouting (arrowhead).

Discussion Figure 2: Proposed model of presynaptic terminal dynamic regulation.
Enhancement of LMTfil dynamics involves local high-frequency stimulation, AMPA-R activation, PKA, and de novo protein synthesis. Enhanced dynamics is transient: it is first detectable at 6h after stimulation, and it reverses to near control values 2 days after stimulation. BDNF release may occur downstream of PKA activation, to stimulate de novo protein synthesis. Reversible enhancement of dynamics may involve transient elevation in the levels of critical protein(s), e.g. actin-regulating proteins. Our results are consistent with the possibility that similar mechanisms enhance the dynamics of other types of presynaptic terminals in the hippocampus (e.g. mossy fiber epV). While high-frequency stimulation leads to enhanced presynaptic dynamics, our data do not discriminate between an activation of pre- or postsynaptic AMPA-R, nor between a requirement for de novo protein synthesis pre- or postsynaptically.

Discussion Video 1: CA1 pyramidal axons in mature hippocampal slice cultures are characterized by short-term axonal dynamics likewise MF. The video shows a CA1 pyramidal neuron axon in the stratum oriens from a *Thy1-mGFP*^{s} slice (26 DIV), imaged over a few minutes. Note prominent (~ 10 μm max lenght) and rapid extension (in 1') of 3 filopodia from a varicosity, consequent retraction (over 1 minutes) and complete absorption (overall 4'). Frames were captured at 10 sec intervals; the video has been time-compressed, and is shown at 15 frames/second.

3.5. OUTLOOK

The main contributions of this PhD work to the study of synaptic plasticity are: 1) the development of new genetic tools to study synapse structure and remodeling, and 2) the demonstration of activity regulated pre-synaptic rearrangements in mature hippocampal networks.

Future studies should be directed towards a more complete characterization of the molecular mechanisms of presynaptic terminal dynamic regulation, as outlined in the discussion.
In summary, what could represent a clear advantage will be to be able to relate structural changes of presynaptic terminals with functional changes. Thus, electrophysiology, or alternatively Ca2+ imaging should be coupled to imaging anatomy. A particular interesting application, because of its implications for LTP mechanisms, will be to probe the functional effects of anatomical rearrangements at LMTs. Along the same line, simultaneous imaging of pre and postsynaptic sites (using e.g. mGFP/spRFP mice) could add new insights into the regulated rearrangement of synapses in adult brain.

Future challenges include determining whether different types of axons in adult animals are characterized by similar dynamic phenomena. Subsequently it will be important to dissect the molecular mechanisms of these structural modifications together with the potential role of experience in regulating such modifications. Finally, if differences in plastic mechanisms of axons were discovered, it will be a major challenge to understand how such specificity of plastic properties is controlled at the cellular and molecular level.
In summary it will be important to determine to what extent the mechanisms that underlie synapse formation and elimination during development are shared by more mature circuits. Or, instead, whether different mechanisms have evolved to achieve the same purpose in the mature brain.
The regulated presynaptic remodeling that we show in a simple mature neuronal network provides a starting point from where to begin to dissect these fascinating questions.

Instrumental for the success of these tasks will likely be the use of the novel genetic tools presented in this study. They enabled us to “track the lives” of several different types and large populations of presynaptic terminals for extended periods of time. As outlined in the discussion several applications of the targeted-GFP mice are possible in many fields of neurobiology, in particular for

the study of the molecular mechanisms of young granule cell development. Finally, the possibility of their exploitation for *in vivo* imaging of presynaptic terminals both in the CNS and in the PNS is a good example of their potential.

4. APPENDIX

4.1. Defining molecular basis of motor neuron subpopulations

4.1.1. OVERVIEW AND RATIONALE OF APPROACH

The introduction of the silver staining technique more than 130 years ago by Camillo Golgi enabled biologists to discover that neurons comprise several distinct morphological classes or types. It is an important question and challenge in neurobiology to understand the molecular mechanisms underlying this diversity because it will help us to clarify the molecular basis of synaptic specificity. One model system that was extensively used to study distinct subtypes of neurons and their specific functions has been the motor pools, the groups of motor neurons that innervate one defined skeletal muscle (Henneman and Mendell, 1991; Burke, 1994). Each muscle unit (that is one muscle and its motor pool) consists of a defined set of functionally distinct motor units (that is one motor neuron and the muscle fibers it innervates). In mammals, there are three subdivisions of motor units, based on functional types: slow (S), fast fatigue resistant (FR) and fast fatigable (FF). Slow motor units develop relatively little force but are extremely resistant to fatigue (e.g. soleus muscle). FF units on the other hand are powerful but rapidly exhausted (e.g. EDL muscle). There are, in addition, functionally intermediate forms within these categories (e.g. among FF and FR motor units). Characteristic type-specific muscle protein isoforms are expressed by these different muscle fiber types. The specific motor unit content of any particular muscle is determined genetically and has species-specific features that reflect behavioural needs (Burke 1994). Mechanistically, the unique functional roles of neuron subpopulations are likely to be the result of the past or current variation in gene expression. Thus it appears that one way to study the molecular basis of neuronal diversity would be to use gene expression analysis. Members of the cadherin family of cell-adhesion proteins, like the protocadherins, have been found to be a source of potential variation and to have an immunoglobulin-like arrangement of their genes that makes them excellent candidate molecules for ensuring neuronal diversity (Kohmura et al., 1998; Obata et al., 1998; Wu and Maniatis, 1999). To investigate the molecular basis of the functional differences in motor neuron subtypes that innervate different muscles we undertook two different approaches.

In a first approach I sought to investigate the expression patterns of mouse homologs of human protocadherins. I therefore cloned by RT-PCR, and characterised by in situ hybridisation on brain tissues, the 3 mouse homologs of human protocadherins (Pcdhα, Pcdhβ, Pcdhγ, see later). The analysis of their expression patterns revealed that they label different subsets of neurons in the mouse spinal cord and dorsal root ganglia indicating that they can be used as molecular tags for subpopulations of motor neurons.

The second approach lead to the isolation of motor neurons innervating muscles with different motor unit composition (soleus and EDL). This was achieved by retrograde labelling of their soma and by dissection from the surrounding spinal cord tissue. This is a prerequisite for the establishment of motor neuron subpopulation-specific cDNA libraries.

4.1.2. RESULTS

Protocadherins cloning and expression pattern in the mouse spinal cord and DRGs.

Protocadherins are cell-cell adhesion proteins that have characteristic structural features. In contrast to classic cadherins, the extracellular domains of protocadherins consist of six instead of five repeats of the cadherin specific motif and the conserved cytoplasmic C terminus is distinct from that of the classic cadherins. In humans three separate gene clusters exist named *Protocadherin* (*Pcdh*) α (homologs of CNRs in the mouse), β and γ. Each complete extracellular domain is encoded by a single large exon. To generate mRNA transcripts one of these variable 5' exons is joined to a conserved cytoplasmic domain encoded by three constant exons at the 3' end. Each gene cluster has its own constant cytoplasmic regions resulting in three distinct families of proteins (Pcdhα, Pcdhβ, Pcdhγ).

To determine whether these protocadherin genes might contribute to the diversity in motor neuron subpopulations, I cloned the mouse homologs. A BLAST search on the non-redundant database using Hs Pcdhα2 lead to the identification of CNR1 (acc. No D86916), or cadherin-related neuronal receptor (Kohmura et al., 1998). The homolog of Pcdhβ12 was identified as Pcdh3 (acc. No L43592) and that one of PcdhγB2 as Pcdh2C (acc. No U88550). The three constant coding sequences were therefore cloned using appropriately designed oligos by RT-PCR. Three bands of the expected sizes were generated and cloned in PCDNA3 (Fig. 1). They were subsequently linearised and RNA probes created by in vitro transcription. In situ

hybridization was then performed on spinal cord and dorsal root ganglia, as well as on CNS sections. The results are clear. Subsets of motor neurons in the lumbar-sacral spinal cord are evident in both longitudinal and cross-sections when compared to cresyl violet "all-cell" staining of adjacent sections (Fig.1 second, third and fourth rows). Also subsets of sensory neurons in dorsal root ganglia express Pcdhα, β, and γ homologs (Fig.1, last row). It is not clear, at the moment, if there is overlap in this expression patterns, or if instead one subset of neurons can co-express members of different families of protocadherins. Nevertheless, these results suggest that members of the protocadherin family can be used as markers of motor neuron and sensory neuron sub populations.

Backlabeling from different skeletal muscles and isolation of correspondent motor neurons

Soleus and EDL contain diverse complements of motor units (lomo). To identify and isolate specifically the motor neurons that innervate them we used retrograde tracers injected directly in the 2 muscles (tracers). Fluorogold injections in the two hind limb muscles, successfully labeled specific motor neuron pools in the spinal cord (Fig. 2). The correspondent spinal cord section (few mm) was dissected and the labeled cells isolated under a fluorescent microscope with the aid of a micropipette. This procedure can be useful for construction of cDNA libraries that contain either slow or fast motor neuron characteristic genes (e.g. through differential display technology).

4.1.3. DISCUSSION

This project aimed at identifying molecular tags of motor neurons subpopulations.

Even though motor neurons could be isolated using the retrograde labeling method, pure labeled-cell preparations were difficult to obtain. This complicated the way towards the construction of cDNA libraries that contained only genes from one subpopulation of motor neurons. As an alternative approach, thus, we cloned and characterized three mouse members of the protocadherin family, CNR1, Pcdh3 and Pcdh2C. Our results are consistent with a role for these proteins in contributing to neuronal diversity in the spinal cord and dorsal root ganglia. Furthermore they could sub serve as molecular markers because of their expression in subsets of

neurons. Both in the spinal cord (Fig 1) and in the dorsal root ganglia, expression of mRNAs is detectable in restricted areas. It will be interesting to characterize in more detail the properties (morphological and electrophysiological as well as with respect to their connectivity) of the neurons that express the same protocadherin gene and to investigate if the same neurons express multiple protocadherins. Further candidate markers of neuronal diversity are K^+ channels and transcription factors. It is interesting to note that recently (Price et al., 2002) other members of the cadherin family have been shown to specify motor neuron pools in the spinal cord. This study analyzed the developmental expression of cadherins in mouse spinal cord and dorsal root ganglia, and found that these cell-cell adhesion proteins are also expressed in subsets of neurons. Thus, our data on the expression patterns of protocadherins in mouse spinal cord and DRGs open the possibility that also this gene family might be involved in specifying motor neuron subpopulations.

4.1.4. MATERIAL AND METHODS

RT-PCR. RT-PCR was used to clone the three Pcdh cDNAs from total mouse mRNA.
Reverse transcription was performed in 20µl volume reaction in two steps.
First, 5µg DNA-free RNA were incubated for 10' at 70º with 2 µM of each oligo-dT primer (4 µl of 0.5 µM), 1µl (40U) RNAsir (from Boeringher) and ddH_20 up to 12 µl volume, to denature the mRNA secondary structure and allow primer annealing. Sequence of the primers were the following (Tm 58-64º):
- forward primer CNR1 (included the BAMHI restriction site sequence):
5'-GCGGGGATCCCAGCCCAACCCTGACTGG-3';
- forward primer Pcdh3 (included the BAMHI restriction site sequence):
5'-GCGGGGATCCGTGGATCGCGACTCTGGG-3';
- forward primer Pcdh2C (included the EcoRI restriction site sequence):
5'-GCGGAATTCCAAGCCCCGCCCAACACTG-3';
- Reverse primer CNR1 (included the XhoI restriction site sequence):
3'-CCTGTTGTCACTGGTCACTGAGCTCCCGGG-5';
- Reverse primer Pcdh3 (included the XhoI restriction site sequence):
3'-CGACAAACACCCCCACTCGAGCTCCCGCG-5';

- Reverse primer Pcdh2C (included the XhoI restriction site sequence):
3'-CCCGTTCTTTCTCTTCTTCATTGAGCTCCCGCG-5';
Everything was chilled quickly on ice and centrifuged briefly.
Second, 4µl of 5x first strand Buffer (GIBCO), 2µl of 0.1 M DTT (dithiothreitol), 1 µl 10 mM dNTP mix (final concentration 0.5 mM) were incubated for 2' at 42 ºC with the RNA/primer before adding 200U of Superscript II (reverse transcriptase). The mix was incubate at 42º for 50'
To inactivate the reverse transcriptase the mix was boiled at 70º for 15' and left on ice for immediate PCR amplification or stored at – 20 ºC for later use.
One microliter of the obtained cDNA was amplified. The PCR reaction was performed in a 50 µl volume with the following reagents: 5 µl of 10x PCR buffer (expand kit), 1 µl dNTPs Mix 10 mM, 2 µl forward primer (50 ng / µl), 2 µl reverse primer (50 ng / µl), 1 µl cDNA, 0.5 µl HiFi Taq DNA Polymerase (5U/µl) and ddH20 up to 50 µl.

In situ hybridization. For in situ hybridization the brain and spinal cord were removed soon after cervical dislocation, frozen in Tissue-Tek (Sakura Finetek, Torrance, CA) and stored at – 80 C°. Sagittal section (12 µm thick) were prepared using a cryostat and thaw-mounted on glass slides.
In *situ* hybridization for each of the protocadherins was carried out with cRNA probe corresponding to the entire constant coding sequence. The cDNA of interest was cloned into a vector such as a pBS+ or pcDNA3 that contained recognition sites for the RNA polymerase (T3, T7 or SP6). 5 µg of plasmid DNA were digested with appropriate restriction enzymes to produce either a sense or an antisense RNA probe. pCDNA3-Pcdh were linearised using Xho1 and then the T7 polymerase was used to generate the sense probe. To have the antisense probe the plasmids were cut with either EcoR1 or BamH1 and the SP6 polymerase was used. Quantification of probe concentration was done using dot-blots with a known RNA marker and control probes (HB9 and EGFP). The hybridized sections were treated with anti-digoxigenin sheep antibody (Boehringer) coupled to alkaline phosphatase. Anti-digoxigenin antibody and therefore cRNAs were visualized in a colour reaction with BCIP-NBT (Baumeister et al., 1997).

Retrograde labelling. Mice were anaesthetized with a mix of ketamine and rampoon (10 µl/g). The muscle exposed with fine scissors. Fluorogold (Fluorochrome, Englethat), 5 µl, was injected in either the soleus or the EDL with a micro syringe under the dissecting microscope. Incisions were closed using a special surgical glue (Vet-Seal, B. Braun Medical).

4.1.5. FIGURES

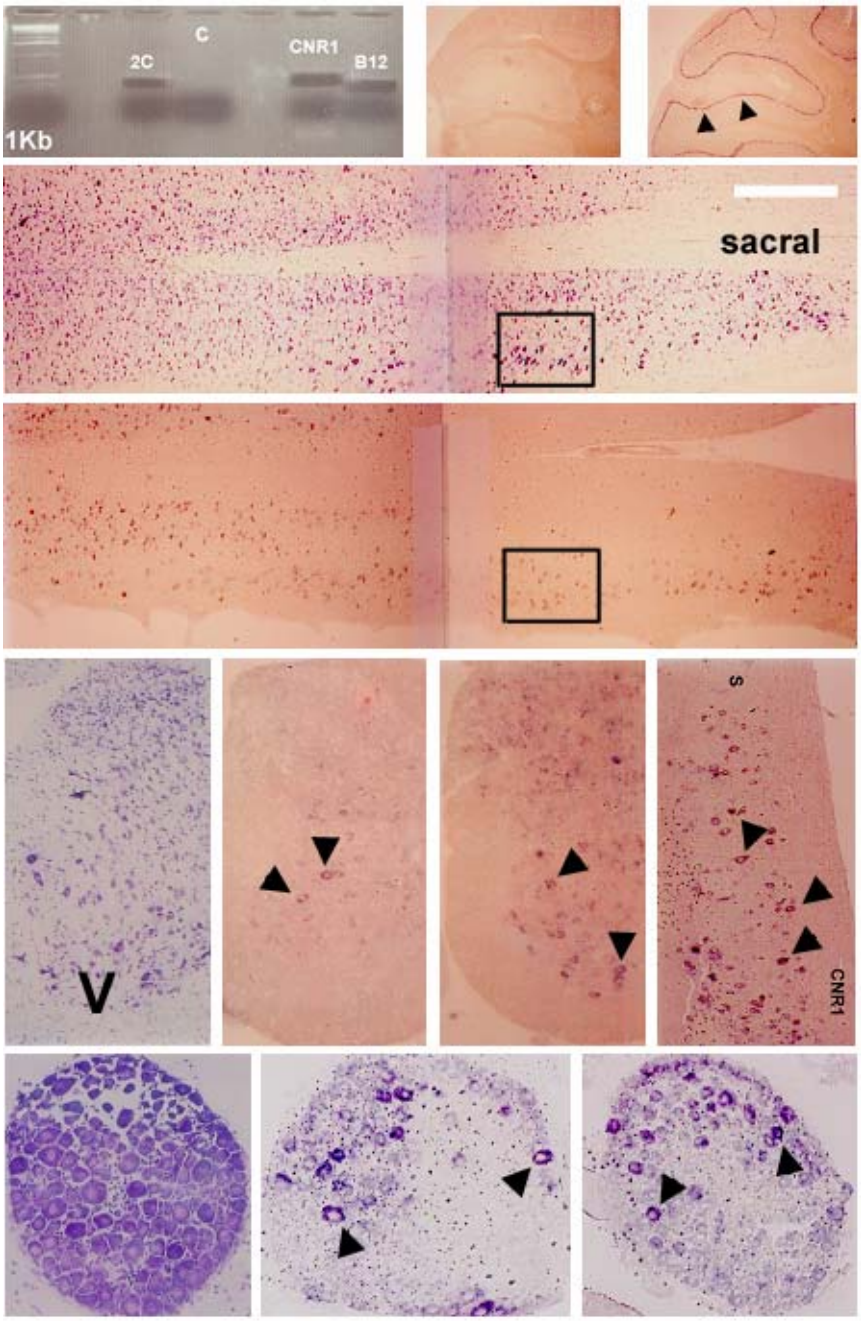

FIGURE 1

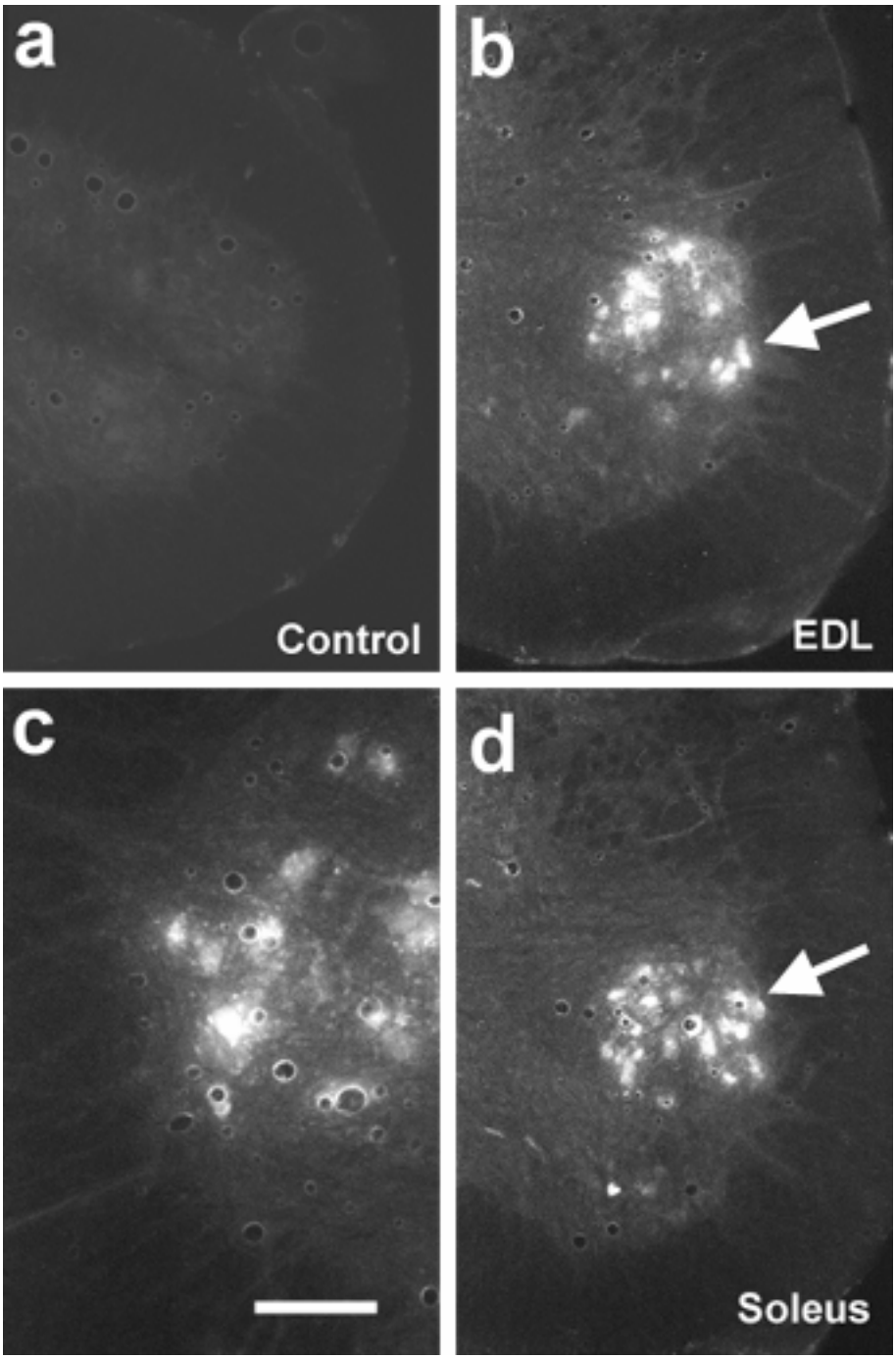

FIGURE 2

4.1.6. FIGURE LEGENDS

Figure 1: Cloning of mouse homologs of human protocadherins and their characterization by in situ hybridization. (First row, first panel) RT-PCR using designed primers (see methods for sequences) on mouse total mRNA. Expected bands were 470, 390, 360 bp for CNR1, Pcdh2C and Pcdh3 (B12) respectively. C is control, 1Kb is the marker. Sense probe gave no signal (second panel) compared to antisense Purkinje cell layer-specific signal in the cerebellum (arrows, third panels). Longitudinal sections of lumbar to sacral, ventral side spinal cord reveal all cells upon cresyl violet staining (second row). Third row and fourth row, 4th panel show the correspondent Pcdh2C and CNR1 *in situ* hybridization. Note colour reaction in subsets of presumably motor neurons (rectangle and arrowheads). In spinal cord cross sections Pcdh3 (4th row, second panel to be compared to first panel which shows cresyl violet staining of adjacent section) and CNR1 (4th row third panel) give also a pattern of expression restricted to the ventral horn where large bodies of motor neurons reside (arrowheads). V, ventral.
Also subsets of dorsal root ganglion neurons (arrowheads in 5th row, second and third panels) appear to express Pcdh3 (second panel) and CNR1 (third panel) when compared to cresyl violet stained ganlia (first panel). Scale bar: 400 μm in first row; 200 in second and third, 150 in fourth, 50 μm in fifth row.

Figure 2: Backlabeling of motor neurons innervating two muscles with different motor unit composition. (a) Contralateral side. (b) Fluorogold signal is detectable in the ventral horn of lumbar spinal cord specifically (arrow indicates groups of motor neurons). (c) Another example of EDL motor neuron-specific labelling in the ventral spinal cord. (d) Motor neurons innervationg the soleus (arrow). Scale bar: 50 μm.

5. REFERENCES

Abel T, Nguyen PV, Barad M, Deuel TA, Kandel ER, Bourtchouladze R (1997) Genetic demonstration of a role for PKA in the late phase of LTP and in hippocampus-based long-term memory. Cell 88:615-626.

Acsady L, Kamondi A, Sik A, Freund T, Buzsaki G (1998) GABAergic cells are the major postsynaptic targets of mossy fibers in the rat hippocampus. JNeurosci 18:3386-3403.

Ahmari SE, Buchanan J, Smith SJ (2000) Assembly of presynaptic active zones from cytoplasmic transport packets. Nat Neurosci 3:445-451.

Aigner L, Arber S, Kapfhammer JP, Laux T, Schneider C, Botteri F, Brenner HR, Caroni P (1995) Overexpression of the neural growth-associated protein GAP-43 induces nerve sprouting in the adult nervous system of transgenic mice. Cell 83:269-278.

Amaral DG (1979) Synaptic extensions from the mossy fibers of the fascia dentata. Anat Embryol (Berl) 155:241-251.

Amaral DG, Witter MP (1989) The three-dimensional organization of the hippocampal formation: a review of anatomical data. Neuroscience 31:571-591.

Amaral DG, Ishizuka N, Claiborne B (1990) Neurons, numbers and the hippocampal network. Prog Brain Res 83:1-11.

Antonova I, Arancio O, Trillat AC, Wang HG, Zablow L, Udo H, Kandel ER, Hawkins RD (2001) Rapid increase in clusters of presynaptic proteins at onset of long-lasting potentiation. Science 294:1547-1550.

Bailey CH, Chen M (1988) Long-term memory in Aplysia modulates the total number of varicosities of single identified sensory neurons. Proc Natl Acad Sci U S A 85:2373-2377.

Bailey CH, Chen M (1989) Time course of structural changes at identified sensory neuron synapses during long-term sensitization in Aplysia. J Neurosci 9:1774-1780.

Bailey CH, Kandel ER (1993) Structural changes accompanying memory storage. Annu Rev Physiol 55:397-426.

Bailey CH, Chen M, Keller F, Kandel ER (1992) Serotonin-mediated endocytosis of apCAM: an early step of learning-related synaptic growth in Aplysia. Science 256:645-649.

Bailey CH, Giustetto M, Huang YY, Hawkins RD, Kandel ER (2000) Is heterosynaptic modulation essential for stabilizing Hebbian plasticity and memory? Nat Rev Neurosci 1:11-20.

Balice-Gordon RJ (1997) In vivo approaches to neuromuscular structure and function. Methods Cell Biol 52:323-348.

Balice-Gordon RJ, Lichtman JW (1990) In vivo visualization of the growth of pre- and postsynaptic elements of neuromuscular junctions in the mouse. J Neurosci 10:894-908.

Balice-Gordon RJ, Lichtman JW (1994) Long-term synapse loss induced by focal blockade of postsynaptic receptors. Nature 372:519-524.

Banker GA, Cowan WM (1977) Rat hippocampal neurons in dispersed cell culture. Brain Res 126:397-342.

Baranes D, Lopez-Garcia JC, Chen M, Bailey CH, Kandel ER (1996) Reconstitution of the hippocampal mossy fiber and associational- commissural pathways in a novel dissociated cell culture system. ProcNatlAcadSciUSA 93:4706-4711.

Baranes D, Lederfein D, Huang YY, Chen M, Bailey CH, Kandel ER (1998) Tissue plasminogen activator contributes to the late phase of LTP and to synaptic growth in the hippocampal mossy fiber pathway. Neuron 21:813-825.

Bashir ZI, Bortolotto ZA, Davies CH, Berretta N, Irving AJ, Seal AJ, Henley JM, Jane DE, Watkins JC, Collingridge GL (1993) Induction of LTP in the hippocampus needs synaptic activation of glutamate metabotropic receptors. Nature 363:347-350.

Bastmeyer M, O'Leary DD (1996) Dynamics of target recognition by interstitial axon branching along developing cortical axons. JNeurosci 16:1450-1459.

Baumeister A, Arber S, Caroni P (1997) Accumulation of muscle ankyrin repeat protein transcript reveals local activation of primary myotube endcompartments during muscle morphogenesis. J Cell Biol 139:1231-1242.

Beaver CJ, Ji Q, Fischer QS, Daw NW (2001) Cyclic AMP-dependent protein kinase mediates ocular dominance shifts in cat visual cortex. Nat Neurosci 4:159-163.

Betz WJ, Bewick GS, Ridge RM (1992) Intracellular movements of fluorescently labeled synaptic vesicles in frog motor nerve terminals during nerve stimulation. Neuron 9:805-813.

Black JE, Isaacs KR, Anderson BJ, Alcantara AA, Greenough WT (1990) Learning causes synaptogenesis, whereas motor activity causes angiogenesis, in cerebellar cortex of adult rats. Proc Natl Acad Sci U S A 87:5568-5572.

Blackstad TW, Brink K, Hem J, Jeune B (1970) Distribution of hippocampal mossy fibers in the rat. An experimental study with silver impregnation methods. J Comp Neurol 138:433-449.

Blair HT, Schafe GE, Bauer EP, Rodrigues SM, LeDoux JE (2001) Synaptic plasticity in the lateral amygdala: a cellular hypothesis of fear conditioning. Learn Mem 8:229-242.

Bliss TV, Lomo T (1973) Long-lasting potentiation of synaptic transmission in the dentate area of the anaesthetized rabbit following stimulation of the perforant path. J Physiol 232:331-356.

Bliss TV, Collingridge GL (1993) A synaptic model of memory: long-term potentiation in the hippocampus. Nature 361:31-39.

Bondareff W, Geinisman Y (1976) Loss of synapses in the dentate gyrus of the senescent rat. Am J Anat 145:129-136.

Bonhoeffer T, Yuste R (2002) Spine motility. Phenomenology, mechanisms, and function. Neuron 35:1019-1027.

Bontempi B, Laurent-Demir C, Destrade C, Jaffard R (1999) Time-dependent reorganization of brain circuitry underlying long-term memory storage. Nature 400:671-675.

Bortolotto ZA, Clarke VR, Delany CM, Parry MC, Smolders I, Vignes M, Ho KH, Miu P, Brinton BT, Fantaske R, Ogden A, Gates M, Ornstein PL, Lodge D, Bleakman D, Collingridge GL (1999) Kainate receptors are involved in synaptic plasticity. Nature 402:297-301.

Bozdagi O, Shan W, Tanaka H, Benson DL, Huntley GW (2000) Increasing numbers of synaptic puncta during late-phase LTP: N-cadherin is synthesized, recruited to synaptic sites, and required for potentiation. Neuron 28:245-259.

Brandon, E.P., et al., Aberrant patterning of neuromuscular synapses in choline acetyltransferase-deficient mice. J Neurosci, 2003. **23**(2): p. 539-49.

Brittis PA, Lu Q, Flanagan JG (2002) Axonal protein synthesis provides a mechanism for localized regulation at an intermediate target. Cell 110:223-235.

Brown V, Jin P, Ceman S, Darnell JC, O'Donnell WT, Tenenbaum SA, Jin X, Feng Y, Wilkinson KD, Keene JD, Darnell RB, Warren ST (2001) Microarray identification of FMRP-associated brain mRNAs and altered mRNA translational profiles in fragile X syndrome. Cell 107:477-487.

Brunelli M, Castellucci V, Kandel ER (1976) Synaptic facilitation and behavioral sensitization in Aplysia: possible role of serotonin and cyclic AMP. Science 194:1178-1181.

Buonomano DV, Merzenich MM (1998) Cortical plasticity: from synapses to maps. Annu Rev Neurosci 21:149-186.

Burke, R.E. (1994) Physiology of motor units. *Myology* (Engel, A.G., Franzini-Armstrong, C., eds) pp464-484. Ney York: McGraw-Hill

Callahan CA, Yoshikawa S, Thomas JB (1998) Tracing axons. Curr Opin Neurobiol 8:582-586.

Capani F, Martone ME, Deerinck TJ, Ellisman MH (2001) Selective localization of high concentrations of F-actin in subpopulations of dendritic spines in rat central nervous system: a three-dimensional electron microscopic study. JComp Neurol 435:156-170.

Carleton A, Petreanu LT, Lansford R, Alvarez-Buylla A, Lledo PM (2003) Becoming a new neuron in the adult olfactory bulb. Nat Neurosci 6:507-518.

Caroni P (1997) Overexpression of growth-associated proteins in the neurons of adult transgenic mice. J Neurosci Methods 71:3-9.

Castillo PE, Malenka RC, Nicoll RA (1997) Kainate receptors mediate a slow postsynaptic current in hippocampal CA3 neurons. Nature 388:182-186.

Castillo PE, Schoch S, Schmitz F, Sudhof TC, Malenka RC (2002) RIM1alpha is required for presynaptic long-term potentiation. Nature 415:327-330.

Chalfie M, Tu Y, Euskirchen G, Ward WW, Prasher DC (1994) Green fluorescent protein as a marker for gene expression. Science 263:802-805.

Chang FL, Greenough WT (1984) Transient and enduring morphological correlates of synaptic activity and efficacy change in the rat hippocampal slice. Brain Res 309:35-46.

Chang S, De Camilli P (2001) Glutamate regulates actin-based motility in axonal filopodia. NatNeurosci 4:787-793.

Chicurel ME, Harris KM (1992) Three-dimensional analysis of the structure and composition of CA3 branched dendritic spines and their synaptic relationships with mossy fiber boutons in the rat hippocampus. JComp Neurol 325:169-182.

Claiborne BJ, Amaral DG, Cowan WM (1986) A light and electron microscopic analysis of the mossy fibers of the rat dentate gyrus. JComp Neurol 246:435-458.

Cline HT (2001) Dendritic arbor development and synaptogenesis. CurrOpinNeurobiol 11:118-126.

Colicos MA, Collins BE, Sailor MJ, Goda Y (2001) Remodeling of synaptic actin induced by photoconductive stimulation. Cell 107:605-616.

Comery TA, Harris JB, Willems PJ, Oostra BA, Irwin SA, Weiler IJ, Greenough WT (1997) Abnormal dendritic spines in fragile X knockout mice: maturation and pruning deficits. Proc Natl Acad Sci U S A 94:5401-5404.

Contractor A, Swanson GT, Sailer A, O'Gorman S, Heinemann SF (2000) Identification of the kainate receptor subunits underlying modulation of excitatory synaptic transmission in the CA3 region of the hippocampus. J Neurosci 20:8269-8278.

Craig AM, Boudin H (2001) Molecular heterogeneity of central synapses: afferent and target regulation. Nat Neurosci 4:569-578.

Cremer H, Lange R, Christoph A, Plomann M, Vopper G, Roes J, Brown R, Baldwin S, Kraemer P, Scheff S, et al. (1994) Inactivation of the N-CAM gene in mice results in size reduction of the olfactory bulb and deficits in spatial learning. Nature 367:455-459.

Dailey ME, Smith SJ (1996) The dynamics of dendritic structure in developing hippocampal slices. JNeurosci 16:2983-2994.

Dailey ME, Buchanan J, Bergles DE, Smith SJ (1994) Mossy fiber growth and synaptogenesis in rat hippocampal slices in vitro. JNeurosci 14:1060-1078.

Darian-Smith C, Gilbert CD (1994) Axonal sprouting accompanies functional reorganization in adult cat striate cortex. Nature 368:737-740.

Davis GW, Bezprozvanny I (2001) Maintaining the stability of neural function: a homeostatic hypothesis. Annu Rev Physiol 63:847-869.

Daw MI, Chittajallu R, Bortolotto ZA, Dev KK, Duprat F, Henley JM, Collingridge GL, Isaac JT (2000) PDZ proteins interacting with C-terminal GluR2/3 are involved in a PKC-dependent regulation of AMPA receptors at hippocampal synapses. Neuron 28:873-886.

De Camilli P, Vitadello M, Canevini MP, Zanoni R, Jahn R, Gorio A (1988) The synaptic vesicle proteins synapsin I and synaptophysin (protein P38) are concentrated both in efferent and afferent nerve endings of the skeletal muscle. J Neurosci 8:1625-1631.

Denk, W. and K. Svoboda, Photon upmanship: why multiphoton imaging is more than a gimmick. Neuron, 1997. **18**(3): p. 351-7.

Dekkers, J., et al., Treatment of the neuromuscular junction with 4-aminopyridine results in improved reinnervation following nerve injury in neonatal rats. Neuroscience, 2001. **103**(1): p. 267-74.

De Paola V, Arber S, Caroni P (2003) AMPA receptors regulate dynamic equilibrium of presynaptic terminals in mature hippocampal networks. Nat Neurosci 6:491-500.

DeChiara TM, Bowen DC, Valenzuela DM, Simmons MV, Poueymirou WT, Thomas S, Kinetz E, Compton DL, Rojas E, Park JS, Smith C, DiStefano PS, Glass DJ, Burden SJ, Yancopoulos GD (1996) The receptor tyrosine kinase MuSK is required for neuromuscular junction formation in vivo. Cell 85:501-512.

Desmond NL, Levy WB (1988) Synaptic interface surface area increases with long-term potentiation in the hippocampal dentate gyrus. Brain Res 453:308-314.

Diamond ME, Armstrong-James M, Ebner FF (1993) Experience-dependent plasticity in adult rat barrel cortex. Proc Natl Acad Sci U S A 90:2082-2086.

Drakew A, Muller M, Gahwiler BH, Thompson SM, Frotscher M (1996) Spine loss in experimental epilepsy: quantitative light and electron microscopic analysis of intracellularly stained CA3 pyramidal cells in hippocampal slice cultures. Neuroscience 70:31-45.

Dunaevsky A, Tashiro A, Majewska A, Mason C, Yuste R (1999) Developmental regulation of spine motility in the mammalian central nervous system. ProcNatlAcadSciUSA 96:13438-13443.

Edwards KA, Demsky M, Montague RA, Weymouth N, Kiehart DP (1997) GFP-moesin illuminates actin cytoskeleton dynamics in living tissue and demonstrates cell shape changes during morphogenesis in Drosophila. Dev Biol 191:103-117.

Eichenbaum H (2000) A cortical-hippocampal system for declarative memory. Nat Rev Neurosci 1:41-50.

Engert F, Bonhoeffer T (1999) Dendritic spine changes associated with hippocampal long-term synaptic plasticity. Nature 399:66-70.

Feng G, Mellor RH, Bernstein M, Keller-Peck C, Nguyen QT, Wallace M, Nerbonne JM, Lichtman JW, Sanes JR (2000) Imaging neuronal subsets in transgenic mice expressing multiple spectral variants of GFP. Neuron 28:41-51.

Fiala JC, Allwardt B, Harris KM (2002) Dendritic spines do not split during hippocampal LTP or maturation. Nat Neurosci 5:297-298.

Fifkova E, Anderson CL (1981) Stimulation-induced changes in dimensions of stalks of dendritic spines in the dentate molecular layer. Exp Neurol 74:621-627.

Fischer M, Kaech S, Knutti D, Matus A (1998) Rapid actin-based plasticity in dendritic spines. Neuron 20:847-854.

Fischer M, Kaech S, Wagner U, Brinkhaus H, Matus A (2000) Glutamate receptors regulate actin-based plasticity in dendritic spines. Nat Neurosci 3:887-894.

Fitzjohn SM, Bortolotto ZA, Palmer MJ, Doherty AJ, Ornstein PL, Schoepp DD, Kingston AE, Lodge D, Collingridge GL (1998) The potent mGlu receptor antagonist LY341495 identifies roles for both cloned and novel mGlu receptors in hippocampal synaptic plasticity. Neuropharmacology 37:1445-1458.

Florence SL, Taub HB, Kaas JH (1998) Large-scale sprouting of cortical connections after peripheral injury in adult macaque monkeys. Science 282:1117-1121.

Fox K (2002) Anatomical pathways and molecular mechanisms for plasticity in the barrel cortex. Neuroscience 111:799-814.

Frey D, Schneider C, Xu L, Borg J, Spooren W, Caroni P (2000) Early and selective loss of neuromuscular synapse subtypes with low sprouting competence in motoneuron diseases. J Neurosci 20:2534-2542.

Friedman HV, Bresler T, Garner CC, Ziv NE (2000) Assembly of new individual excitatory synapses: time course and temporal order of synaptic molecule recruitment. Neuron 27:57-69.

Frisk V, Milner B (1990) The role of the left hippocampal region in the acquisition and retention of story content. Neuropsychologia 28:349-359.

Gaarskjaer FB (1986) The organization and development of the hippocampal mossy fiber system. Brain Res 396:335-357.

Gahwiler BH, Capogna M, Debanne D, McKinney RA, Thompson SM (1997) Organotypic slice cultures: a technique has come of age. Trends Neurosci 20:471-477.

Gan WB, Grutzendler J, Wong WT, Wong RO, Lichtman JW (2000) Multicolor "DiOlistic" labeling of the nervous system using lipophilic dye combinations. Neuron 27:219-225.

Garner CC, Kindler S, Gundelfinger ED (2000) Molecular determinants of presynaptic active zones. Curr Opin Neurobiol 10:321-327.

Geiger JR, Jonas P (2000) Dynamic control of presynaptic Ca(2+) inflow by fast-inactivating K(+) channels in hippocampal mossy fiber boutons. Neuron 28:927-939.

Geinisman Y, deToledo-Morrell L, Morrell F (1991) Induction of long-term potentiation is associated with an increase in the number of axospinous synapses with segmented postsynaptic densities. Brain Res 566:77-88.

Gilbert CD (1998) Adult cortical dynamics. Physiol Rev 78:467-485.

Glass DJ, Bowen DC, Stitt TN, Radziejewski C, Bruno J, Ryan TE, Gies DR, Shah S, Mattsson K, Burden SJ, DiStefano PS, Valenzuela DM, DeChiara TM, Yancopoulos GD (1996) Agrin acts via a MuSK receptor complex. Cell 85:513-523.

Grutzendler J, Kasthuri N, Gan WB (2002) Long-term dendritic spine stability in the adult cortex. Nature 420:812-816.

Gurney ME, Pu H, Chiu AY, Dal Canto MC, Polchow CY, Alexander DD, Caliendo J, Hentati A, Kwon YW, Deng HX, et al. (1994) Motor neuron degeneration in mice that express a human Cu,Zn superoxide dismutase mutation. Science 264:1772-1775.

Haas K, Sin WC, Javaherian A, Li Z, Cline HT (2001) Single-cell electroporation for gene transfer in vivo. Neuron 29:583-591.

Harris KM (1999a) Structure, development, and plasticity of dendritic spines. Curr Opin Neurobiol 9:343-348.

Harris KM (1999b) Calcium from internal stores modifies dendritic spine shape. Proc Natl Acad Sci U S A 96:12213-12215.

Harris RM, Woolsey TA (1981) Dendritic plasticity in mouse barrel cortex following postnatal vibrissa follicle damage. J Comp Neurol 196:357-376.

Hatada Y, Wu F, Sun ZY, Schacher S, Goldberg DJ (2000) Presynaptic morphological changes associated with long-term synaptic facilitation are triggered by actin polymerization at preexisting varicositis. JNeurosci 20:RC82.

Hausser M, Spruston N, Stuart GJ (2000) Diversity and dynamics of dendritic signaling. Science 290:739-744.

Henneman, E., Mendell, L.M. (1991) Functional organization of the motoneuron pool and its inputs. *Handbook of physiology: the nervous system II* (Brooks, H., ed) pp423-507, Baltimore: Williams and Wilkins

Henze DA, Urban NN, Barrionuevo G (2000) The multifarious hippocampal mossy fiber pathway: a review. Neuroscience 98:407-427.

Herrera AA, Banner LR, Nagaya N (1990) Repeated, in vivo observation of frog neuromuscular junctions: remodelling involves concurrent growth and retraction. J Neurocytol 19:85-99.

Higashijima S, Hotta Y, Okamoto H (2000) Visualization of cranial motor neurons in live transgenic zebrafish expressing green fluorescent protein under the control of the islet-1 promoter/enhancer. J Neurosci 20:206-218.

Honig MG, Hume RI (1989) Dil and diO: versatile fluorescent dyes for neuronal labelling and pathway tracing. Trends Neurosci 12:333-335, 340-331.

Horch HW, Kruttgen A, Portbury SD, Katz LC (1999) Destabilization of cortical dendrites and spines by BDNF. Neuron 23:353-364.

Hubel DH, Wiesel TN (1970) The period of susceptibility to the physiological effects of unilateral eye closure in kittens. J Physiol 206:419-436.

Huber KM, Kayser MS, Bear MF (2000) Role for rapid dendritic protein synthesis in hippocampal mGluR-dependent long-term depression. Science 288:1254-1257.

Isokawa M, Levesque MF (1991) Increased NMDA responses and dendritic degeneration in human epileptic hippocampal neurons in slices. Neurosci Lett 132:212-216.

Jiang C, Schuman EM (2002) Regulation and function of local protein synthesis in neuronal dendrites. Trends Biochem Sci 27:506-513.

Jones TA, Schallert T (1994) Use-dependent growth of pyramidal neurons after neocortical damage. J Neurosci 14:2140-2152.

Kaech S, Brinkhaus H, Matus A (1999) Volatile anesthetics block actin-based motility in dendritic spines. Proc Natl Acad Sci U S A 96:10433-10437.

Kafitz KW, Rose CR, Thoenen H, Konnerth A (1999) Neurotrophin-evoked rapid excitation through TrkB receptors. Nature 401:918-921.

Kaibara T, Leung LS (1993) Basal versus apical dendritic long-term potentiation of commissural afferents to hippocampal CA1: a current-source density study. J Neurosci 13:2391-2404.

Kang H, Schuman EM (1996) A requirement for local protein synthesis in neurotrophin-induced hippocampal synaptic plasticity. Science 273:1402-1406.

Kang H, Welcher AA, Shelton D, Schuman EM (1997) Neurotrophins and time: different roles for TrkB signaling in hippocampal long-term potentiation. Neuron 19:653-664.

Keller-Peck CR, Walsh MK, Gan WB, Feng G, Sanes JR, Lichtman JW (2001) Asynchronous synapse elimination in neonatal motor units: studies using GFP transgenic mice. Neuron 31:381-394.

Khalilov I, Esclapez M, Medina I, Aggoun D, Lamsa K, Leinekugel X, Khazipov R, Ben-Ari Y (1997) A novel in vitro preparation: the intact hippocampal formation. Neuron 19:743-749.

Kirov SA, Harris KM (1999) Dendrites are more spiny on mature hippocampal neurons when synapses are inactivated. NatNeurosci 2:878-883.

Knott GW, Quairiaux C, Genoud C, Welker E (2002) Formation of dendritic spines with GABAergic synapses induced by whisker stimulation in adult mice. Neuron 34:265-273.

Kohmura N, Senzaki K, Hamada S, Kai N, Yasuda R, Watanabe M, Ishii H, Yasuda M, Mishina M, Yagi T (1998) Diversity revealed by a novel family of cadherins expressed in neurons at a synaptic complex. Neuron 20:1137-1151.

Kolb B, Petrie B, Cioe J (1996) Recovery from early cortical damage in rats, VII. Comparison of the behavioural and anatomical effects of medial prefrontal lesions at different ages of neural maturation. Behav Brain Res 79:1-14.

Kramar EA, Lynch G (2003) Developmental and regional differences in the consolidation of long-term potentiation. Neuroscience 118:387-398.

Lahtinen H, Autere AM, Paalasmaa P, Lauri SE, Kaila K (2001) Post-insult activity is a major cause of delayed neuronal death in organotypic hippocampal slices exposed to glutamate. Neuroscience 105:131-137.

Lendvai B, Stern EA, Chen B, Svoboda K (2000) Experience-dependent plasticity of dendritic spines in the developing rat barrel cortex in vivo. Nature 404:876-881.

Leuner B, Falduto J, Shors TJ (2003) Associative memory formation increases the observation of dendritic spines in the hippocampus. J Neurosci 23:659-665.

Li Z, Murthy VN (2001) Visualizing postendocytic traffic of synaptic vesicles at hippocampal synapses. Neuron 31:593-605.

Liao D, Zhang X, O'Brien R, Ehlers MD, Huganir RL (1999) Regulation of morphological postsynaptic silent synapses in developing hippocampal neurons. Nat Neurosci 2:37-43.

Lichtman JW, Colman H (2000) Synapse elimination and indelible memory. Neuron 25:269-278.

Lichtman JW, Magrassi L, Purves D (1987) Visualization of neuromuscular junctions over periods of several months in living mice. J Neurosci 7:1215-1222.

Lin W, Burgess RW, Dominguez B, Pfaff SL, Sanes JR, Lee KF (2001) Distinct roles of nerve and muscle in postsynaptic differentiation of the neuromuscular synapse. Nature 410:1057-1064.

Lisman J, Malenka RC, Nicoll RA, Malinow R (1997) Learning mechanisms: the case for CaM-KII. Science 276:2001-2002.

Livet J, Sigrist M, Stroebel S, De Paola V, Price SR, Henderson CE, Jessell TM, Arber S (2002) ETS gene Pea3 controls the central position and terminal arborization of specific motor neuron pools. Neuron 35:877-892.

Lnenicka GA, Atwood HL, Marin L (1986) Morphological transformation of synaptic terminals of a phasic motoneuron by long-term tonic stimulation. J Neurosci 6:2252-2258.

Lo DC, McAllister AK, Katz LC (1994) Neuronal transfection in brain slices using particle-mediated gene transfer. Neuron 13:1263-1268.

Lu YM, Jia Z, Janus C, Henderson JT, Gerlai R, Wojtowicz JM, Roder JC (1997) Mice lacking metabotropic glutamate receptor 5 show impaired learning and reduced CA1 long-term potentiation (LTP) but normal CA3 LTP. J Neurosci 17:5196-5205.

Luscher C, Nicoll RA, Malenka RC, Muller D (2000) Synaptic plasticity and dynamic modulation of the postsynaptic membrane. Nat Neurosci 3:545-550.

Ma L, Zablow L, Kandel ER, Siegelbaum SA (1999) Cyclic AMP induces functional presynaptic boutons in hippocampal CA3- CA1 neuronal cultures. NatNeurosci 2:24-30.

Magrassi L, Purves D, Lichtman JW (1987) Fluorescent probes that stain living nerve terminals. J Neurosci 7:1207-1214.

Maguire EA, Gadian DG, Johnsrude IS, Good CD, Ashburner J, Frackowiak RS, Frith CD (2000) Navigation-related structural change in the hippocampi of taxi drivers. Proc Natl Acad Sci U S A 97:4398-4403.

Majewska A, Tashiro A, Yuste R (2000) Regulation of spine calcium dynamics by rapid spine motility. J Neurosci 20:8262-8268.

Malenka RC, Nicoll RA (1999) Long-term potentiation--a decade of progress? Science 285:1870-1874.

Maletic-Savatic M, Malinow R, Svoboda K (1999) Rapid dendritic morphogenesis in CA1 hippocampal dendrites induced by synaptic activity. Science 283:1923-1927.

Marrs GS, Green SH, Dailey ME (2001) Rapid formation and remodeling of postsynaptic densities in developing dendrites. Nat Neurosci 4:1006-1013.

Martin KA (2002) Microcircuits in visual cortex. Curr Opin Neurobiol 12:418-425.

Martin SJ, Grimwood PD, Morris RG (2000) Synaptic plasticity and memory: an evaluation of the hypothesis. AnnuRevNeurosci 23:649-711.

Marty S, Wehrle R, Sotelo C (2000) Neuronal activity and brain-derived neurotrophic factor regulate the density of inhibitory synapses in organotypic slice cultures of postnatal hippocampus. J Neurosci 20:8087-8095.

Maskos U, Kissa K, St Clement C, Brulet P (2002) Retrograde trans-synaptic transfer of green fluorescent protein allows the genetic mapping of neuronal circuits in transgenic mice. Proc Natl Acad Sci U S A 99:10120-10125.

Matus A (2000) Actin-based plasticity in dendritic spines. Science 290:754-758.

Matus A, Ackermann M, Pehling G, Byers HR, Fujiwara K (1982) High actin concentrations in brain dendritic spines and postsynaptic densities. Proc Natl Acad Sci U S A 79:7590-7594.

McAllister AK, Katz LC, Lo DC (1999) Neurotrophins and synaptic plasticity. Annu Rev Neurosci 22:295-318.

McKinney RA, Capogna M, Durr R, Gahwiler BH, Thompson SM (1999) Miniature synaptic events maintain dendritic spines via AMPA receptor activation. NatNeurosci 2:44-49.

Meng Y, Zhang Y, Tregoubov V, Janus C, Cruz L, Jackson M, Lu WY, MacDonald JF, Wang JY, Falls DL, Jia Z (2002) Abnormal spine morphology and enhanced LTP in LIMK-1 knockout mice. Neuron 35:121-133.

Merzenich M (1998) Long-term change of mind. Science 282:1062-1063.

Mizuhashi S, Nishiyama N, Matsuki N, Ikegaya Y (2001) Cyclic nucleotide-mediated regulation of hippocampal mossy fiber development: a target-specific guidance. J Neurosci 21:6181-6194.

Mombaerts P, Wang F, Dulac C, Chao SK, Nemes A, Mendelsohn M, Edmondson J, Axel R (1996) Visualizing an olfactory sensory map. Cell 87:675-686.

Moriyoshi K, Richards LJ, Akazawa C, O'Leary DD, Nakanishi S (1996) Labeling neural cells using adenoviral gene transfer of membrane-targeted GFP. Neuron 16:255-260.

Moser MB, Trommald M, Andersen P (1994) An increase in dendritic spine density on hippocampal CA1 pyramidal cells following spatial learning in adult rats suggests the formation of new synapses. Proc Natl Acad Sci U S A 91:12673-12675.

Moser MB, Trommald M, Egeland T, Andersen P (1997) Spatial training in a complex environment and isolation alter the spine distribution differently in rat CA1 pyramidal cells. J Comp Neurol 380:373-381.

Naisbitt S, Kim E, Tu JC, Xiao B, Sala C, Valtschanoff J, Weinberg RJ, Worley PF, Sheng M (1999) Shank, a novel family of postsynaptic density proteins that binds to the NMDA receptor/PSD-95/GKAP complex and cortactin. Neuron 23:569-582.

Nakazawa K, Quirk MC, Chitwood RA, Watanabe M, Yeckel MF, Sun LD, Kato A, Carr CA, Johnston D, Wilson MA, Tonegawa S (2002) Requirement for hippocampal CA3 NMDA receptors in associative memory recall. Science 297:211-218.

Narisawa-Saito M, Carnahan J, Araki K, Yamaguchi T, Nawa H (1999) Brain-derived neurotrophic factor regulates the expression of AMPA receptor proteins in neocortical neurons. Neuroscience 88:1009-1014.

Nimchinsky EA, Sabatini BL, Svoboda K (2002) Structure and function of dendritic spines. Annu Rev Physiol 64:313-353.

Nonet ML (1999) Visualization of synaptic specializations in live C. elegans with synaptic vesicle protein-GFP fusions. J Neurosci Methods 89:33-40.

Nottebohm F (1981) A brain for all seasons: cyclical anatomical changes in song control nuclei of the canary brain. Science 214:1368-1370.

Obata S, Sago H, Mori N, Davidson M, St John T, Suzuki ST (1998) A common protocadherin tail: multiple protocadherins share the same sequence in their cytoplasmic domains and are expressed in different regions of brain. Cell Adhes Commun 6:323-333.

Okabe S, Kim HD, Miwa A, Kuriu T, Okado H (1999) Continual remodeling of postsynaptic density and its regulation by synaptic activity. NatNeurosci 2:804-811.

O'Keefe J (1979) A review of the hippocampal place cells. Prog Neurobiol 13:419-439.

O'Rourke NA, Fraser SE (1990) Dynamic changes in optic fiber terminal arbors lead to retinotopic map formation: an in vivo confocal microscopic study. Neuron 5:159-171.

Ostroff LE, Fiala JC, Allwardt B, Harris KM (2002) Polyribosomes redistribute from dendritic shafts into spines with enlarged synapses during LTP in developing rat hippocampal slices. Neuron 35:535-545.

Pak DT, Yang S, Rudolph-Correia S, Kim E, Sheng M (2001) Regulation of dendritic spine morphology by SPAR, a PSD-95-associated RapGAP. Neuron 31:289-303.

Paradis S, Sweeney ST, Davis GW (2001) Homeostatic control of presynaptic release is triggered by postsynaptic membrane depolarization. Neuron 30:737-749.

Patterson SL, Pittenger C, Morozov A, Martin KC, Scanlin H, Drake C, Kandel ER (2001) Some forms of cAMP-mediated long-lasting potentiation are associated with release of BDNF and nuclear translocation of phospho-MAP kinase. Neuron 32:123-140.

Pennetta G, Hiesinger P, Fabian-Fine R, Meinertzhagen I, Bellen H (2002) Drosophila VAP-33A Directs Bouton Formation at Neuromuscular Junctions in a Dosage-Dependent Manner. Neuron 35:291.

Penzes P, Johnson RC, Sattler R, Zhang X, Huganir RL, Kambampati V, Mains RE, Eipper BA (2001) The neuronal Rho-GEF Kalirin-7 interacts with PDZ domain-containing proteins and regulates dendritic morphogenesis. Neuron 29:229-242.

Personius KE, Balice-Gordon RJ (2002) Activity-dependent synaptic plasticity: insights from neuromuscular junctions. Neuroscientist 8:414-422.

Polo-Parada L, Bose CM, Landmesser LT (2001) Alterations in transmission, vesicle dynamics, and transmitter release machinery at NCAM-deficient neuromuscular junctions. Neuron 32:815-828.

Poo MM (2001) Neurotrophins as synaptic modulators. Nat Rev Neurosci 2:24-32.

Pouille F, Scanziani M (2001) Enforcement of temporal fidelity in pyramidal cells by somatic feed-forward inhibition. Science 293:1159-1163.

Price SR, De Marco Garcia NV, Ranscht B, Jessell TM (2002) Regulation of motor neuron pool sorting by differential expression of type II cadherins. Cell 109:205-216.

Pun S, Sigrist M, Santos AF, Ruegg MA, Sanes JR, Jessell TM, Arber S, Caroni P (2002) An intrinsic distinction in neuromuscular junction assembly and maintenance in different skeletal muscles. Neuron 34:357-370.

Purves D, Hadley RD (1985) Changes in the dendritic branching of adult mammalian neurones revealed by repeated imaging in situ. Nature 315:404-406.

Purves D, Voyvodic JT, Magrassi L, Yawo H (1987) Nerve terminal remodeling visualized in living mice by repeated examination of the same neuron. Science 238:1122-1126.

Rajan I, Cline HT (1998) Glutamate receptor activity is required for normal development of tectal cell dendrites in vivo. J Neurosci 18:7836-7846.

Ramón y Cajal, S. (1891). Sur la structure de l' ècorce cèrèbrale de quelques mammifères. La Cellule 7, 125–176.

Rampon C, Tang YP, Goodhouse J, Shimizu E, Kyin M, Tsien JZ (2000) Enrichment induces structural changes and recovery from nonspatial memory deficits in CA1 NMDAR1-knockout mice. Nat Neurosci 3:238-244.

Reid B, Slater CR, Bewick GS (1999) Synaptic vesicle dynamics in rat fast and slow motor nerve terminals. J Neurosci 19:2511-2521.

Rihn LL, Claiborne BJ (1990) Dendritic growth and regression in rat dentate granule cells during late postnatal development. Brain ResDevBrain Res 54:115-124.

Schallert T, Kozlowski DA, Humm JL, Cocke RR (1997) Use-dependent structural events in recovery of function. Adv Neurol 73:229-238.

Scheetz AJ, Nairn AC, Constantine-Paton M (1997) N-methyl-D-aspartate receptor activation and visual activity induce elongation factor-2 phosphorylation in amphibian tecta: a role for N-methyl-D-aspartate receptors in controlling protein synthesis. Proc Natl Acad Sci U S A 94:14770-14775.

Schuman EM (1997) Synapse specificity and long-term information storage. Neuron 18:339-342.

Schwegler H, Crusio WE (1995) Correlations between radial-maze learning and structural variations of septum and hippocampus in rodents. Behav Brain Res 67:29-41.

Segal I, Korkotian I, Murphy DD (2000) Dendritic spine formation and pruning: common cellular mechanisms? Trends Neurosci 23:53-57.

Shepherd GM, Raastad M, Andersen P (2002) General and variable features of varicosity spacing along unmyelinated axons in the hippocampus and cerebellum. Proc Natl Acad Sci U S A 99:6340-6345.

Shi S, Hayashi Y, Esteban JA, Malinow R (2001) Subunit-specific rules governing AMPA receptor trafficking to synapses in hippocampal pyramidal neurons. Cell 105:331-343.

Shi SH, Hayashi Y, Petralia RS, Zaman SH, Wenthold RJ, Svoboda K, Malinow R (1999) Rapid spine delivery and redistribution of AMPA receptors after synaptic NMDA receptor activation. Science 284:1811-1816.

Shigemoto R, Kinoshita A, Wada E, Nomura S, Ohishi H, Takada M, Flor PJ, Neki A, Abe T, Nakanishi S, Mizuno N (1997) Differential presynaptic localization of metabotropic glutamate receptor subtypes in the rat hippocampus. JNeurosci 17:7503-7522.

Shimada A, Mason CA, Morrison ME (1998) TrkB signaling modulates spine density and morphology independent of dendrite structure in cultured neonatal Purkinje cells. J Neurosci 18:8559-8570.

Shimizu E, Tang YP, Rampon C, Tsien JZ (2000) NMDA receptor-dependent synaptic reinforcement as a crucial process for memory consolidation. Science 290:1170-1174.

Siegel JM (2001) The REM sleep-memory consolidation hypothesis. Science 294:1058-1063.

Skrede KK, Westgaard RH (1971) The transverse hippocampal slice: a well-defined cortical structure maintained in vitro. Brain Res 35:589-593.

Smart FM, Halpain S (2000) Regulation of dendritic spine stability. Hippocampus 10:542-554.

Squire LR, Knowlton B, Musen G (1993) The structure and organization of memory. Annu Rev Psychol 44:453-495.

Steward O, Levy WB (1982) Preferential localization of polyribosomes under the base of dendritic spines in granule cells of the dentate gyrus. J Neurosci 2:284-291.

Stoppini L, Buchs PA, Muller D (1991) A simple method for organotypic cultures of nervous tissue. JNeurosciMethods 37:173-182.

Stryker MP, Harris WA (1986) Binocular impulse blockade prevents the formation of ocular dominance columns in cat visual cortex. J Neurosci 6:2117-2133.

Tanzi, E. (1893). I fatti e le induzioni nell'odierna istologia del sistema nervoso. Riv. Sper. Freniatr. 19, 419–472.

Teng E, Squire LR (1999) Memory for places learned long ago is intact after hippocampal damage. Nature 400:675-677.

Toni N, Buchs PA, Nikonenko I, Bron CR, Muller D (1999) LTP promotes formation of multiple spine synapses between a single axon terminal and a dendrite. Nature 402:421-425.

Toth K, McBain CJ (2000) Target-specific expression of pre- and postsynaptic mechanisms. JPhysiol 525 Pt 1:41-51.

Toth K, Suares G, Lawrence JJ, Philips-Tansey E, McBain CJ (2000) Differential mechanisms of transmission at three types of mossy fiber synapse. JNeurosci 20:8279-8289.

Trachtenberg JT, Chen BE, Knott GW, Feng G, Sanes JR, Welker E, Svoboda K (2002) Long-term in vivo imaging of experience-dependent synaptic plasticity in adult cortex. Nature 420:788-794.

Tsien JZ, Huerta PT, Tonegawa S (1996) The essential role of hippocampal CA1 NMDA receptor-dependent synaptic plasticity in spatial memory. Cell 87:1327-1338.

Turner AM, Greenough WT (1985) Differential rearing effects on rat visual cortex synapses. I. Synaptic and neuronal density and synapses per neuron. Brain Res 329:195-203.

Tzounopoulos T, Janz R, Sudhof TC, Nicoll RA, Malenka RC (1998) A role for cAMP in long-term depression at hippocampal mossy fiber synapses. Neuron 21:837-845.

Urban NN, Henze DA, Barrionuevo G (2001) Revisiting the role of the hippocampal mossy fiber synapse. Hippocampus 11:408-417.

Valverde F (1971) Rate and extent of recovery from dark rearing in the visual cortex of the mouse. Brain Res 33:1-11.

van den Pol AN, Ghosh PK (1998) Selective neuronal expression of green fluorescent protein with cytomegalovirus promoter reveals entire neuronal arbor in transgenic mice. J Neurosci 18:10640-10651.

van Praag H, Schinder AF, Christie BR, Toni N, Palmer TD, Gage FH (2002) Functional neurogenesis in the adult hippocampus. Nature 415:1030-1034.

Vickery RM, Morris SH, Bindman LJ (1997) Metabotropic glutamate receptors are involved in long-term potentiation in isolated slices of rat medial frontal cortex. J Neurophysiol 78:3039-3046.

Walsh MK, Lichtman JW (2003) In vivo time-lapse imaging of synaptic takeover associated with naturally occurring synapse elimination. Neuron 37:67-73.

Wang F, Nemes A, Mendelsohn M, Axel R (1998) Odorant receptors govern the formation of a precise topographic map. Cell 93:47-60.

Wang YT, Linden DJ (2000) Expression of cerebellar long-term depression requires postsynaptic clathrin-mediated endocytosis. Neuron 25:635-647.

Whitton PS (1997) Glutamatergic control over brain dopamine release in vivo and in vitro. Neurosci Biobehav Rev 21:481-488.

Wiederkehr A, Staple J, Caroni P (1997) The motility-associated proteins GAP-43, MARCKS, and CAP-23 share unique targeting and surface activity-inducing properties. Exp Cell Res 236:103-116.

Wong WT, Faulkner-Jones BE, Sanes JR, Wong RO (2000) Rapid dendritic remodeling in the developing retina: dependence on neurotransmission and reciprocal regulation by Rac and Rho. J Neurosci 20:5024-5036.

Woolley CS (1999) Effects of estrogen in the CNS. Curr Opin Neurobiol 9:349-354.

Woolley CS, McEwen BS (1994) Estradiol regulates hippocampal dendritic spine density via an N-methyl-D-aspartate receptor-dependent mechanism. J Neurosci 14:7680-7687.

Woolley CS, Wenzel HJ, Schwartzkroin PA (1996) Estradiol increases the frequency of multiple synapse boutons in the hippocampal CA1 region of the adult female rat. J Comp Neurol 373:108-117.

Woolsey TA, Van der Loos H (1970) The structural organization of layer IV in the somatosensory region (SI) of mouse cerebral cortex. The description of a cortical field composed of discrete cytoarchitectonic units. Brain Res 17:205-242.

Wu Q, Maniatis T (1999) A striking organization of a large family of human neural cadherin-like cell adhesion genes. Cell 97:779-790

Yang X, Arber S, William C, Li L, Tanabe Y, Jessell TM, Birchmeier C, Burden SJ (2001) Patterning of muscle acetylcholine receptor gene expression in the absence of motor innervation. Neuron 30:399-410.

Yankova M, Hart SA, Woolley CS (2001) Estrogen increases synaptic connectivity between single presynaptic inputs and multiple postsynaptic CA1 pyramidal cells: a serial electron-microscopic study. Proc Natl Acad Sci U S A 98:3525-3530.

Yuste R, Denk W (1995) Dendritic spines as basic functional units of neuronal integration. Nature 375:682-684.

Yuste R, Bonhoeffer T (2001) Morphological changes in dendritic spines associated with long-term synaptic plasticity. AnnuRevNeurosci 24:1071-1089.

Zhai RG, Vardinon-Friedman H, Cases-Langhoff C, Becker B, Gundelfinger ED, Ziv NE, Garner CC (2001) Assembling the presynaptic active zone: a characterization of an active one precursor vesicle. Neuron 29:131-143.

Zhang X, Poo MM (2002) Localized synaptic potentiation by BDNF requires local protein synthesis in the developing axon. Neuron 36:675-688.

Zhou H, Glass DJ, Yancopoulos GD, Sanes JR (1999) Distinct domains of MuSK mediate its abilities to induce and to associate with postsynaptic specializations. J Cell Biol 146:1133-1146.

Zhou Q, Xiao M, Nicoll RA (2001) Contribution of cytoskeleton to the internalization of AMPA receptors. Proc Natl Acad Sci U S A 98:1261-1266.

Zhu JJ, Qin Y, Zhao M, Van Aelst L, Malinow R (2002) Ras and Rap control AMPA receptor trafficking during synaptic plasticity. Cell 110:443-455.

Zimmer J, Gahwiler BH (1984) Cellular and connective organization of slice cultures of the rat hippocampus and fascia dentata. JComp Neurol 228:432-446.

Ziv NE, Smith SJ (1996) Evidence for a role of dendritic filopodia in synaptogenesis and spine formation. Neuron 17:91-102.

Ziv NE, Garner CC (2001) Principles of glutamatergic synapse formation: seeing the forest for the trees. Curr Opin Neurobiol 11:536-543.

Zucker RS, Regehr WG (2002) Short-term synaptic plasticity. Annu Rev Physiol 64:355-405.